ABSTRACT

LATE DEFLATION STUDY: HEMODYNAMIC EFFECTS OF IAB TIMING IN HUMANS

by
Manal Morcos

Conventional IABP timing deflates 100% of the balloon volume before the onset of left ventricular ejection and has been well established in the literature as a safe and effective method. Yet, recent studies suggest that deflation of the IAB at or near the onset of systole improve myocardial efficiency (Kern, 1999, 1129). To test whether deflation of the IAB at a later deflation time reduces left ventricular workload and enhances coronary perfusion, four timing methods were evaluated in 20 patients: T_1 (100% IAB volume deflated before onset of ejection), T_2 (60% IAB volume deflated before and 40% volume during ejection), T_3 (25% IAB volume deflated before and 75% volume during ejection) and T_4 (100% deflation simultaneous with left ventricular ejection).

To identify an optimal timing point for the deflation of the IAB, data was analyzed. Data analysis consisted of three main parts: elimination of files containing noise artifact, normalization of data for ease of analysis, and correction for variations in mean aortic pressure and heart rate which take into account the dynamic state of the heart. Late IAB deflation at 50% of the volume deflated prior to left ventricular ejection produced significantly greater percentage changes in systolic pressure time index (SPTI), diastolic pressure time index (DPTI), the SPTI/DPTI ratio, systemic vascular resistance (SVR) as compared to conventional timing, T_1. No significant change in heart rate or cardiac output was established.

LATE DEFLATION STUDY: HEMODYNAMIC EFFECTS OF IAB TIMING IN HUMANS

by
Manal Morcos

A Thesis
Submitted to the Faculty of
New Jersey Institute of Technology
in Partial Fulfillment of the Requirements for the Degree of
Master of Science in Biomedical Engineering

Biomedical Engineering Committee

January 2000

APPROVAL PAGE

LATE DEFLATION STUDY: HEMODYNAMIC EFFECTS OF IAB TIMING IN HUMANS

Manal Morcos

Dr. Raj Sodhi, Thesis Advisor — Date
Associate Professor of Mechanical Engineering, NJIT

Dr. David Kristol, Committee Member — Date
Director of Biomedical Engineering and Professor of Chemistry

---

Dr. John Tavantzis, Committee Member — Date
Director of Life Sciences Program and Professor of Mathematics, NJIT

BIOGRAPHICAL SKETCH

Author: Manal Morcos

Degree: Master of Science in Biomedical Engineering

Date: January 2000

Undergraduate and Graduate Education:

- Master of Science in Biomedical Engineering
  New Jersey Institute of Technology, Newark, NJ, 2000

- Bachelor of Science in Engineering Science
  New Jersey Institute of Technology, Newark, NJ, 1998

Major: Biomedical Engineering

This thesis is dedicated to my wonderful family who provided me with constant encouragement and moral support.

ACKNOWLEDGMENT

I wish to express my gratitude and sincere appreciation to Dr. Raj Sodhi, who provided me with guidance, support, and encouragement. Special thanks to Dr. David Kristol and Dr. John Tavantzis for serving as members of the committee.

I would also like to express my deepest appreciation and gratitude to John Lucas, without whom none of this would have been possible. He not only provided me with the topic for the thesis but also provided valuable and countless resources, guidance, and support. He spent countless hours reviewing my work and providing the necessary information to fully understand the topic at hand.

I am especially grateful to employees at Datascope Corporation, specifically, Bob Hamilton, Kent McCune, Jon Williams, and Anna Zastrozna who have been extremely patient and understanding with me. They allowed me to dedicate time to completion of my thesis and have constantly provided me with reassurance and encouragement to complete a task that was once seen as impossible to me. I also wish to thank Sally Shady, Shrenik Draftary, Bob Hoff, and Lara Sarraf for their assistance, friendship, and encouragement.

TABLE OF CONTENTS

TABLE OF CONTENTS
(Continued)

TABLE OF CONTENTS
(Continued)

LIST OF TABLES

LIST OF FIGURES

CHAPTER 1

PHYSIOLOGICAL BACKGROUND RELEVANT TO IAB COUNTERPULSATION

1.1 Introduction: Heart Failure and Intra-Aortic Balloon Pump Therapy

In the United States, nearly 2.3 million individuals are affected with chronic heart failure. Each year, approximately 400,000 people develop heart failure, and "this number is likely to increase as greater numbers of patients who might have died of an acute myocardial infarction are surviving, but with compromised ventricular function" (Quaal 1993, 41). This disorder is the cause of 1,000 deaths each day and now represents the most common medical discharge diagnosis for patients over the age of 65 years.

In a general population study conducted by Kannel, heart failure was found to be greater in men than in women due to a higher incidence of coronary artery disease. Within six years of diagnosis, the mortality rate was 82% for men and 67% for women, corresponding to a mortality rate that is four to eight times greater than that of the general population for the same age group. Sudden death occurred to a greater degree in men than in women with an incidence of 28% versus 14% respectively.

"HF is not a specific disease, but rather the inability of the heart to pump blood commensurate with body tissue metabolic needs. Delivery of oxygen becomes inadequate, leading to cellular dysfunction and imminent organ failure" (Quaal 1993, 43). Deterioration and impairment of cardiac function is a result of a decline in cardiac output and systemic blood flow. Braunwald described heart failure as a secondary occurrence to a massive MI (myocardial infarction), sudden onset of tachyrhthmia, or bradyrhythmia. He further explains that when the heart is subjected to pressure or volume overload for a long duration, a more gradual but progressive state of heart failure may occur.

Heart failure can occur one of two ways: inadequate emptying of the venous reservoirs (backward failure) or reduced ejection of blood under pressure into the aorta and pulmonary artery (forward failure). These two cases are not fully independent, however, because the circulatory system is a closed system (i.e. blood flows in a circle). Therefore, if failure in the ventricle causes a reduction in ejection, then filling will also be reduced and vice versa.

The intra-aortic balloon pump (IABP) has become a useful method for providing temporary mechanical support to those patients diagnosed with heart failure. Downing, et al cited that the single largest groups of patients who benefit from IABP support consist of cardiac surgical patients in whom IABP support has been instituted intraoperatively. Several applications of IABP support that have been suggested but considered controversial include: acute myocardial ischemia or unstable angina, left main coronary artery disease, postinfarction ventricular septal defect, acute cardiogenic shock, hemorrhagic shock, septic shock, intractable ventricular tachyarrhythmias, and major noncardiac operations in patients with severe left ventricular dysfunction (Downing 1981, 112).

In this 7-year study, it was concluded that high complication rates sustained by IABP patients appear to be related to the "severity of underlying disease than to technical features of IABP counterpulsation per se". Therefore, follow-up after 2 years from discharge of patients given IABP support showed that survival rate was $45\pm3\%$ but the functional status of the surviving patients was markedly improved (90% of survivors in New York Heart Association Class I or II).

Another study conducted by Arafa et al suggested that although there was no association between IAB-related complications and death, the average mortality rate over a ten-year period of 344 patients undergoing cardiac operations and who required the use of IABP support was 53% (Arafa 1998, 745). This percentage is consistent with other studies that report mortality rates between 36% and 61% of patients undergoing cardiac operations including those experiencing cardiogenic shock (references cited on page 745 of this article). Survival rates are at a higher rate if the IABP is inserted prophylactically "before operation in high-risk patients with unstable angina, left main coronary artery stenosis, and left ventricular dysfunction". Yet, this study confirmed the results of Downing's research that hospital survivors usually had a relatively good probability of late survival (see Figure 1 below). Although the mortality rates discussed above are high for patients who received IABP support, "the long term prognosis was relatively good for patients who survived the early postoperative period" (Arafa 1998, 746).

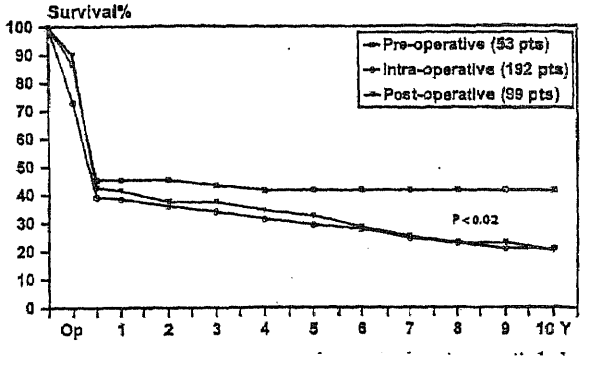

Figure 1: (Source: Arafa)

From these two studies, it is evident that the use of intra-aortic balloon pump therapy for assisting the failing heart can reduce the mortality rate and is critical to saving thousands of lives each year. In order for the reader to understand this importance, it is

essential to gain a fundamental basis for the heart by examining the physiological background relevant to the heart in a healthy state. In other words, "essential to an understanding of physiological benefits derived from intra-aortic balloon counterpulsation (IABC) is a foundation of normal cardiac anatomy and physiology" (Quaal 1993, 3). Thus, it is the intent of this chapter to provide the necessary foundation to fully understand and appreciate the benefits of IABC discussed in subsequent chapters.

Although intra-aortic balloon pump therapy is employed when the left ventricle fails to provide an adequate pumping effort, this chapter will not concentrate on characteristics and function of the left ventricle as a single entity. The interaction between the left ventricle with other muscular chambers of the heart and with the circulatory system as a whole is significant because the consequence of such an interaction provides the essential nutrients to all aspects of the human body. Therefore, the general properties of the heart will be noted prior to focus on the subject at hand-the left ventricle.

1.2 Background

1.2.1 Gross Anatomy of the Human Heart

The human heart is a hollow muscular organ positioned in the thoracic cavity midline between the sternum (breastbone) and the vertebrae (backbone), specifically between the third and sixth ribs. Barely the size of a clenched fist of the individual in whom it resides, the heart measures 12 to 13 cm from base to apex and 7 to 8 cm at its widest point, weighing about .474% of the individual's body weight (approximately 0.75 lb.). Serving as the center of the cardiovascular system, it is considered a "vital pipeline for

transporting materials on which the cells of the body are absolutely dependent" (Sherwood 1997, 266). The heart serves as a pump that imparts pressure to the blood to establish adequate pressure gradients necessary for blood to flow to the tissues.

The muscular wall of the heart is divided into three parts: the epicardium, the myocardium, and the endocardium. The outer surface of the heart is covered by the epicardium, a thin, transparent layer, continuous with the pericardium at the base of the heart. The ventricular myocardium lies between the epicardium and the endocardium The heart is enclosed and held in place within the thorax by a tough connective tissue sac, the pericardium, which maintains the heart's position while still allowing the free movement of the heart during vigorous beating (Fried 1990, 573).

The heart is divided by the interatrial-interventricular septum into a crescent-shaped right side and a cylindrically shaped left side, each side being as a pump that together are connected in series. The heart is composed of four muscular chambers that collectively serve the role of a double pump to deliver oxygenated blood from the lungs to the rest of the body and deoxygenated blood from the body back to the lungs. The two upper chambers are the right and left atria, and the two lower chambers are the right and left ventricles.

The degree of musculature of each of the chamber walls is a function of pressure gradients encountered during the pumping state of the heart. The atria's muscular chambers are thin walled, the thinness of their walls is appropriate due to the low pressures normally developed in the atrial cavities (Katz 1992, 6). The ventricles develop much higher pressures than the atria, and therefore, have thicker muscular walls. However, the muscular walls of the right and left ventricles are not equivalent in

thickness in which the left ventricle has three times the mass and twice the thickness of the right ventricle (Katz 1992, 2).

The thickness of the ventricles can also be appreciated by comparing the work demands of each. Work required of the right ventricle is modest compared to the demands placed on the left ventricle. The pulmonary bed offers little resistance to right ventricular contraction while, in contrast, the left ventricle is required to generate high pressure to overcome systemic circulation resistance and eject blood through the aortic valve and to all aspects of the body. The output of the left ventricle is distributed throughout systemic circulation, a series of parallel pathways that consists of muscles, kidneys, the digestive tract, brain, and all other organs (Katz 1992, 6; Quaal 1993, 6; Sherwood 1997, 268).

Blood flows in a unidirectional fashion from veins to atria to ventricles to arteries through the presence of four one-way valves. The valves open and close in a similar manner to that of the atria and ventricles. A greater pressure (forward pressure gradient) behind the valve will cause the valve to open whereas a greater pressure (backward pressure gradient) in front of the valve will force the valve to close. Located between the atrium and ventricle in each half of the heart are atrioventricular valves, which permit blood flow from the atrium to the ventricle but not from the ventricle to atrium as shown in Figure 2 (Katz 1992, 3). The right AV valve is termed the tricuspid valve (three cusps or leaflets) while the left is the mitral or bicuspid valve (two cusps or leaflets). The two remaining heart valves, the semilunar ("half-moon") valves are the aortic and pulmonary valves located at the juncture between the left ventricle and major arteries (Sherwood 1997, 270).

1.2.2 Circulation

Blood flow is a direct result of the contraction of the cardiac muscle cells in two dimensions, thus wringing blood out of the heart. Blood travels through a series of complex pathways called the cardiovascular system (Figure 2).

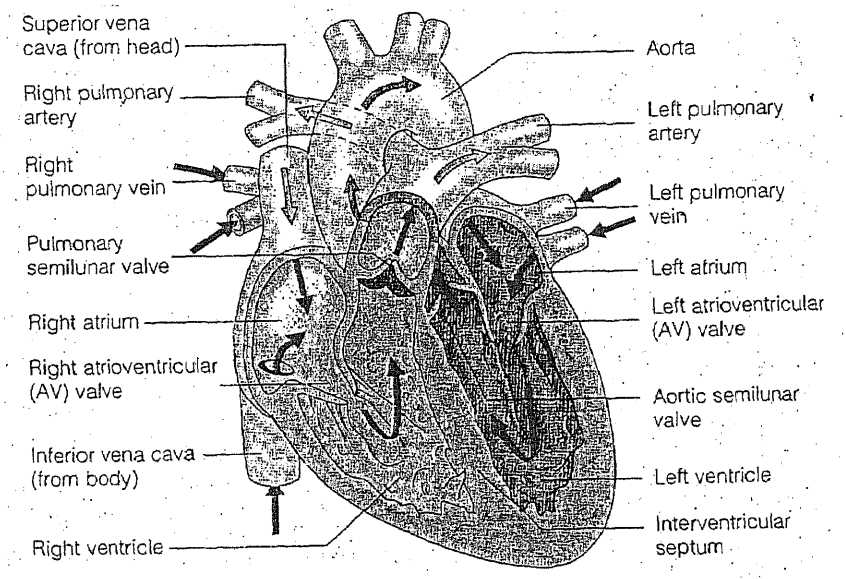

Figure 2: (Source: Sherwood)

The role of the right atrium is to receive dark red, oxygen poor blood from systemic circulation through three veins: the superior vena cava, the inferior vena cava, and the coronary sinus. Blood from the upper part of the body and the upper limbs (parts of the body superior to the heart) travels to the right atrium via the superior vena cava. Blood from the lower part of the body and the lower limbs (parts of the body inferior to the heart) travels via the inferior vena cava and finally, the coronary sinus brings blood from most of the vessels supplying the wall of the heart. Direction of flow occurs

passively from the right atrium through the tricuspid valve into the right ventricle. The right ventricle ejects blood into the pulmonary bed with little resistance whereby the exchange of carbon dioxide and oxygen takes place.

The oxygenated blood returns to the heart, namely the left atrium, via four pulmonary veins, through the mitral valve, and into the left ventricle. Most of ventricular filling occurs passively but an additional 20% occurs during atrial contraction. Finally, the ventricle pumps blood into the ascending aorta where it is transported to all aspects of the body.

1.2.3 Heartbeat Coordination

Although the heart is innervated by the autonomic nervous system, it can contract and relax without any direct stimulus from the nervous system. The cardiac tissue possess the properties of automaticity (ability to initiate an electrical impulse), conductivity (ability to conduct an electrical impulse), rhythmicity (regularity of the pacemaking activity) (Katz 1992, 473; Sherwood 1997, 274).

The heart has its own intrinsic regulating system called the conduction system which is composed of specialized muscle tissue that generates and distributes the electrical impulse that stimulate the cardiac muscle fibers to contract. These tissues are the sinoatrial (SA) node, atrioventricular (AV) node, the atrioventricular bundle, the bundle branches, and the Purkinje fibers, which, like all myocardial cells, are self-excitable and able to rhythmically generate action potentials. This activity is recorded using the electrocardiogram, a scalar quantity that consists of three clearly recognizable waves: the P wave, the QRS complex, and the T wave (Figure 3).

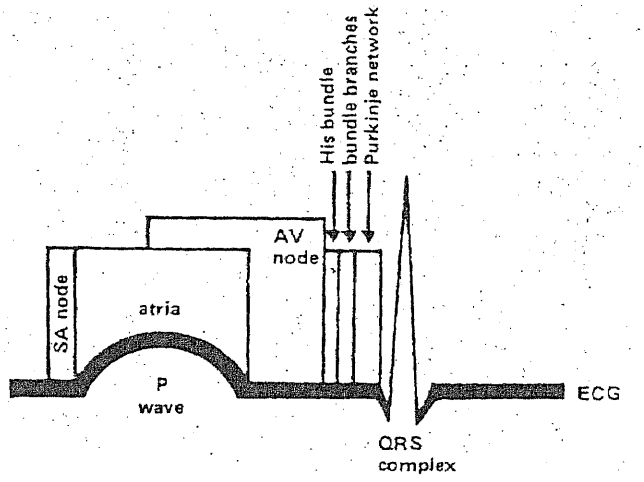

Figure 3: (Source: Katz)

In a healthy human heart, a heartbeat is a two-phase process as follows: atria contract while the ventricles relax, and then the atria relax while the ventricle contract. Thus, a complete mechanical cardiac cycle (one heartbeat) corresponds to these two phases, each portion defined as systole (contraction or propulsion of blood) or diastole (relaxation or filling of blood) depending on the particular function being performed by the heart. The mechanical cardiac cycle is represented as eight divisions of the aortic pressure waveform, which is known as the Wiggers diagram (section 1.2.5.2).

1.2.4 Electrical Events of the Cardiac Cycle and the Electrocardiogram

The electrocardiogram is primarily a tool for evaluating the electrical events within the heart and is used as a trigger for Intra-aortic balloon counterpulsation. The manifestation of these events represents "the sum of the action potentials occurring simultaneously in many individual cells and can be detected by recording electrodes at the surface of the skin" (Vander 1994, 415).

Contraction of myocardial cells is triggered by initial depolarization of group of conducting-system cells, the SA node, located in the right atrium near the entrance of the superior vena cava. The SA node is considered the primary pacemaker of the heart because of its characteristic of having the fastest discharge rate of any of the myocardial cells with pacemaker activity. "Its depolarization normally generates the current that leads to depolarization of all other cardiac-muscle cells, and so its discharge rate determines the heart rate, the number of times the heart contracts per minute" (Vander 1994, 413).

The wave of depolarization that originates in the SA node spreads into the right atrium and then to the left atrium. The time for the wave of depolarization to travel over the atria is reflected as the first deflection in the electrocardiogram, the P wave (Figure 3). It is important to realize at this point, that the depolarization of the SA node is not visible in the ECG because the "SA node is too small to generate electrical potential differences great enough to be recorded from the body surface" (Katz 1992, 482).

After the occurrence of the P wave, the ECG returns to its baseline because the electrical potentials that follow are no longer recorded at the body surface prior to ventricular depolarization (QRS complex). This interval, the P-R interval, is noted as the time when wave of depolarization is propagated through the AV (atrioventricular) node, the AV bundle (also called His bundle or common bundle) and bundle branches.

The second deflection as evidenced in the ECG is the QRS complex, occurring approximately 0.15 seconds later, and is the result of ventricular depolarization. The complexity of this deflection is due to both the paths taken by the wave of depolarization through the thick ventricular walls and the change in current direction in body fluids

accordingly. Therefore, the form of the complex itself varies from instant to instant and the absence of the Q and/or S portions may result. Since the R portion is always present in ECG recordings, it is the wave of choice for triggering of intra-aortic balloon counterpulsation (see Chapter 2).

Comparison of the P wave to the QRS complex shows that the amplitude of the QRS complex is greater than that of the P wave, yet, the duration of the complex is about the same as that of the P wave. The difference in amplitude is due to the fact that ventricular mass is greater than that of the atria while the similarity in duration can be explained by the presence of the Purkinje network in the ventricle that causes rapid propagation of the wave depolarization (Figure 3). Following the QRS complex, the ECG returns once again to its baseline where the final deflection, the T wave, occurs. The T wave, normally rounded and unsymmetrical, represents ventricular repolarization. Occasionally, a small wave with the same polarity as the T wave is visible in the electrocardiogram. The source of this wave, the U wave, is uncertain but it has been hypothesized to represent the repolarization of the papillary muscles or the Purkinje system (Katz; Sherwood; Vander).

In addition to the presence of the major waves listed above, ECG segment intervals, measured between deflections (P, Q, R, S, and T), are used for clinical diagnosis. The P-R interval already discussed, is a measure of the time taken by the impulse to travel from the SA node to the ventricular muscle fibers. The Q-T interval, measured from the beginning of the QRS complex to the end of the T-wave, is the total duration of ventricular systole. The S-T interval, measured from the end of the S wave to the beginning of the T-wave, is the time between the end of the spread of the impulse

throughout the ventricles and the repolarization of the ventricles (Vander; Sherwood; Katz).

1.2.5 Mechanical Events of the Cardiac Cycle

1.2.5.1 Mechanics of the Left Ventricle: The left ventricle is governed by changes in the physical state that ultimately, determine the cardiac output to systemic circulation. This section will discuss the mechanics of the left ventricle in terms of pressure and volume changes. The relationship of pressure and volume is critical to application of counterpulsation techniques to the diseased heart, which will be the topic of Chapter 2.

When the left ventricle is in the filling phase, the volume of blood in that chamber increases even when intraventricular pressure remains constant. This increase in volume leads to dilation of the ventricle to consequently, an increase in tension on each muscle fiber in the ventricular walls. In the diseased heart, higher tensions in the endocardial region of the ventricle makes the region vulnerable to a reduction in coronary flow. Thus, to reduce tension in the muscle fibers, an increase in wall thickness developed during systole is required. This is accomplished by simply distributing tension among a greater number of active sarcomeres in the overloaded heart. Distribution of tension can be accomplished by the utilization of an Intra-Aortic Balloon Pump, which distributes this tension during the inflation phase of the catheter (Chapter 2). The variables discussed above define the Laplace Law:

$$T = \frac{P \times R}{2 \times h} \quad \text{where}$$

T = stress or force exerted across an area
P = pressure
R = radius
h = wall thickness

The Laplace Law is significant because understanding the relationships between left ventricular physical variables in a healthy heart can lead to understanding its application in a heart that is diseased. For example, it is evident from the equation above that increase in the diameter of the ventricle will also increase tension or stress. In congestive heart failure, the dilation of the heart to increase the radius factor not only causes a decrease in coronary flow (ejection of blood is inadequate), but can result in a dilation throughout the contractile cycle, and both end-diastolic and end-systolic tensions are higher (Opie 1998, 362). Katz explains that a decrease in coronary flow can result in a "greater vulnerability of the endocardium to an imbalance between energy demands and energy supply. This is due to the fact that the coronary arteries penetrate the ventricles from the epicardium, and so must traverse a greater distance of contracting myocardium before they can supply the endocardial portion of the ventricles" (355).

In a healthy heart, the contraction of the heart during the systolic phase requires energy. Transfer of metabolic energy to ventricular pressure causes an increase in tension, which consequently, is affected by ventricular volume. Displacement of ventricular volume during contraction is defined as cardiac work. Hence, cardiac work is the addition of external and internal work involved in the transfer of energy from its metabolic substrate to the pressure developed in contraction (Quaal 1993, 37). Internal work is defined as the energy dissipated in the form of heat or used to govern the opening or closing of valve cusps. External work is the work done by the left ventricle and is reflected in a "Work Diagram" or "PV Loop" (Katz 1992, 358; Opie 1998, 365; Quaal

1993, 38). This diagram illustrates the principle of left ventricular work by relating ventricular pressure and volume to the cardiac cycle (Figure 4).

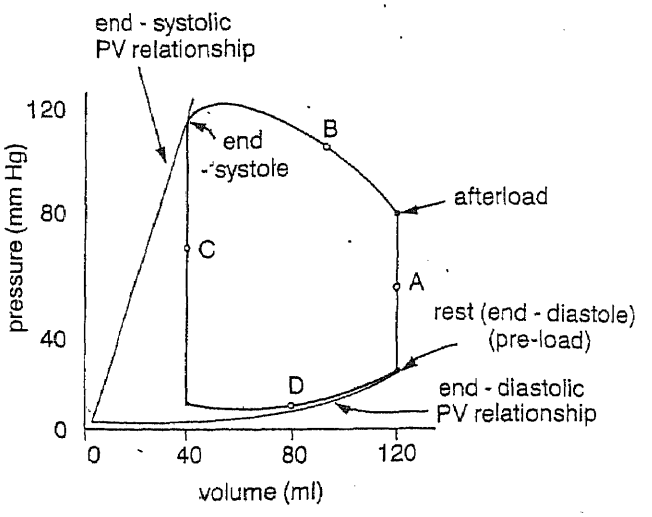

Figure 4: (Source: Quaal)

Preload and afterload determine ventricular pressure and volume. The concept of preload, also known as the Frank-Starling law of the heart, suggests that ventricular fiber length before contraction (fiber stretch caused by end-diastolic volume) determines the strength of the contraction that ensues. Therefore, an increase in end-diastolic volume in the ventricle will result in a greater contractile effort due to the stretching of the cardiac fibers (Quaal 1993, 11). Afterload is defined as resistance to left ventricular ejection. This impedance, for the left ventricle, reflects both peripheral resistance and compliance of the aorta. Aortic impedance is encountered when the left ventricle must overcome aortic end-diastolic pressure to push open the aortic valve during isovolumic contraction (Quaal 1993, 13). During this isovolumic phase, the heart works against the afterload and thus consumes about 90% of myocardial oxygen. Due to this fact, one of the goals of balloon

counterpulsation is to reduce the aortic end-diastolic pressure and, thus, reduce myocardial oxygen consumption.

The Pressure-Volume Loop diagram shown above illustrates the work performed by the left ventricle. The sequence of events that follow portray the cardiac cycle as it pertains to that ventricle and it will thus, give aid in understanding the conventional method of counterpulsation encountered in Chapter 2. The reader is referred to the books written by Katz, Quaal, and Opie for a more in-depth look at this topic.

The diagram, moving in a counterclockwise direction, is divided into four phases. The first phase, isovolumic contraction, defines the period when pressure begins to rise with constant volume caused by the development of tension within the walls of the left ventricle. Rising pressure causes the mitral valve to close and blood can neither enter nor leave until the aortic valve opens. The pressure build-up at this time is end-diastolic pressure.

The second phase, systole defines the period when left ventricular pressure exceeds aortic pressure and causes aortic valve to open. At the onset of aortic valve opening, ejection begins. Aortic pressure at this time rises suddenly as blood rushes in and then falls because the blood travels to systemic circulation. Tension in the walls of the left ventricle decreases owing to the Law of Laplace because less volume is present in the left ventricle during ejection (radius decreases).

The third phase defines beginning of diastole or end-systole and occurs at the end of ejection. Ventricular myocardium begins to relax and pressure in the aorta exceeds ventricular pressure which causes the aortic valve to close. Ventricular relaxation "is unloaded because aortic valve closure, by disconnecting the load (aortic pressure) from

the relaxing left ventricle, relieves the ventricular myocardium of its afterload during all subsequent phases of relaxation" (Katz 1992, 360).

Phase number four is the period defined as diastole when pressure in the left ventricle falls below that of the left atrium, and thus, causes the mitral valve to open. The filling of the ventricle facilitates preload and prepares it for contraction. The state of the fully relaxed ventricle is defined at point D, end-diastolic PV relationship, when pressure and volume have risen gradually to this point.

The importance of understanding the pressure and volume relationships of the left ventricle is its application toward the alleviation of the diseased heart. As will be seen in Chapter 2, IABP Counterpulsation is a cardiac assist mechanism that is timed in synchronization with the cardiac cycle, specifically with the pressure and volume phases occurring in the left ventricle.

1.2.5.2 Mechanics of the Aorta in Conjunction with the Left Ventricle: Section 1.2.5.1, although useful in gaining a perception of the mechanics of the left ventricle, it lacks information on the mechanics of the aorta. The placement of the Intra-Aortic Balloon occurs in the proximal descending aorta, just below the left subclavian artery. Therefore, the effectiveness of the balloon is measured by identifying the events of the patient's cardiac cycle synonymous with the phasically pulsed balloon. In an Intra-Aortic Balloon Pump display, the left ventricular PV relationship or LV pressure waveform is not available and the clinician relies on another means of obtaining information. The diagram that follows, the "Wiggers Diagram", precedes the description on the mechanical events of the cardiac cycle (Figure 5). This diagram is "now an integral part of modern

cardiology and must be understood fully by all who wish to know the basis for the pumping action of the heart" (Katz 1992, 361).

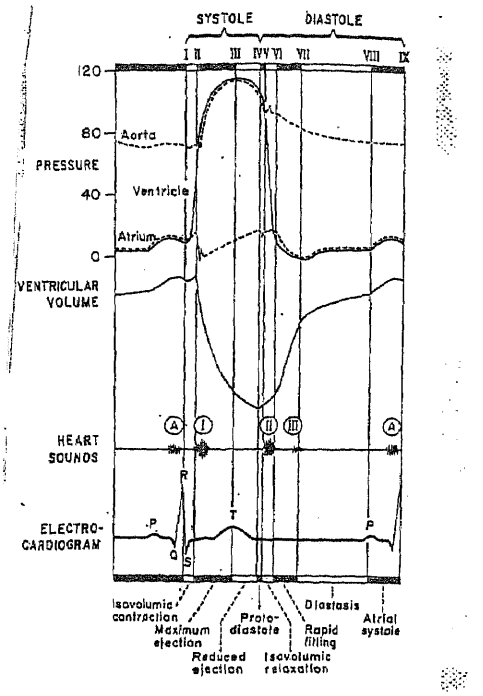

Figure 5: (Source: Katz)

The superimposed curves above summarize the cardiodynamic events, which are summarized as follows:

At the onset of ventricular systole (I), the pressures in both the atrium and ventricle are approximately equal and the AV valves are in the act of apposition to one another. Pressure slowly rises within the left ventricle because both the semilunar valves and AV valves are closed at this time. The slight rise in pressure leads to the contraction of the ventricle isovolumically and thus defines the period when pressure rises rapidly (I-II). The rapid rise in pressure causes a "bulging of both the semilunar and AV valves, which accounts for the small positive oscillations in the aorta and atrium during this

period" (Katz 1992, 361). When pressure in the ventricle exceeds the pressure in the aorta, the semilunar valves open and as a result, the aorta and ventricle become a "common cavity" (II). In the figure above, the opening of the semilunar valves at this time is represented by the close tracking of the aortic and ventricular pressure curves to each other.

The early moments of ventricular ejection is marked by a volumetric change in the ventricle because blood rapidly rushes out of the ventricle and into the aorta. In the figure, this is represented by the rise in pressure of aortic pressure to a summit peak (III) because the rate at which blood enters the aorta is greater than the rate at which it is expelled to the arterioles. The end of systole is indicated as a decline in aortic and ventricular pressures as the rate of ejection diminishes (III-IV). Dr. Wigger's further reduces the period of ejection into two phases: the period at which there is maximum ejection (II-III), and the period at which there is reduced ejection (III-IV). The period of diastole (IV) is defined as relaxation of the ventricle and aorta defined in the diagram as a sharp drop in pressure terminated by the closure of the semilunar valves (V). As left ventricular pressure declines, intra-atrial pressure rises slowly. The AV valves are once again opened when a pressure difference is present, specifically, when atrial pressure exceeds that of the ventricle (VI). Rapid flow of blood occurs at this period (VI-VII) and continues while the pressures in the atria and ventricle decline together, but the atrial pressure is slightly higher than the ventricular. "In long cycles, this is followed by a diastasis phase (VII-VIII), during which ventricular inflow is exceedingly slow, and the pressure rises very gradually both in the atrium and ventricle" (Katz 1992, 363).

1.3 Summary

The goal of this chapter was to provide the reader with a brief overview of the mechanics and physiology of the heart. The concepts presented in this chapter provide a basis for understanding the interaction of the heart and IABP during therapy and will thus, lead to the establishment of the objective of this study.

The purpose of this study is to determine the optimal time to deflate the IAB relative to systole so that left ventricular efficiency is improved to a greater extent than with conventional timing. Hence, the goals of this study is to apply a method of analyzing the data that can take into account the dynamic state of the heart as well as eliminate technical error and motion artifact from the data.

Prior to a discussion of the results obtained from the data analysis, this thesis will provide the following:

- Physiological background pertaining to IAB counterpulsation
- Discussion of the advantages and disadvantages of the current counterpulsation technique
- Discussion of late deflation theory as well as a comparison to conventional timing
- Data analysis: methodology, method, and results
- Summary of data including results and discussion

CHAPTER 2

CURRENT COUNTERPULSATION TECHNIQUE & THE IABP

2.1 Introduction

In Chapter 1, statistical data was presented that indicated the mortality rate of individuals affected with heart failure (Section 1.1). Evidence was provided that demonstrated the decrease in mortality rate by application of the intra-aortic balloon pump. To fully appreciate the extent at which this mechanical device aids the failing heart, fundamental knowledge regarding the healthy heart, specifically, the left ventricle was introduced.

Because the principles of counterpulsation rely on prior knowledge of the mechanics of the cardiac cycle, this information was also provided as part of the background. The cardiac cycle includes the mechanics of the interaction of the left ventricle with the aorta, yet only the aortic pressure waveform appears on the intra-aortic balloon pump screen. Therefore, we must rely on this waveform alone to provide all the necessary information to properly time the IAB in synchronization with the cardiac cycle.

Since the purpose of this thesis is to identify an optimal timing point for deflation of the IAB, it is appropriate to gain a clear indication of the current method of counterpulsation. Thus, it is the intent of this chapter to explain the advantages and disadvantages of the current timing method as well provide a brief overview of the theory of intra-aortic balloon pump therapy.

2.2 Theory of IABP

The first proposal of a device that provides mechanical assistance to the failing heart was first published in the May, 1962 issue of American Heart Journal. In this study, Moulopoulos, Topaz, and Kolff inserted latex tubing tied around the end of a polyethylene catheter into the descending aorta of an anesthetized dog. Through a pressure system, the latex tube was rhythmically inflated with carbon dioxide. The electrocardiogram of the dog served as a trigger so that the latex tubing was inflated during diastole and remained deflated throughout systole. Results showed that "it was possible to increase the diastolic blood flow in the arterial system and lower the end-diastolic arterial pressure" (674). The test also indicated that "intra-aortic pumping may be of help by relieving the left ventricle of its work, and by increasing the blood flow and possibly the coronary blood flow during diastole" (674).

Nearly four decades later the same theory of mechanical assistance to the left ventricle is applied. Intra-Aortic Balloon Counterpulsation (IABC) is instituted by the insertion of polyurethane balloon (mounted on a vascular catheter, which has multiple pores) in the patient's descending thoracic aorta. The most common of insertions is through the femoral artery. The femorally inserted IAB is then passed retrogradely up the descending thoracic aorta to a position just distal to the left subclavian artery.

The IAB is attached to an intra-aortic balloon pump console and helium is shuttled from the IABP to the balloon, escapes through the pores of the vascular catheter and inflates the balloon. Timing of the inflation and deflation of the balloon is phasically counterpulsed with the patient's cardiac cycle. Inflation occurs upon onset of diastole while deflation occurs during isovolumetric contraction or early systole.

2.3 Principles of Counterpulsation: The Conventional Timing Method

2.3.1 Introduction

The word, counterpulsation, is a clinical term that describes balloon inflation in diastole and deflation during isometric contraction or early systole. Inflation of the balloon during diastole displaces the blood in the aorta both proximally (aortic root and coronary arteries) and distally (systemic circulation). The volume displacement of blood enhances coronary circulation as well as potentially increasing system perfusion and perfusion to the aortic arch trifurcated vessels (Quaal 1993, 96). At the time of balloon deflation, intra-aortic blood volume is decreased which lowers the end diastolic pressure in the aorta (afterload). The decrease in pressure reduces the impedance against which the left ventricle must overcome to eject and therefore, cardiac work is also reduced.

2.3.2 Conventional Timing and the Arterial Pressure Waveform

2.3.2.1 Proper Timing of Inflation and Deflation of the IAB: Proper timing of the IAB results in effective interaction between the heart's electrical activity, hemodynamic activity of the left ventricle, and the mechanical activity of the counterpulsation method (Quaal 1993, 246). Kantrowicz stated "The hemodynamic efficacy of balloon pumping is critically dependent on precise timing of both inflation and deflation in relation to the events of the cardiac cycle." (1992, 819).

The IABP console requires a "trigger signal" from which it determines systole and diastole. The most common trigger signal is the R-wave extracted from the patient's ECG. ECG trigger signals is simply obtained from a set of electrodes and lead wires in which the electrodes are placed on the patient's chest and lead to the pump console.

Other methods of triggering include activation of the balloon from the patient's arterial pressure waveform or an internal trigger mechanism available in some IABP's which provide continuous counterpulsation at an established heart rate.

The arterial waveform is the reference from which clinicians adjust for proper inflation and deflation. The clinician moves the inflation and deflation controls manually until proper inflation and deflation morphological landmarks are achieved. As the clinician manually adjusts the settings on the pump console, the console software relates these inflation and deflation points to either R-R intervals from the ECG or intervals between arterial pressure cycles ("trigger signals"). The pump then stores the time (in milliseconds) between each R-R interval or between arterial pressure cycles and relates these times to inflation based upon where the clinician positioned the inflation control and deflation based upon where the clinician positioned the deflation control. For regular R-R rhythm, the pump's logistics system can automatically initiate signal inflation and deflation based on the clinician's adjustments. Irregular R-R intervals can be properly tracked by using the "Real Timing" Method (see Quaal for further reading).

The IAB is timed to inflate at the beginning of diastole right after closure of the aortic valve, thus elevating diastolic pressure termed "augmented diastolic pressure". On the arterial waveform, inflation of the IAB should occur at the midpoint of the dicrotic notch. However, proper timing needs to account for a delay in waveform propagation that exists between the aortic root and peripheral vessels. The delay is a result of a pressure pulsation developed during the systolic phase where ejection of the stroke volume distends the arterial wall and thereby, producing the pulse wave.

To adjust for the dicrotic notch time delay, Quaal describes a common procedure followed by clinicians and healthcare providers (see diagram below). The figure below shows that the cumulative delay is approximately 50 milliseconds: approximately 25 milliseconds of delay exist for the time of aortic valve closure to be relayed to the subclavian artery, and another 25 millisecond delay exists in transmission of an IAB pressure pulse to the aortic root. If properly timed to inflate the IAB 40-50 milliseconds earlier than the midpoint of the dicrotic notch, the morphology of the dicrotic notch should change from the U-shape to the V-shape as is evident in Figure 6 below.

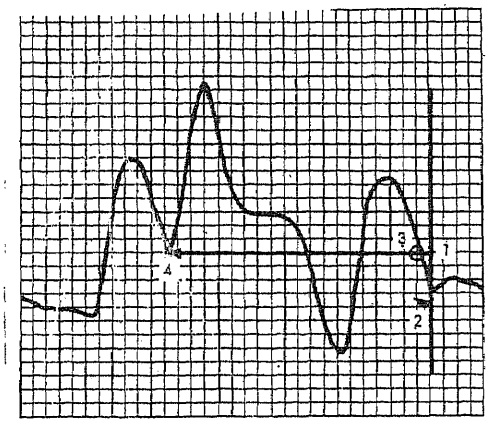

Figure 6: (Source: Quaal)

While the dicrotic notch is a critical landmark for proper inflation, aortic end-diastolic pressure is a critical landmark for proper deflation. Recall from the PV loop that during isovolumetric contraction, aortic end-diastolic pressure is lowered due to the displacement of stroke volume during inflation. Proper deflation should produce two results evident in the aortic pressure waveform. The end-diastolic pressure following balloon assist should be lower than the unassisted aortic end-diastolic pressure. The

decrease in this pressure will reduce left ventricular work because afterload is decreased. As a result, the "assisted systole (the systole that occurs after the balloon counterpulsed) should be ideally lower than but at least not higher than the unassisted systole" (Quaal 1993, 253).

2.3.2.2 Improper Timing of Inflation and Deflation of the IAB: Although no particular timing method has proven to be superior than the rest, there is a widespread acceptance of when IAB counterpulsation can potentially harm the patient rather than provide the necessary therapy it was meant to accomplish. It is significant that IAB inflation or deflation does not compete with systolic ejection, which would increase left ventricular work and therefore, oxygen requirements.

Currently, there is a widespread agreement that inflation of the balloon should occur at the beginning of diastole just after aortic valve closure. Inflation earlier than this point can increase the pressure in the aorta and prematurely close the aortic valve. Stroke volume and cardiac output decrease because the left ventricle does not completely empty. The volume that remains in the left ventricle also causes an increase in pressure or preload which shift the characteristics of the pressure volume loop (see chapter 1). Inflation that occurs far after aortic valve closure can reduce diastolic augmentation and thus, decrease coronary and systemic perfusion. The following diagram illustrates the concepts of both early inflation and late inflation in comparison to conventional timing as witnessed in the aortic pressure waveform:

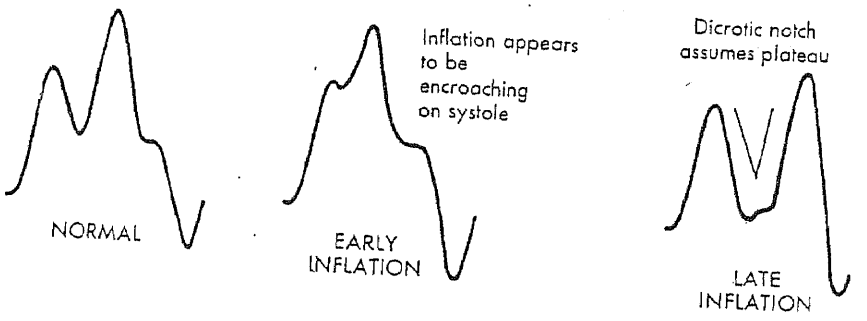

Figure 7: (Source: Quaal)

Improper deflation of the IAB is defined as deflation that occurs too early or too late in reference to systole. Early deflation is characterized by a higher assisted systolic pressure than unassisted systole as evidenced in the aortic pressure waveform. This increase in systolic pressure does not reduce the workload of systolic ejection and therefore, the benefit associated with therapy is not obtained. Other potential consequences include occurrence of retrograde flow that will flow from arterial vessels of higher pressure to the aorta of lower pressure which can be detrimental leading to angina (if flow initiates from coronary arteries) or to a transient ischemia attack (if flow initiates from the cerebrals). Since isovolumetric contraction does not coincide with IAB deflation, myocardial work and oxygen demands are not reduced.

Late deflation is described in terms of inflation timing. If the IAB is still inflated in competition with systolic ejection, the left ventricle must work harder to eject against the increase in aortic impedance and the rate at which systolic pressure rises is prolonged (Figure 8). Consequences include an increase in myocardial work and oxygen consumption as well as a decrease in cardiac output.

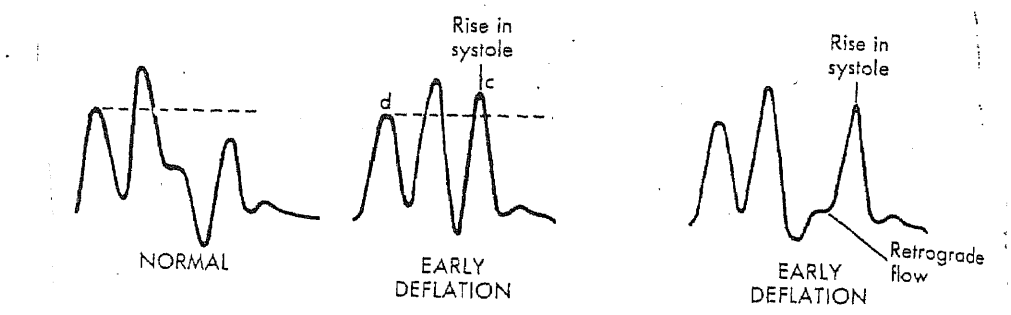

Figure 8: (Source: Quaal)

2.4 Support for Conventional Timing

Over the years, articles and books have been written to support and validate the present practice of conventional timing. Many investigators have chosen not only to examine the benefits of IABP therapy by implementation of the standard timing method but also to examine the risks versus benefits associated with variation of this method. Thus, conclusions derived from such experiments either support conventional timing or propose a timing method whereby indices are improved as a result.

Various groups, including Wolf et al, conducted experiments with the timing method. Using a mock circulation system, they conducted a series of experiments to determine the effects of balloon inflation and deflation timing on systolic left ventricular pressure and cardiac output. Results showed that if balloon deflation occurred after systole, no reduction of left ventricular pressure was obtained. As deflation duration is increased with late deflation, a marked increase in left ventricular pressure and cardiac output occur. It was concluded that even with balloon sizes smaller than 19.5 millimeters, the "most desirable timing occurs when balloon deflation begins at the start of systole" (Wolf 1972, 45).

Literature has also been generated that point out the difficulty in optimization of timing, and thus, is the reason why conventional timing has been the method of choice for clinicians. A performance index should first be formulated based on objective criteria using clinically measurable hemodynamic variables. Choosing a performance index has been a controversial issue in the clinical field since there are numerous variables to consider. It is widely believed that properly timed deflation reduces systolic pressure (conventional timing). Barnea et al point "this effect increases stroke volume and decreases left ventricular energy requirement. However, published data reflect inconsistent results for both augmentation of coronary perfusion and ventricular unloading" (171). They also demonstrated that "as deflation was started in systole, coronary perfusion was enhanced but at the expense of increased workload". Thus, the timing of deflation that reduces workload was found to be different from the timing, which maximally reduces coronary perfusion. Therefore, a measure of IABP performance relies on the hemodynamic variables chosen which can either fully support the standard timing method or provide enough reason for investigators to develop an optimal method.

2.5 Summary

Conventional timing is a "safe" method that reduces myocardial work and oxygen requirements. The range set for inflation and deflation of the balloon is such that it does not compete with left ventricular ejection. Inflation of the balloon during systolic ejection can potentially harm the patient and provide more risks to the patient in comparison to his/her unassisted state. While support exists for utilization of

conventional timing to aid the patient suffering from heart failure, it is well understood that this method has not been optimized. "No single timing setting can be expected to provide optimal hemodynamics for various modalities of heart failure, such as biochemical structural, and viral" (Quaal 1993, 259). However, as discussed in subsection 2.3.2.2, there are risks involved with the conventional timing method. Human error is a factor that can contribute to a great degree in improper timing of the IAB. These errors can be traumatic to the patient and can even lead to death in the worst case scenario. In evaluating the proper timing method, it is essential to determine the risks versus benefits to the patient.

It is difficult to identify hemodynamic indices related to IAB effectiveness (Sun 1991, 1309) since certain parameters can improve with variation in IAB characteristics while others will worsen. Therefore, contradictions exist as to what constitutes the optimal deflation time. As will be discussed in subsequent chapters, there are benefits as well as risks associated with deflation of the balloon at a later time period in comparison to conventional timing depending on which hemodynamic indices are examined.

CHAPTER 3

LATE DEFLATION TIMING STUDY: HEMODYNAMIC EFFECTS OF IAB TIMING IN HUMANS (Late Deflation Theory and Methodology)

3.1 Introduction

The intra-aortic balloon pump is the most commonly used circulatory assist device for the failing heart. Benefits include arterial diastolic augmentation and reduction of afterload resistance with decreased systolic pressure (Bolooki 1998, 4; Kern 1999, 1129; Quaal 1993, 101). This counterpulsation device has saved thousands of lives since its creation and continues to provide therapy to those that need it (see chapter 2).

The hemodynamics of the intra-aortic balloon have been documented and demonstrate that a significant increase in diastolic augmentation as well as a decrease in afterload and systolic pressure results in patients with IABP support in comparison to patients without assist. Currently, these benefits are gained by the utilization of the conventional timing method in which complete balloon deflation is completed prior to ejection of the left ventricle (Bolooki 1998, 4).

Although the theory of conventional timing is widely practiced and accepted in the clinical field, it is not considered an optimal timing method (Barnea 1990, 175). This classical method has remained unchanged for the past 25 years (Datascope Protocol-Lucas 1994, 2). Several disadvantages are cited and thus, leave room for improvement. In Chapter 2, it was explained that conventional timing is a "safe" method. While its benefits are well documented in literature, several issues are still being investigated. The first issue deals with incorrect timing (e.g. early or late inflation/deflation) discussed in

Chapter 2. The second issue deals with optimization of hemodynamic indices associated with IABP therapy such as oxygen supply to the myocardial tissue (i.e. diastolic augmentation) and reduction of afterload and therefore, systolic pressure.

The proper timing of deflation is still an issue. It is well understood that it should occur so as not to compete with ventricular ejection. Yet, the possibilities for deflation of the balloon encompass a broader range than that available for correct inflation. Thus, it has been the intent of investigators to define what that particular optimal deflation time is. Currently, contradictions still exist in the data obtained from these experiments since benefits as well as risks are associated with deflating the balloon at a later period. Because no one can agree on which performance index provides the best clinical indication of hemodynamic efficacy of IABP support, the results of this study will be presented using several hemodynamic variables that encompass the wide range of variables cited in the literature.

3.2 Late Deflation Study: Theory

"Although the effects of the IABP on systemic and coronary hemodynamics have been extensively described (7-12), little information exists in patients regarding optimal myocardial efficiency with IABP timing techniques" (Kern 1999, 1129). As explained in Chapter 2, conventional IAB timing has previously been set to ensure 100 percent of balloon deflation prior to left ventricular ejection. Yet, recent experimental studies have demonstrated that myocardial efficiency may be optimal when balloon deflation coincides with the pre-systolic ejection period (isovolumetric contraction) and is completed at some point during left ventricular ejection (Kern 1999, 1129-1130). These

studies, referenced in the article by Kern et al, have demonstrated that a later IAB deflation resulted in improved diastolic augmentation and further reduction in afterload.

Benefits for later deflation are not only supported by experimentation with animals and mock circulatory systems but are mathematically modeled as well. Mathematical modeling of the dynamic interaction between the left ventricle and the intra-aortic balloon pump predicted that progressive postponing of the deflation point does not significantly impact left ventricular work and stroke volume until approximately 50 milliseconds after the R-wave (Sun 1991, H1310). Yet, maximum stroke volume was found to occur when the deflation transition matched the opening of the aortic valve because it was hypothesized that the deflating balloon sucks additional blood from the left ventricle (H1310).

As discussed in this section, the theory of deflating the balloon at a later time period than standard deflation is valid because it demonstrates an increase in hemodynamic efficacy. Yet, the theory is still vague since no one has been able to state what that optimal timing point is. This study will attempt to define that optimal timing point as well as provide information on hemodynamic efficacy of intra-aortic balloon pumping using different timing methods as compared to the unassisted state (i.e. IABP turned off).

3.3 Objective

The purpose of this study is to identify an optimal deflation of the IAB at which IABP efficacy is modified and thus, improved as compared to conventional timing. The hypothesis tested was that deflation of the IAB approaching or simultaneous with left

ventricular ejection would improve myocardial efficiency and systemic hemodynamics. It is the goal of this study that identification of hemodynamic efficiency of IABP deflation could lead to implementation of a new IABP timing technique that can further aid the sick patient.

This analysis has been triggered by a previous study conducted by Datascope Corporation and Kern et al. The purpose of the study was to determine the potential benefits of deflating the IAB closer to ventricular ejection than is currently being done with conventional timing. The study examined four timing methods described in the following chapter. Results showed that a delay in IABP deflation approaching left ventricular ejection appears to provide "optimal reduction of afterload without producing adverse effects on cardiac output, stroke volume, or indices of oxygen consumption" as evidenced by the differences between conventional timing and late deflation (1999, 1135). Yet, identification of the "optimal" deflation timing point was not established and the findings do not conclusively demonstrate that deflation at or after the R-wave is completely appropriate in each patient. Inconclusiveness of Kern's study may be due, in part, to a faulty analysis technique, which resulted in intra- and inter-patient inconsistency and variability (Paul Nigroni & John Lucas, Datascope Corp.). Therefore, a new analysis method that excludes this variability is provided in this thesis.

The results obtained by Kern et al will be identified for comparison with results obtained in this study. The following will be considered as constants that will remain the same for both the focus of this thesis and was used for the study conducted by Kern et al:

- Patient files containing the aortic pressure waveforms as well as the EKG (electrocardiogram). Therefore, patient selection/criteria and data acquisition described in Appendix A pertains to both this study as well as Kern et al's.
- Four timing methods, T_1-T_4 (section 3.4)
- Hemodynamic indices utilized to determine effectiveness of IAB performance at a particular timing method (Chapter 4).

Differences between the two studies, Kern et al's versus my study, exist in the method utilized to analyze the data and is summarized as follows:

- Correction of data for change in mean pressures including mean systolic pressure, mean diastolic pressure, and mean aortic pressure (pressure was found in this study to change with change in heart rate which will be discussed in Chapter 4)
- Selection of a consistent starting point for systole, which ultimately had a significant impact on reduction of variability (see Chapter 4)
- Correction of data for improper timing, specifically, early or late inflation/deflation (the four predetermined timing points did not occur exactly as theoretically described in the protocol and will be further discussed in Chapter 4)

3.4 Four Timing Methods for IAB Deflation

The four timing methods below were utilized for the purpose of this thesis as well as for the study conducted by Kern et al. The methodology for choosing each setting is discussed below but the exact time (in milliseconds) in relation to left ventricular ejection is not mentioned since it varies with each patient depending on the length of the cardiac cycle.

The time setting, T_1, is defined as the conventional or standard timing setting whereby the entire 40cc volume of the IAB is deflated prior to left ventricular ejection. The end of deflation of the IAB coincides with the onset of left ventricular ejection and thus, provides maximum pre-systolic decline in pressure. A potential consequence of using this experimental point is retrograde coronary blood flow.

The time setting, T_2, is defined as an intermediate time setting between T_1 and T_3 whereby 60% of the 40cc volume (24cc) of the IAB is deflated prior to the onset of left ventricular ejection. Therefore, 40% of the volume (16cc) will still be inflated at the onset of ejection and it is hypothesized that this will cause a decline in the pre-systolic pressure but not to as great a degree as T_1. Just like the T_1 setting, a possibility exists that retrograde flow will occur.

The T_3 time setting is defined as 25% of the IAB volume (10cc) deflated prior to the onset of left ventricular ejection. Thus, 75% of the volume (30cc) will be deflated during left ventricular ejection and will provide "the best degree of pre-systolic unloading (i.e. pressure decline) realizable in the absence of significant retrograde flow" (Lucas, 1994). Cited in Datascope's test protocol is the rationale for choosing this time period: "T_3 is based upon data in the literature which indicates that 10cc is about the maximum volume which can be deflated in pre-systole without incurring retrograde blood flow into the central aortic reservoir from the coronary circulation, and perhaps from cerebral vessels and other vascular beds" (Lucas, 1994).

T_4 is the time setting whereby the onset of IAB deflation occurs simultaneously with left ventricular ejection. Thus, it is set so that 40cc volume of the IAB is inflated at the onset of left ventricular ejection and starts to deflate at that moment, providing the

best in-phase match of IAB deflation to left ventricular ejection. It was hypothesized that no pre-systolic decline in pressure will occur with this time setting since inflation of the IAB might pose as a large resistance or impedance to LV ejection. In this chapter, the potential risks associated with late deflation were described and it was possible that with this time setting, these risks could have become an issue at the patient's bedside. As with implementation of all time settings, the patient was continually monitored and was removed from the study if a negative effect to IABP therapy was recognized.

3.5 Summary

It is critical when looking at all sections in subsequent chapters that there exists a clear understanding of the purpose of this study. Datascope Corporation has instituted a study to determine an optimal timing point for deflation of the IAB as well as to determine the hemodynamic effects of IAB timing in man. Thus, it is the goal of my study to present this information using an analysis technique different from the one that was utilized in the past (e.g. Kern et al's study). The data collected prior to this study and utilized by Kern et al will remain the same data that is analyzed in this thesis. The similarities and differences between this study and Kern et al's investigation will be cited as deemed necessary in the body of text that follows, specifically in Appendix A.

The objective of Chapter 4 is to present the test methodology including extraction of information from aortic pressure waveforms and the ECG as well as selection of patients' files utilized in this study. The graphs generated for each file represent the correction factors that take into account the dynamic state of the heart and are contained in Appendix B. Chapter 5 will include the results, discussion, and conclusion. Results

are presented in Appendix C in graphical form for all files analyzed which will serve as a visual tool for ease of comparison.

CHAPTER 4

LATE DEFLATION TIMING STUDY: HEMODYNAMIC EFFECTS OF IAB TIMING IN HUMANS (PARAMETERS INVOLVED IN DATA EXTRACTION)

4.1 Introduction

The purpose of this chapter is to provide the reader with information regarding the steps taken to analyze the data. Equipment necessary for data analysis will be described as well as the number of files analyzed following elimination of data containing artifact. Corrections for deflation time, heart rate, and pressure are also included in this chapter.

4.2 Data Reduction: Elimination of Files with Substantial Artifact (Catheter Whip)

Although the total number of patients accepted according to the inclusion/exclusion criteria were 43, it was evident from evaluation of patients' files that not all files can be analyzed, specifically, due to pressure or motion artifact (i.e. catheter whip). Based on the limitations of the data playback software utilized (CODAS), extraction of artifact from the waveforms was not possible. Therefore, analysis of data that contained artifact would not have provided meaningful clinical results. Evaluation of these files resulted in a reduction of patients' files to a total of 35.

The data presented in this thesis represent a total of twenty patients' files out of those 35 files mentioned above. The number twenty was chosen because analysis of each file encompasses a great deal of time that was not available given the time span of this study. The twenty files were chosen randomly from the list of 35 files shown in Table 1 which are indicated with a check mark (✓) next to the file name:

Table 1 Twenty Patients' Files Randomly Chosen for this Study

PATIENT FILE: A		PATIENT FILE: B		PATIENT FILE: C		PATIENT FILE: D	
A2	✓	B1	✓	C1		D2	✓
A3	✓	B2	✓	C2	✓	D3	✓
A4		B3	✓	C3	✓	D6	✓
A7	✓	B4	✓	C4	✓	D8	✓
A8		B5		C5	✓	D9	✓
A11	✓	B6	✓	C6	✓	D10	✓
A14		B7		C10		D12	
		B8		C11		D13	
		B9		C12		D14	
		B10		C13			
Total Files Evaluated in this Study:	4		5		5		6

Each patient file contained a total number of ninety cardiac cycles that were evaluated (18 cardiac cycles for each of the timing settings and standby multiplied by 5 (4 time settings + standby)). The number eighteen represents the number of cardiac cycles previously evaluated by Datascope Corporation, specifically Lynn Antonelli and John Lucas, and were incorporated in Kern et al's study. Previously analyzed cycles are found in CODAS by looking for the cycles with inserted marks.

4.3 Software Utilized for Data Analysis

The same P.C. software package utilized for data acquisition was utilized for data analysis. This software, Windaq Playback Software (also called CODAS), contained the same channels present in the data acquisition files described in Appendix A. This software was specifically utilized to obtain the following raw hemodyamic data:

- R-R Interval (RR) = total cardiac cycle = time between IABP R-wave trigger signals
- Diastolic Time Index (DTI) = time from dicrotic notch or IAB inflation to the next systolic aortic pressure upstroke
- Left Ventricular Ejection Time (LVET) = time from systolic aortic pressure upstroke to dicrotic notch or IAB inflation point.
- Mean Aortic Pressure (MAP) = total mean aortic pressure during one complete R-R interval
- Mean Systolic Aortic Pressure (MSAP) = mean systolic pressure during LVET time interval
- Mean Diastolic Aortic Pressure (MDAP) = mean diastolic pressure during DTI

The parameters listed above were later entered into Excel spreadsheets for further analysis. Graphs and correlation factors were generated which are explained in Chapter 5 and included in Appendices B and C of this thesis.

4.4 Waveform Analysis Technique: Normalization of Data

The method of extracting raw hemodynamic data from the CODAS files is outlined below. This method normalizes the data so that a relevant statistical comparison can be established. Hemodynamic data was then entered into Excel spreadsheets for further analysis and is attached in Appendix B of this manuscript. The data points extracted included: RR, LVET, DTI, MSAP, MDAP, and MAP.

4.4.1 Methodology

The data represented four timing methods as well as standby data (intra-aortic balloon pump was turned off). According to the figure below (Figure 9), as the deflation point is increasingly delayed, the systolic aortic pressure of the subsequent cycle is artificially shortened. For example, the deflation point, T_4, intersected the systolic aortic pressure waveform at a later time period than T_1. Therefore, the total area under the systolic aortic pressure curve artificially decreases as the deflation timing point occurs later into systole (i.e. the area to the left of the intersection of the timing points is eliminated).

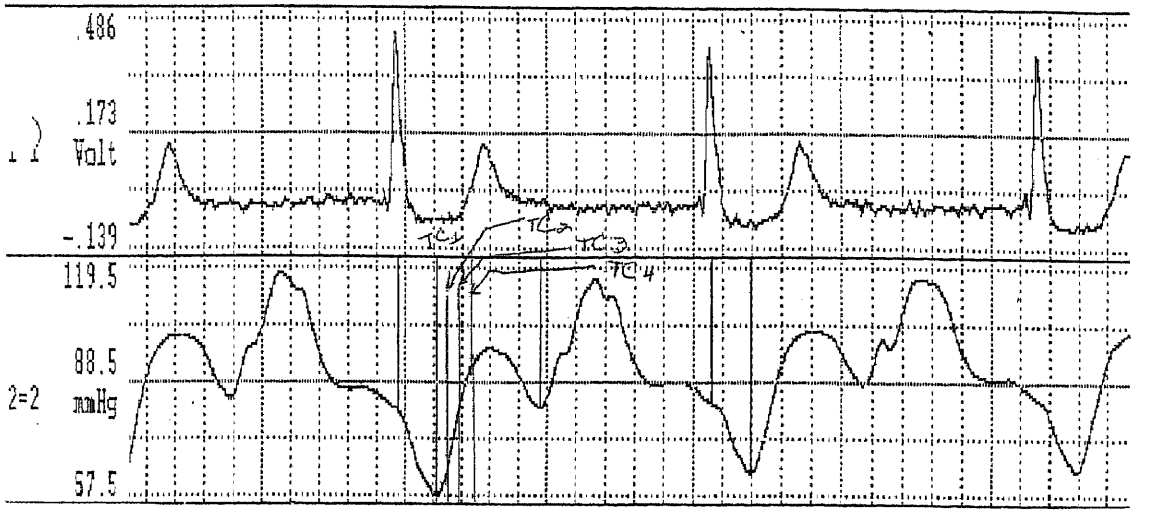

Figure 9: (Source: Lucas)

The area under the aortic pressure curve that was eliminated could not be measured for the following reason. The deflation timing points did not occur exactly as described in Chapter 3 relative to systole. Because the data did not include the left ventricular pressure, we do not know when ventricular ejection really occurred. Knowing

the time period of ventricular ejection is critical because the deflation timing points, T_1-T_4 are timed to occur relative to systole. Thus, we do not have a clear indication of how much of the aortic pressure curve was eliminated with each time setting.

To account for these timing errors, the data was normalized so that a comparison can be made between the four deflation timing points and at standby. Normalization of the data was established by obtaining the hardcopy of each of the patients' files and then measuring the largest distance between the R-wave and systole. From CODAS, this distance was then translated into a time period, RS_{max}, which was used as a starting point for that particular file. That way, systole was assumed to start at a particular location for the patient's cardiac cycle for all deflation time settings as well as at standby. Analysis consisted of a comparison of these normalized values to standby data and is contained in Appendices B and C.

4.4.2 Method

The procedure that follows lists the necessary steps required to obtain the raw hemodynamic data. In CODAS, Channel 1 (ECG) and Channel 2 (aortic pressure waveform) were utilized for extraction of this information.

1. For each patient, obtain the hard copy files.
2. On the bottom of each sheet is the timing method represented by the waveforms on that page. Analysis should consist of "standby" data as well as the four timing methods, T_1-T_4.
    - Using a ruler or straight edge, draw a vertical line at the R-wave of the ECG reading (Channel 1 in CODAS-See Appendix A).

- Draw another line at systole, where systole is defined by the upstroke of the aortic pressure waveform (Channel 2 in CODAS- See Appendix A).
- Use a vernier caliper to measure the first three cycles on that page. Particularly, measure the distance between the R-wave of the ECG and systole as indicated by the two vertical lines drawn from the above steps.
- Once the above procedure is completed for the time settings labeled standby and T_1 through T_4, compare the distances measured by the vernier caliper and note the largest distance along with the time setting associated with it. This distance, RS_{max}, is defined as the maximum distance between the R-wave and systole.

3. Go to that particular patient's file on the computer (using CODAS software) and look for the time setting that corresponds to the RS_{max} noted. It is important to understand that the maximum distance measured, in inches, is only relevant to locate the particular time setting on the computer where the longest cardiac cycle occurs. Once the cardiac cycle is found using the steps below, that distance was converted into a time period, in seconds, defined as Rs_{max}.

- Move the cursor to the ECG of Channel 1, specifically, the R-wave, and press the F4 button to zero out the time at that point.

- Using the time, in seconds, found in the last step of instruction #2 above, move the cursor from time=0 seconds to time found in that step (defined as RS_{max}).
- Again zero the out the time at that point by pressing the F4 key and insert an event mark (press the insert key on your keyboard). This is the starting point, systole, at which deflation of the IAB is assumed to occur.
- Move the cursor from systole to the dicrotic notch. It is critical that the location of the cursor be defined as the least pressure in millimeters of mercury (mmHg) at the dicrotic notch. Insert an event mark, which will make it easier to find this point at a later time period (press the insert key on your keyboard). This time period, from systole to the dicrotic notch (LVET) should be noted for further analysis. Also, the area under the curve from systole to the dicrotic notch, defined as the mean systolic aortic pressure (MSAP), is obtained by pressing the <control> key and the letter T (or from the toolbar, go to the statistics function in the Edit menu). Also, note this value for further analysis.
- From the dicrotic notch, move the cursor to the next R-wave. Zero that point and move the cursor to the specific time period noted in the last step of instruction # 2 defined as RS_{max}.
- From systole, at time=0 seconds, move the cursor back to the event mark located at the dicrotic notch. Record this time period as DTI.

Go to "Statistics" and record the mean diastolic aortic pressure (MDAP).

- Move the cursor from its current location to the left at systole (i.e. location of inserted event mark). Record this time period as R-R interval. Again, go to "Statistics" and record the mean aortic pressure (MAP).

4.5 Correction for Mean Aortic Pressure and Heart Rate

Following completion of data extraction, the correlation between heart rate and pressure at standby was deduced and incorporated as a correction factor for all time settings as well as standby data. The method included in this section was applied to all files and represents the dynamic state of the heart. The heart's properties vary with time and are not held at a constant static rate. Bolooki stated this critical point: "variations in factors such as impedance, diastolic properties of the ventricle, and heart rate may significantly influence the interpretations of data" (1998, 30). If this data is to be considered a true representation of IABP efficacy, then this dynamic state must not only be quantified but must also be incorporated into the analysis via substitution of the data into the linear equations extracted from Excel graphs.

4.5.1 Methodology

In the clinical field, it is well understood that there exists an inverse relationship between heart rate and pressure. This relationship is explained in the textbook written by Susan Quaal and is summarized as follows: "Intraaortic balloon inflation elevates diastolic

pressure, which stretches the baroreceptors. Heart rate is therefore lowered and systemic vascular resistance decreases with IAB inflation due to the baroreceptor response" (1993, 110). Basically, balloon inflation in diastole displaces stroke volume directly toward aortic baroreceptors. These baroreceptors then send a message to inhibit peripheral vasoconstrictor activity, thereby, decreasing peripheral resistance and improving blood flow.

As heart rate increases, the duration of balloon inflation decreases. Thus, it is critical to incorporate the change in systolic and diastolic time intervals as well as the change in mean aortic pressure associated with increased heart rate.

4.5.2 Method and Results

To demonstrate and quantify these relationships, graphs were generated which represent hemodynamic indices while the IABP is in the "standby" state. The "standby" state is recorded following implementation of each time setting when the IABP was turned off for a specific time interval. Thus, two graphs were generated as follows: 1) Mean aortic pressure (mmHg) versus Systolic & Diastolic Aortic Pressure (mmHg) and 2) Heart Rate (BPM) versus Systolic & Diastolic Interval (msec).

Theoretically, mean aortic pressure is the time-average of systolic aortic pressure and diastolic aortic pressure. Therefore, if the total pressure increases with time, it is expected that this increase is a result of an increase in a portion of the mean pressure, either systolic, diastolic, or both. This was indeed the case as evident in the first graph titled "Effect of Mean AoP on Systolic & Diastolic AoP" included in Appendix B. The equations that represent this relationship are incorporated as a correction factor by

substitution of systolic or diastolic aortic pressure into the x-value of the equations on that graph. Thus, the standby data was adjusted to correspond to the mean pressure and heart rate of each of the four time settings.

As previously indicated in the above subsection, an increase in heart rate decreases the systolic and diastolic time intervals. The graph labeled "Effect of Heart Rate on Systolic & Diastolic Intervals" demonstrates this inverse relationship and is also included in Appendix B. The quantitative relationship of heart rate and time intervals are also incorporated as a correction factor by substitution of systolic or diastolic time intervals into the x-value of the equations on that graph.

4.6 Summary

Data analysis consisted of three main parts: elimination of files containing noise artifact, standardization of the start of systole (RS_{max}) for consistency, and correction for variations in mean aortic pressure and heart rate which take into account the dynamic state of the heart. The goal of applying these methods is to be able to interpret the data in a way that can provide an accurate representation of the hemodynamic state of the heart following IABP therapy using the four timing methods. Barnea et al stated that we must account for such changes in mean aortic pressure and heart rate because the "state of the cardiovascular system may be constantly changing during balloon assistance" as witnessed in the graphs included in Appendix B (1990, 171). Doing so will help answer the following questions:

- Compared to the conventional timing method (T_I), does deflating the IAB at predetermined volumes relative to systole improve efficacy in man?

- What is the optimal point to deflate the IAB relative to systole?

These methods led to data extraction and generation of graphs for all 20 patients, which were compared not only to each other but also to standby data. Thus, results were summarized in one chart representing relevant hemodynamic variables used in the clinical field to indicate IABP efficacy. The following chapter summarizes the results obtained using these methods as well as provides the answers to the two questions above.

CHAPTER 5

LATE DEFLATION TIMING STUDY: HEMODYNAMIC EFFECTS OF IAB TIMING IN HUMANS (DATA ANALYSIS: RESULTS & CONCLUSION)

5.1 Introduction

It is imperative to keep in mind that several variables influence the magnitude and duration of diastolic pressure augmentation with balloon inflation. Cited in the textbook by Quaal is a framework of biological and physical variables published by Weber and Janicki nearly 20 years ago (1993, 114). Physical variables include balloon position within the aorta, volume of shuttle gas entering the balloon, balloon shape and diameter, occlusion of the balloon within the aorta, type of shuttle gas utilized, and timing of inflation. Biological variables include arterial pressure, heart rate, and aortic pressure-volume relation.

Studies have been conducted to maximize efficacy related to each of these variables and while literature exists to propose such methods, the optimization of timing of the IAB is still a controversial issue. It is significant to realize that while the goal of this thesis is to define an optimal timing point to deflate the IAB, the variables above need to be considered as important factors that may influence results of further testing into this matter.

It is the attempt of this chapter to summarize the results of all files analyzed. Prior to providing the final results, each variable will be explained. For clarity and ease of understanding, one patient file will be chosen and used as an example throughout the course of this chapter.

5.2 Correction for Deflation Timing Errors

Although the protocol devised by Datascope Corporation outlined the method for deflation of the IAB at different points relative to systole, it was possible that a discrepancy existed between the measured values and the theoretical values sought after due to technical error. To test this hypothesis and to also determine the timing point at which deflation actually occurred relative to systole, graphs were generated for each patient, which plotted the % of deflation time versus pressure efficacy (either DPTI/SPTI or SPTI). These graphs are included as part of Appendix C.

Evaluation of these graphs led to the optimal timing point for late deflation of the IAB. In most patients, pressure efficacy seemed to occur with late deflation between T_2 and T_3, particularly, 50% of the volume was evacuated prior to the initiation of systole. Therefore, deflation of the balloon at 50% of the volume prior to systole was chosen as the timing method that will be compared against conventional timing, T_1. The results are outlined in the following section and are included as part of Appendix C.

5.3 Discussion

5.3.1 Variables Utilized in the Clinical Field as Indications of IABP Efficacy

In Chapter 3, difficulties associated with determining the effectiveness of the intra-aortic balloon pump in providing mechanical assistance to the failing heart was discussed. Because no one can agree on which performance index provides the best clinical indication of hemodynamic efficacy of IABP support, the results of this study are presented using several hemodynamic variables that encompass the wide range of variables cited in the literature. Each variable is explained below serving as an

introduction to the next subsection, which is a discussion of the results. The term "corrected" refers to the implementation of all the correction factors mentioned in Chapter 4.

- SPTI or TTI (corrected) = This variable, systolic pressure-time index, is directly related to myocardial oxygen demands. SPTI is expected to decrease with IABP due to a decrease in systolic blood pressure.
- DPTI (corrected) = DPTI, diastolic pressure-time index, describes pressure-time events during diastole and can be used to estimate diastolic subendocardial blood flow (Bolooki, 1998, 103; Quaal, 1993, 101). It is directly related to myocardial oxygen supply and is expected to increase with intra-aortic balloon counterpulsation due to an increase in diastolic blood pressure.
- DPTI/SPTI (corrected) = This ratio, also known as an endocardial viability ratio, is a useful indicator of oxygen supply and demand. An endocardial viability ratio (EVR) of 1.0 signifies a normal supply/demand balance. In order for this ratio to be utilized as a determinant of increased blood flow with balloon support, a period of "EVR without balloon support may assist in determining prognosis" (cited in Quaal, 103). Therefore, this variable will be compared with standby data.
- [SPTI] + CO = The benefits of IABP include 1) decreasing the amount of work required by the left ventricle to eject blood resulting in 2) an increase in cardiac output. Each patient is different and therefore, the benefits associated with IABC vary. Because there is no way to control the percentage associated with each of these variables, the addition of the two will provide a clearer indication of IABC efficacy.
- Mean HR = Heart rate reflects the status of cardiac performance.

- Mean AoP = The clinician often wants to increase the mean aortic pressure to increase systemic perfusion.
- SVR = Systemic Vascular Resistance offers information regarding resistance to ventricular ejection. As systemic vascular resistance decreases, cardiac output is expected to increase.
- CO = Cardiac output decreases due to left ventricular failure and is expected to increase with IABP support. Freedman states that the increase associated with IABC is minimal ranging between 0.5 and 1.0 liters per minute and is a reminder that "the balloon pump best functions as an assisting circulatory support device" (Quaal, 1993, 101).

5.3.2 Results

In Section 5.2, it was noted that technical error could have occurred during the timing of the IAB. This hypothesis was tested by graphing deflation time relative to systole versus pressure efficacy. Results showed that 2 of the 20 patients' files contained mis-timed inflation points. That is, inflation of the IAB at a later time period caused outliers in the data and thus, were eliminated from the final analysis. Patient files B3 and B6 demonstrated a late inflation time of approximately 120 milliseconds. These files also did not contain information on cardiac output that was not available during the previous analysis (e.g. Kern et al's). Therefore, the data could not be accurately compared to data obtained in this study.

The results of the 18 files are summarized in a graph attached in Appendix C providing a comparison of hemodynamic indices between conventional timing (e.g. 0%

deflation) and late deflation (e.g. 50% of the volume of the IAB remaining at the start of systole). Improvement was noted for SPTI, DPTI, DPTI/SPTI, and [SPTI] + CO using the late deflation timing method as compared to conventional timing. No difference was noted in mean heart rate for late deflation but with conventional timing, mean heart rate decreased by 1%, which is considered an insignificant reduction in heart rate. Systemic vascular resistance decreased by 10% using conventional timing as compared to the 4.2% decrease witnessed with late deflation and mean aortic pressure increased by 3.4% with late deflation.

5.4 Conclusion

The results of this analysis indicate that a significant improvement in hemodynamic indices is established by deflation of the IAB at a later time period than conventional timing. If 50% of the volume of the IAB is present at the start of systole, IABP therapy can be optimized. This agrees with Sakamote's analysis which states: "IAB deflation during isovolumic contraction reduces LV end-systolic pressure and significantly optimizes VA coupling and LV efficiency during IABP support, compared with conventional timing" (1995, M580). It also agrees with Quaal's analysis that presystolic deflation lowers impedance to systolic ejection (1993, 96).

The analysis method utilized in this thesis indicated that cardiac workload was reduced with late deflation. As evident in the graph in Appendix C, the index that best represents cardiac workload, SPTI, was reduced at 50% deflation as compared to conventional timing. Yet, cardiac workload is represented by different variables depending on the preference of the investigators. Therefore, if SPTI is considered as a

valid representation, then late deflation shows a positive effect but if mean aortic pressure is considered, late deflation demonstrates a negative effect. The paragraph that follows demonstrates the use of mean aortic pressure as the cardiac workload index.

Late deflation does have a negative effect on systolic and diastolic pressures combined (mean aortic pressure) and thus, increases the afterload. Barnea et al accounted for this observation during their study. In an attempt to determine IABP efficacy by deviating from conventional timing, they concluded that there exists a "tradeoff between timing for minimal workload on the heart and timing to maximize quantities related to coronary supply. As deflation was started later in diastole, coronary perfusion was enhanced but at the expense of increased cardiac workload" (1970, 171). Despite the increase in workload, they concluded that optimal deflation time occurred when balloon volume was "decreased to approximately half of its fully inflated volume prior to end-diastole and deflation continued into next systole" (174).

It should be noted that this research is based on a limited number of patients and further study involving a larger population is recommended.

APPENDIX A

SELECTION CRITERIA FOR PATIENTS UNDERGOING LATE DEFLATION STUDY

In this appendix, the test protocol utilized to obtain the data relevant to both this study and Kern et al's study is presented. This information was extracted from a test protocol written by employees of Datascope Corporation, Fairfield, NJ.

A.1 Investigational Sites and Prinicipal Investigators

The IAB Timing Study that has been utilized by Kern et al (Prinicipal Investigators) and in this late deflation study was conducted at four clinical centers. The study was sponsored by Datascope Corporation and conducted under an Investigational Device Exemption.

1. St. Louis University, St. Louis, Mo., Prinicipal Investigator: Dr. M.J. Kern
2. Methodist Hospital, San Antonia, Tx., Prinicipal Investigator: Dr. R. Schnitzler
3. Alleghany Hospital, Pittsburgh, PA., Prinicipal Investigator: Dr. D. Lasorda
4. Duke University Medical Center, Durham, NC., Principal Investigator: Dr. E.M. Ohman

A.2 Patient Selection

Patients selected in Kern et al's study were based on the criteria listed in the preceding sections. The following sections, therefore, not only apply to the study conducted by that group but also pertain to this study since the data collected was reanalyzed for the purpose of this thesis. Because analysis of data encompasses a great deal of time that

was not available for the scope of this study, reduction of the amount of patient files analyzed was necessary.

A.2.1 Patient Recruitment and Inclusion/Exclusion Criteria

A maximum of 43 patients undergoing IABP therapy was recruited from the four clinical centers listed above. Investigators and a physician were at the bedside to assure those patients' hemodynamics did not become unstable during the period of this study. For the purposes of this study, hemodynamic instability is defined as either a change in heart rate of greater than or equal to 10 beats per minute (BPM) or a change in mean aortic blood pressure of greater than or equal to 10 millimeters of mercury (mmHg). Those patients that demonstrated hemodynamic instability throughout the course of the study were removed from further participation and treated accordingly.

One hour prior to the start of the protocol, the following requirements were established:

1. no change in the intravenous infusion rate of inotropic drugs (drugs utilized to increase cardiac contractility that can affect heart rate and ventricular stroke volume)
2. no change in vasodilator drugs (drugs utilized to reduce systemic vascular resistance that can affect end diastolic volume, blood pressure, and heart rate)
3. no change in the requirement for volume loading

A.2.2 Patient Profile

According to the patient information collected by Kern et al (reference Kern's article), diagnosis of patients requiring mechanical assistance (IABP support) include acute

myocardial infarction, coronary artery disease, and unstable angina. Their mean age is 59±11 years with a mean height of 68±5 inches and mean weight of 182±35 pounds.

A.2.3 Informed Consents and Patient Confidentiality

The purpose of the IABP Timing Study as well as potential risks associated with it was explained to each participant. Participation was on a voluntary basis and therefore, informed consent was obtained from each patient before enrollment into this study. In order for participants to undergo testing in this study, participants must meet all of the following criteria (i.e. clinician must check off "Yes" for all questions on the Informed Consent Sheet):

1. The patient must possess the ability to provide informed consent. This means that the patient must be aware and understand the extent of the study as well as agree to volunteer despite possible risks.
2. All patients enrolled in this study will have passed clinical criteria of needing mechanical assistance. The IAB utilized for each patient must be Datascope Percor Stat-DL 9.5 Fr. 40cc to eliminate variation in test results due to the difference in variables associated with the IAB (e.g. volume, diameter).
3. The patients' ages ranged from 18 years of age to 85 years of age.
4. The intra-aortic balloon pump was programmed to provide assistance to the patient on a 1:1 frequency (heart beat frequency: device beat frequency).
5. During each heartbeat, systolic time interval accounts for approximately one-third of the cardiac cycle while the remainder is ventricular relaxation (diastolic time interval) (Bolooki, 1998, 28). During IABP support, this allows for sufficient time for the

balloon to fill during diastole and rapid deflation during systole. "With an increase in heart rate or atrial pacing (>120/minute), the diastolic filling time decreases to an extent that preload (PCWP) becomes pressure dependent to achieve rapid (and sufficient) ventricular filling to maintain stroke volume" (Bolooki, 1998, 28). Thus, to achieve adequate balloon inflation, it is required that the heart rate of each patient is less than 120 beats per minute.

6. Mean blood pressure for each participant must be greater than 60 mmHg (i.e. patient must not be hypotensive). Patients in this category have severe LV failure, which may occur simultaneously with the onset of AMI. If proper treatment is not provided, the survival rate may be as low as 10% (Bolooki, 34). IABP support is required to reduce mechanical afterload in addition to intravenous treatment.
7. Cardiac index must be greater than 2.0 liters/min/m^2. Patients with a lower cardiac index may develop acute pulmonary edema, or may fall into the group of hospital survival approaching 50%. They may not respond to large dosages of medication or infusion and, as a result, experience a steep rise in ventricular end-diastolic pressure.
8. Limb ischemia is the most frequent early complication of IABP assistance and can be attributed to balloon catheter/femoral artery mismatch, method of insertion, preexisting peripheral vascular disease, claudication, female gender, diabetes, hypertension, urgency of balloon catheter insertion, and duration of IABP assist (Bolooki, references indicated on page 220). Therefore, the most effective way in recognition of ischemia is to check the limb (IAB insertion site) for the presence of a peripheral pulse.

Patient confidentiality was maintained by assigning individual ID numbers that will specify the patient and the site. The letters A-D designate the four clinical centers specified in section 3.1. The sponsor, Datascope Corporation, was given access to the research data but patient-related information was kept in a confidential portfolio at the designated site of IABP support. The same holds true for data presented in this study. Included in Appendix B is data represented with ID numbers and will not include personal patient profiles.

A.3 Equipment and software

A.3.1 Equipment

The IAB catheter (Datascope Percor STAT-DL 9.5 40 cc) was connected to a Datascope System 95 IABP console and interfaced with a digital tape recorder (TEAC RD-111T PCM recorder) for simultaneous recording of the ECG, aortic blood pressure, IAB pressure waveform and timing signals. Patient ECG and aortic blood pressure were monitored via the central lumen of the catheter and input into the IABP console.

Data was recorded at the four pre-determined timing points as well as at the pump-off condition (i.e. "standby"). The pump-off condition is considered a baseline whereby results of the deflation timing points, particularly, hemodynamic data representing efficiency, can be compared.

A.3.2 Software utilized for Data Acquisition

A P.C. data acquisition package, CODAS™, was utilized in this study to record the following signals on the respective channel numbers. Prior to initiation of data

acquisition, the software was calibrated by placing a 1-volt direct current signal at each of the input channels and observing 1-volt at each of the output channels through the CODAS™ software.

Table 2 Signals recorded with CODAS™ software

SIGNAL DESCRIPTION	UNIT OF MEASUREMENT
Electrocardiogram	(Volts)
Aortic Blood Pressure	(mmHg) [1 volt=100 mmHg]
IABP shuttle gas pressure waveform	(Volts)
IABP drive pressure waveform	(Volts)
R wave trigger	(Volts)
Tri-level IABP trainer signal	(Volts)

APPENDIX B

CALCULATED HEMODYNAMIC DATA

B.1 Introduction

Hemodynamic data values were obtained from each cardiac cycle during data reduction (Chapter 4) and were then utilized for further analysis. The subsequent columns are listed as they appear in the Excel spreadsheets. The Excel spreadsheets are numerous in volume and therefore, could not all be included as part of this Appendix. Instead, one file will be included as an example.

Columns A through I pertain to the raw hemodynamic data extracted during data reduction and Columns J through U pertain to the calculated hemodynamic data. The term "assisted" refers to data obtained while the IABP is in the pump-on state while "unassisted" refers to data obtained while the IABP is in the pump-off state. Data is presented in graphical form and is presented for each patient file in this Appendix.

Column A "Timing ID" identifies the IABP timing setting (e.g. standby, T_1, etc.)

Column B "Time (sec)" identifies the time of the R-wave trigger (in seconds) of the analyzed cardiac cycle relative to the beginning of the recorded file.

Column C "HR (BPM)" identifies the calculated heart rate in beats per minute.

Equation: ***HR = 60/R-R***

(R-R is obtained from Column D)

Column D "R-R (sec)" is the measured time interval (in seconds) between R wave triggers for a cardiac cycle obtained from the CODAS files, specifically, the interval between the RS_{max} of one cardiac cycle.

Column E "LVET (sec)" identifies the left ventricular ejection time interval which initiates from the point of RS_{max} to the dicrotic notch.

Column F "DTI (sec)" identifies the diastolic time interval from the dicrotic notch to RS_{max}.

Column G "MSAP (mmHg)" defines the mean systolic aortic pressure which is the area under the curve during the LVET period.

Column H "MDAP (mmHg)" defines the mean diastolic aortic pressure which is the area under the curve during the DTI period.

Column I "MAP (mmHg)" defines the mean aortic pressure which is the area under the curve during the R-R interval.

Column J "SPTI (sec)" defines the systolic pressure time index which is an indication of oxygen demand needed by the heart.

Equation: ***SPTI = MSAP*LVET***

(SPTI is obtained from Column G multiplied by Column E)

Column K "DPTI/SPTI-assisted (sec)" defines the diastolic pressure time index divided by the systolic pressure time index which is an indication of myocardial oxygen supply to oxygen demand ratio.

Equation: ***DPTI/SPTI = (MDAP*DTI)/(MSAP*LVET)***

DPTI/SPTI = (Column H Column F)/(Column G* Column E)*

Column L "% Change (uncorrected)" is the change in the oxygen supply to oxygen demand ratio prior to IABP therapy as compared to the ratio after therapy. The "uncorrected" value is the value obtained prior to the correction made for pressure or heart rate (see above section for details) and is calculated

using the mean value in column K (for each timing setting) as compared to the mean value in column K for "standby".

Equation: ***% Change = ((Mean DPTI/SPTI$_{TC}$ – Mean DPTI/SPTI$_{standby}$)/ DPTI/SPTI$_{standby}$) * 100***

*% Change=((Column K40$_{TC}$ - Column K40$_{standby}$)/ Column K40$_{standby}$) *100*

Columns N-S: Using the "standby" data (baseline), graphs were generated to determine the effect of heart rate and mean aortic pressure on diastolic and systolic intervals. There is a strong correlation between heart rate and mean aortic pressure on these intervals which demonstrate that even with the IABP turned off, these variables are dynamic (i.e. both heart rate and mean aortic pressure change with time). Thus, it is critical to take this into account when analyzing the data. The following columns have been generated based on these graphs with the substitution of the raw hemodynamic data (Columns E-K) into the linear regression equations. Results and discussion of all evaluated files are included in Chapter 4 as well as this Appendix.

Column N "LVET (calc)" is defined as the calculated left ventricular ejection time, which takes into account the effect of heart rate on the systolic interval.

Equation: ***LVET (calc) is found as follows:***

Use linear equation from the graph labeled "Effect of Heart Rate on Systolic & Diastolic Intervals" which represents a plot of heart rate versus systolic interval. For each cell in Excel, substitute each heart rate value from Column C for the x-value in this equation. These calculated

values take into effect the change in systolic time intervals due to a change in heart rate.

Column O "MSAP (calc)" is defined as the calculated mean systolic aortic pressure. The equation explained below demonstrates the relationship between mean aortic pressure and mean systolic pressure.

Equation: ***MSAP (calc) is found as follows:***

Use linear equation from the graph labeled "Effect of Mean AoP on Systolic & Diastolic AoP" which represents a plot of mean aortic pressure versus mean systolic pressure. For each cell in Excel, substitute each mean aortic pressure value from Column I for the x-value in this equation. These calculated values take into effect the relationship between total mean aortic pressure and mean systolic pressure.

Column P "DTI (calc)" is defined as the calculated diastolic mean interval, which takes into account the effect of heart rate on the diastolic time interval.

Equation: ***DTI (calc) is found as follows:***

Use the linear equation from the graph labeled "Effect of Heart Rate on Systolic & Diastolic Intervals" which represents a plot of heart rate versus diastolic time interval. For each cell in Excel, substitute each heart rate value from Column C for the x-value in this equation. These calculated values take into effect the change in diastolic time intervals due to a change in heart rate.

Column Q "MDAP (calc)" is defined as the calculated mean diastolic aortic pressure. The equation explained below demonstrates the relationship between mean aortic pressure and mean diastolic pressure.

Equation: ***MDAP (calc) is found as follows:***

Use linear equation from the graph labeled "Effect of Mean AoP on Systolic & Diastolic AoP" which represents a plot of mean aortic pressure versus mean diastolic pressure. For each cell in Excel, substitute each mean aortic pressure value from Column I for the x-value in this equation. These calculated values take into effect the relationship between total mean aortic pressure and mean diastolic pressure.

Column R "SPTI (calc)" is defined as the calculated mean systolic pressure time index. The equation explained below demonstrates the effect of change in heart rate and change in mean pressure.

Equation: ***SPTI (calc) = LVET (calc) * MSAP (calc)***

*SPTI (calc) = Column O * Column N*

Column S "DPTI/SPTI (calc)" is defined as the calculated index that gives an indication of oxygen supply versus oxygen demand. The equation explained below demonstrates the effect of change in heart rate and change in mean pressure.

Equation: ***DPTI/SPTI (calc) = (MDAP (calc) * DTI (calc)) /(LVET (calc) * MSAP (calc))***

*DPTI/SPTI (calc) = (Column Q * Column P)/(Column O * Column N)*

Column T "Corr. % Change" is defined as the percent change in calculated index that gives an indication of oxygen supply versus oxygen demand, defined as the ratio of DPTI to SPTI. The equation explained below demonstrates the effect of change in heart rate and change in mean pressure.

Equation: ***Corr. % Change (calc) = ((DPTI/SPTI (calc) assisted - DPTI/SPTI (calc) unassisted / DPTI/SPTI (calc) unassisted)*100***

*Corr. % Change (calc) = ((Column K - Column S)/(Column S)) * 100*

Column U "Corr. % Change" is defined as the percent change in the calculated index that gives an indication of oxygen demand, defined as SPTI. The equation explained below demonstrates the effect of change in heart rate and change in mean pressure.

Equation: ***Corr. % Change (calc) = ((SPTI (calc) assisted - SPTI (calc) unassisted / SPTI (calc) unassisted)*100***

*Corr. % Change (calc) = ((Column J - Column R)/(Column R)) * 100*

B.3 Graphical Representation of Hemodynamic Data

The attached graphs were generated using Excel. There are four graphs presented for each patient's file and are titled below. Analysis and discussion are included in Chapter 4. The first three graphs include data acquired when the intra-aortic balloon pump was in the "standby" state and thus, represent patients' hemodynamics prior to IABP support. The fourth graph provides a comparison of pressure efficacy for each of the deflation timing points tested. It also compares the correlation factor associated with the original analysis (generated in the study conducted by Kern et al), uncorrected analysis (analyzed

using Rsmax to define systole, but not corrected for pressure and heart rate), and corrected analysis (correcting the "uncorrected" analysis for pressure and heart rate).

- Effect of Heart Rate on Systolic & Diastolic Intervals
- Effect of Mean Aortic Pressure (MAP) on Systolic & Diastolic Aortic Pressure
- Comparison of Calculated & Actual DPTI/SPTI
- Pressure Efficacy vs. Deflation Timing-Original, Uncorrected, & Corrected

The graphs below indicate the correlation between heart rate and pressure. They are further explained in Chapter 4.

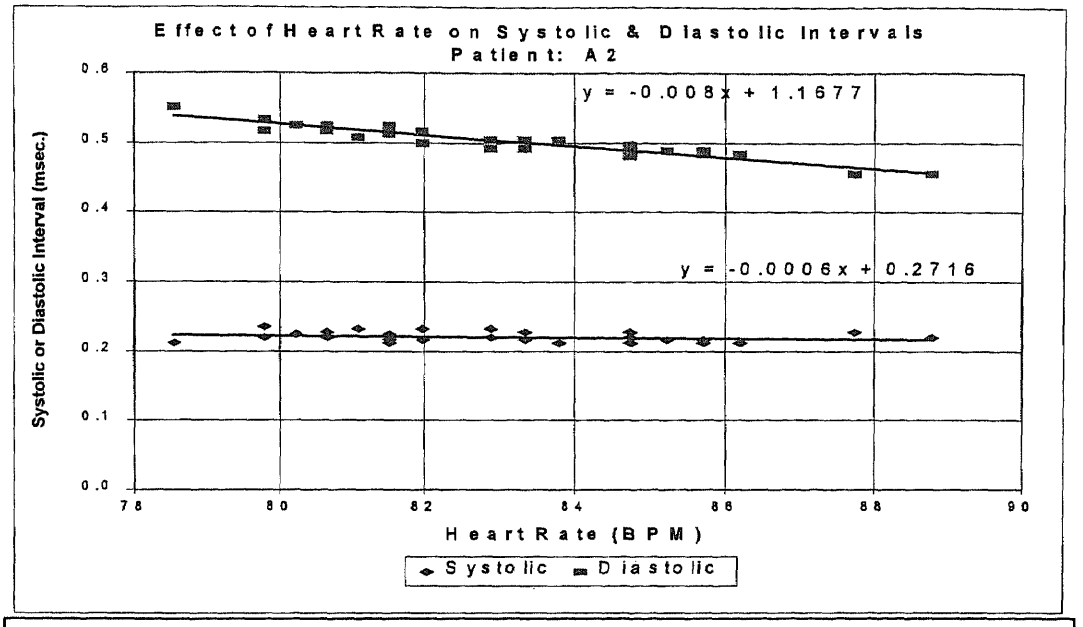

Figure 1B

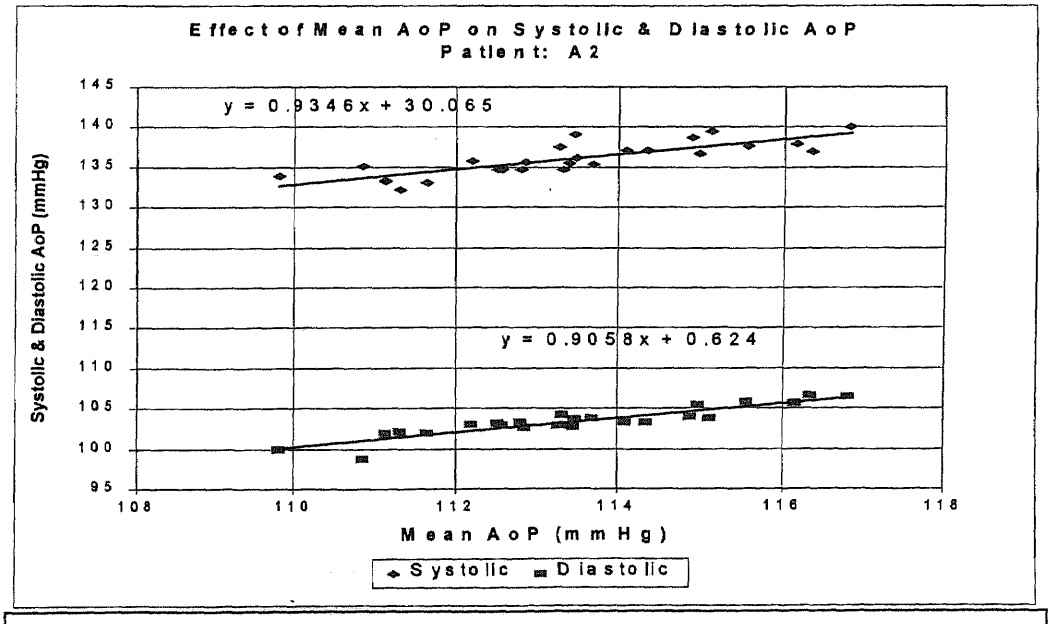

Figure 2B

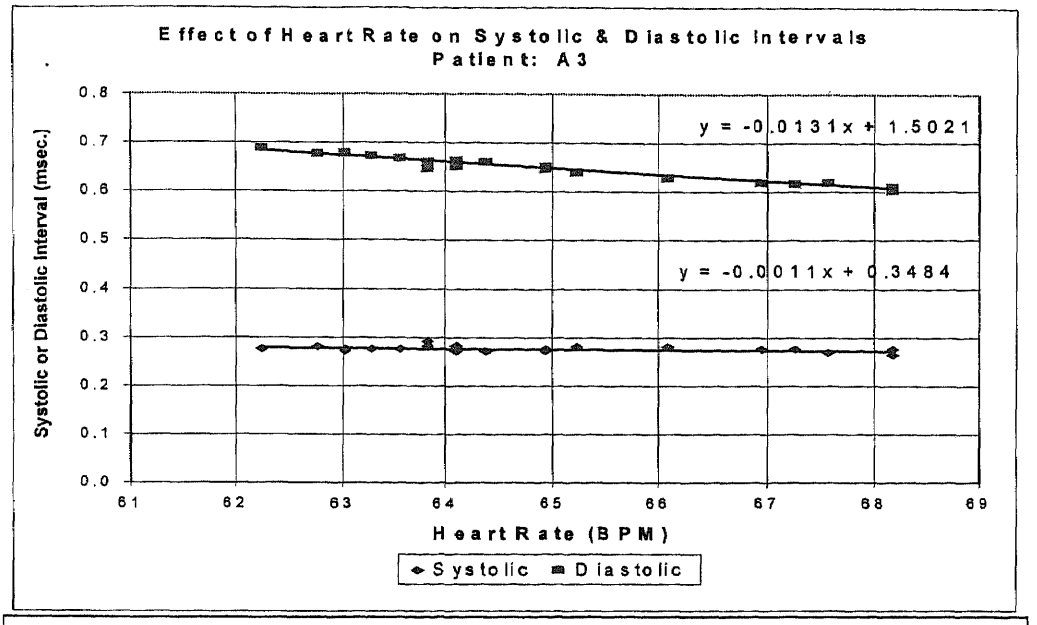

Figure 3B

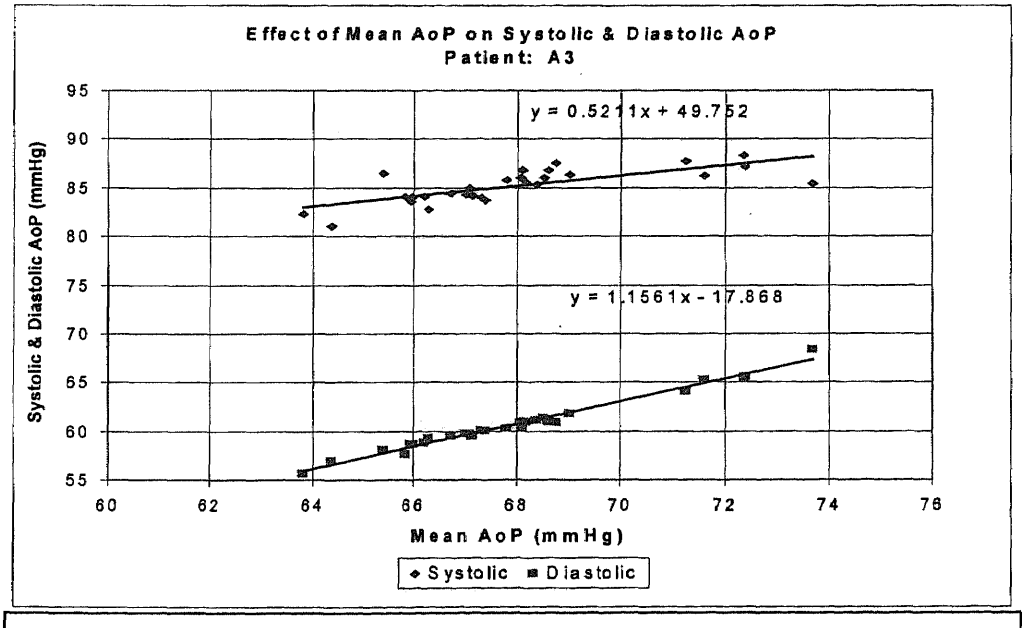

Figure 4B

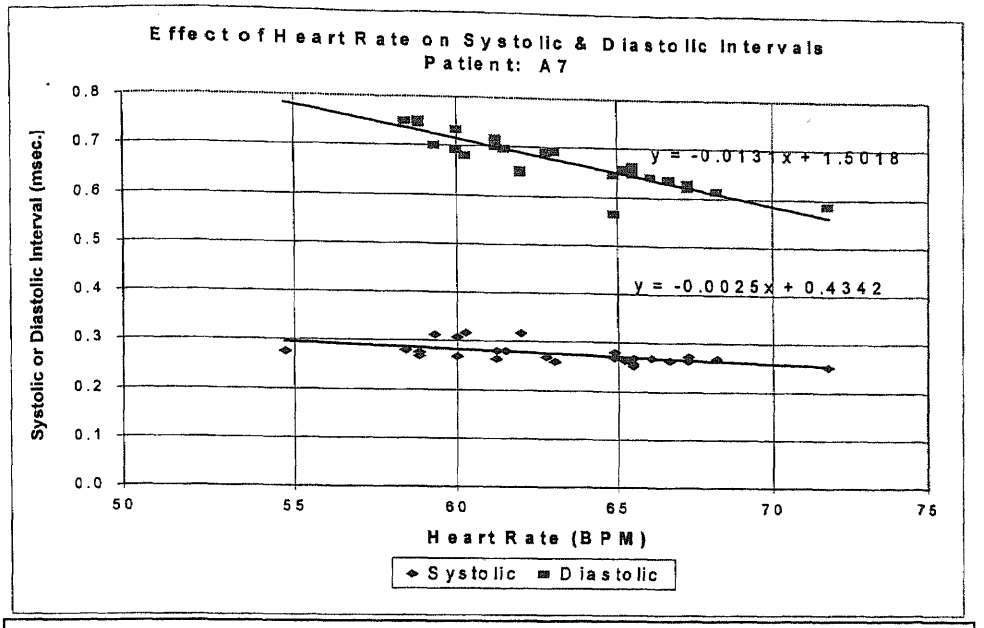

Figure 5B

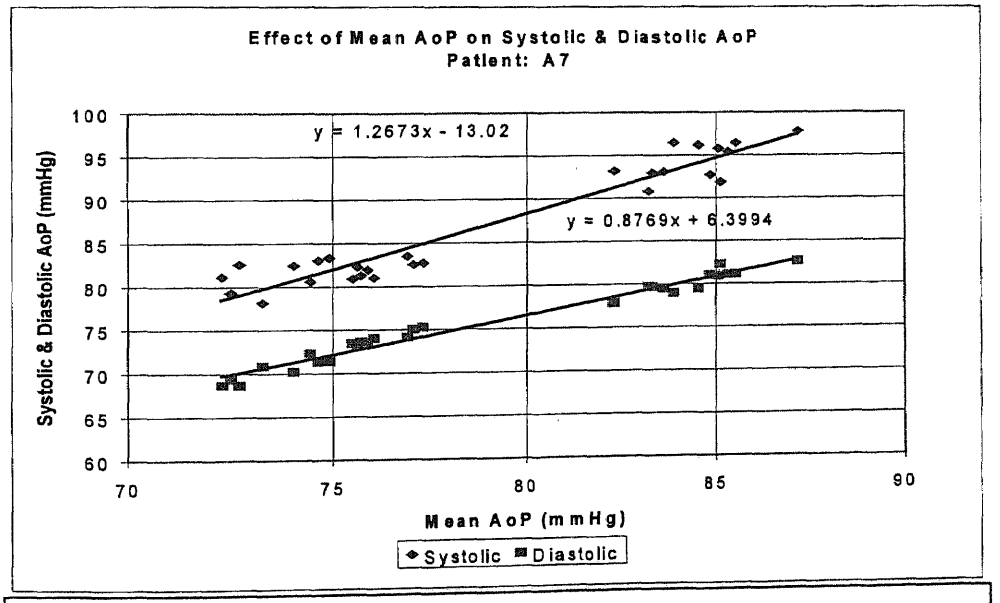

Figure 6B

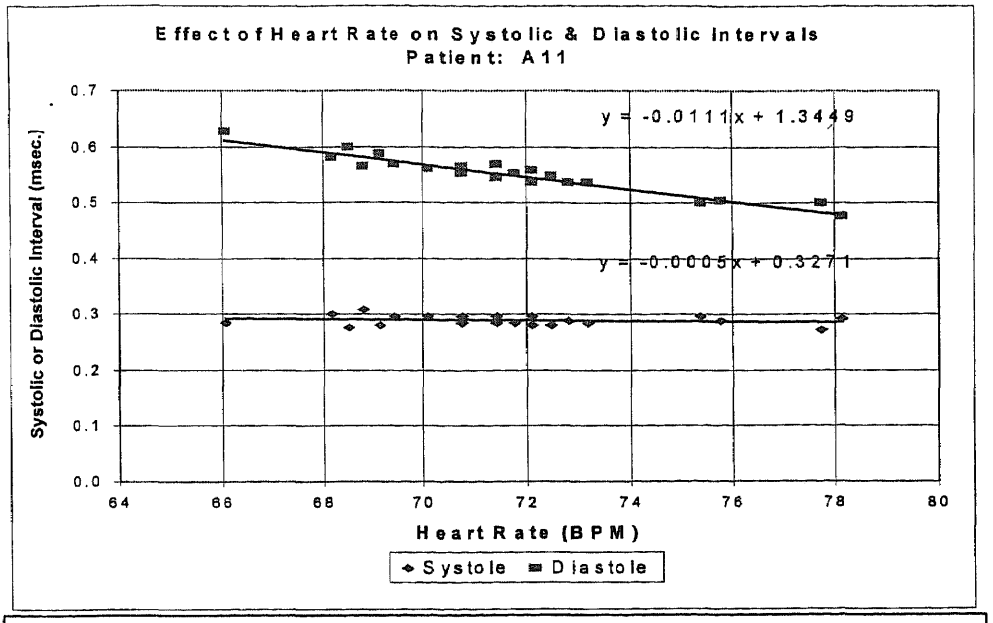

Figure 7B

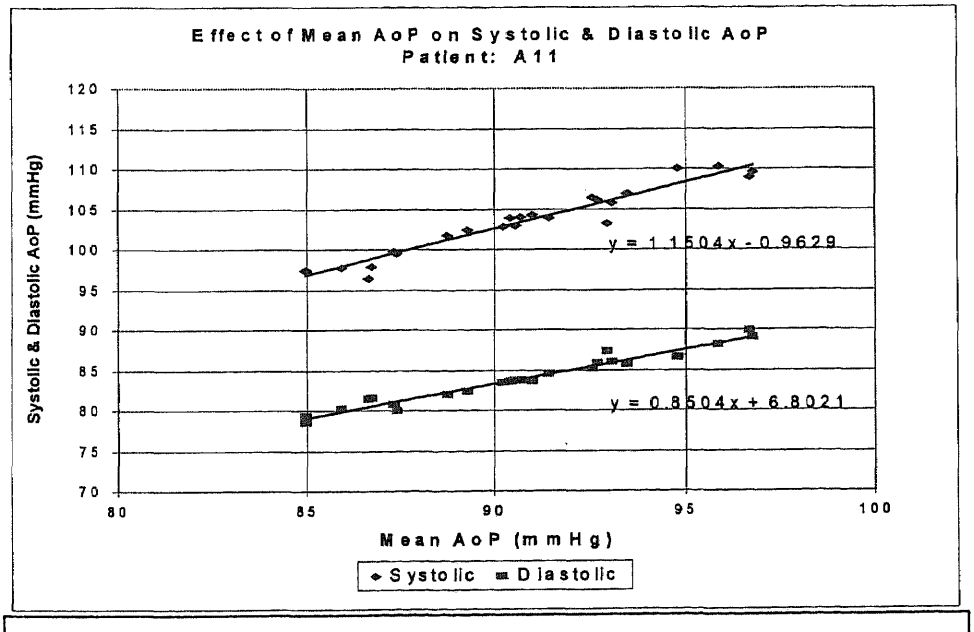

Figure 8B

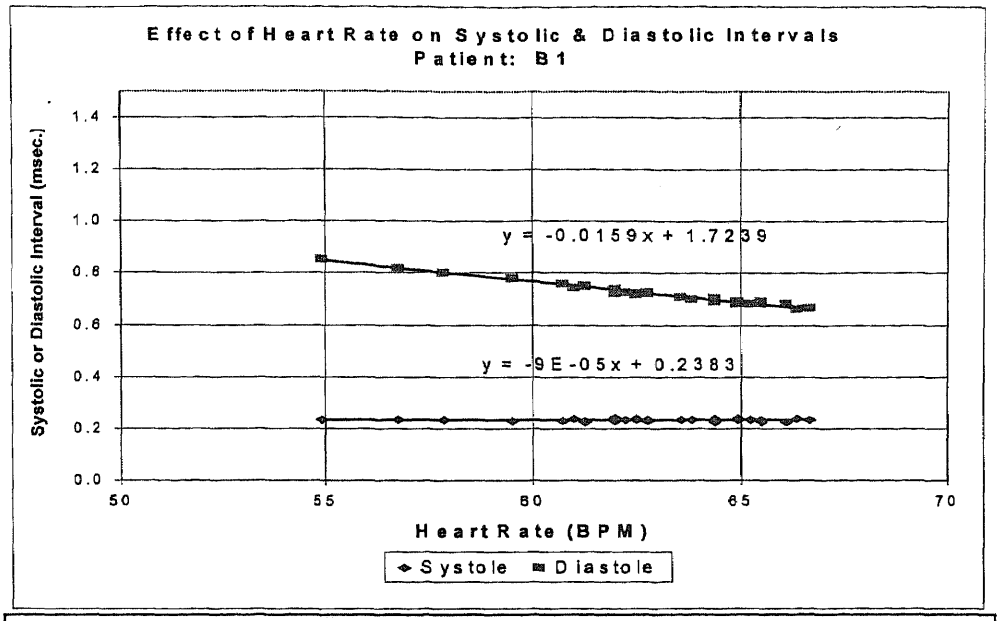

Figure 9B

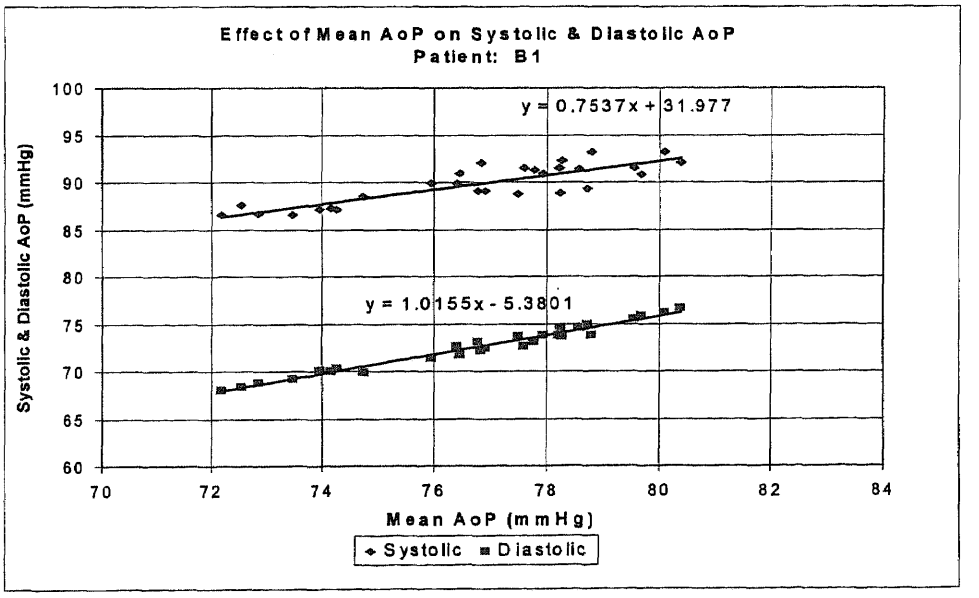

Figure 10B

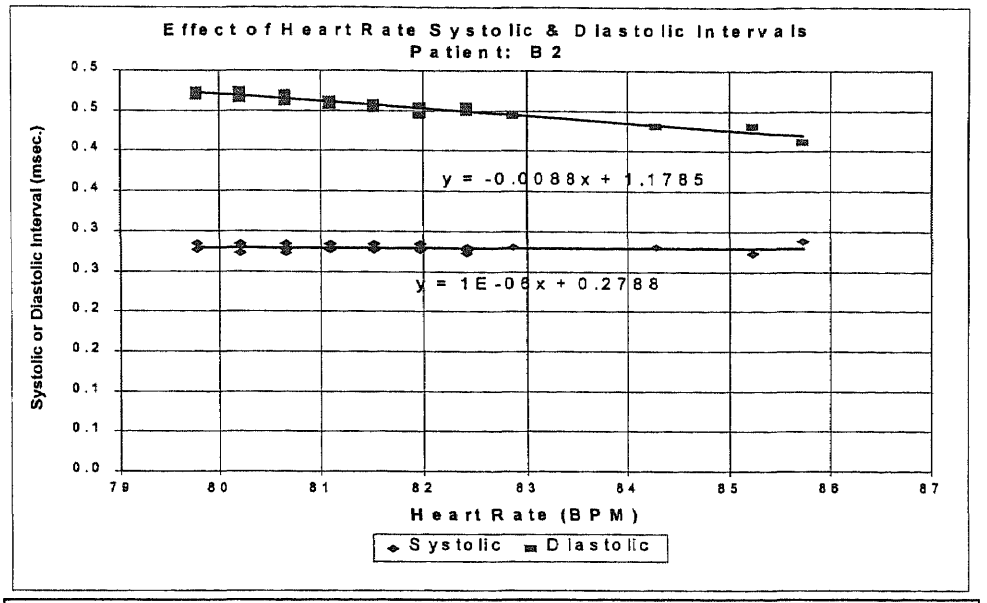

Figure 11B

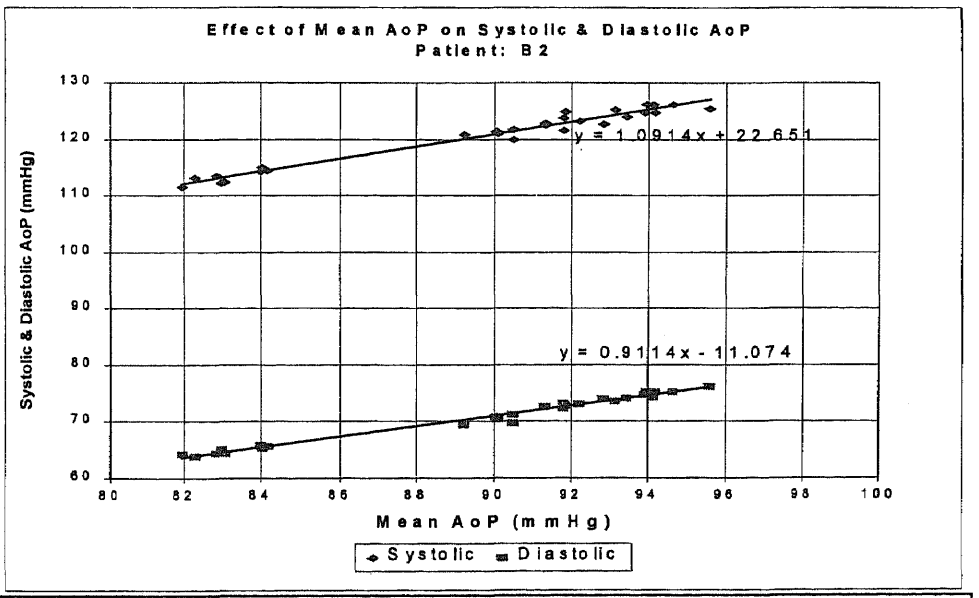

Figure 12B

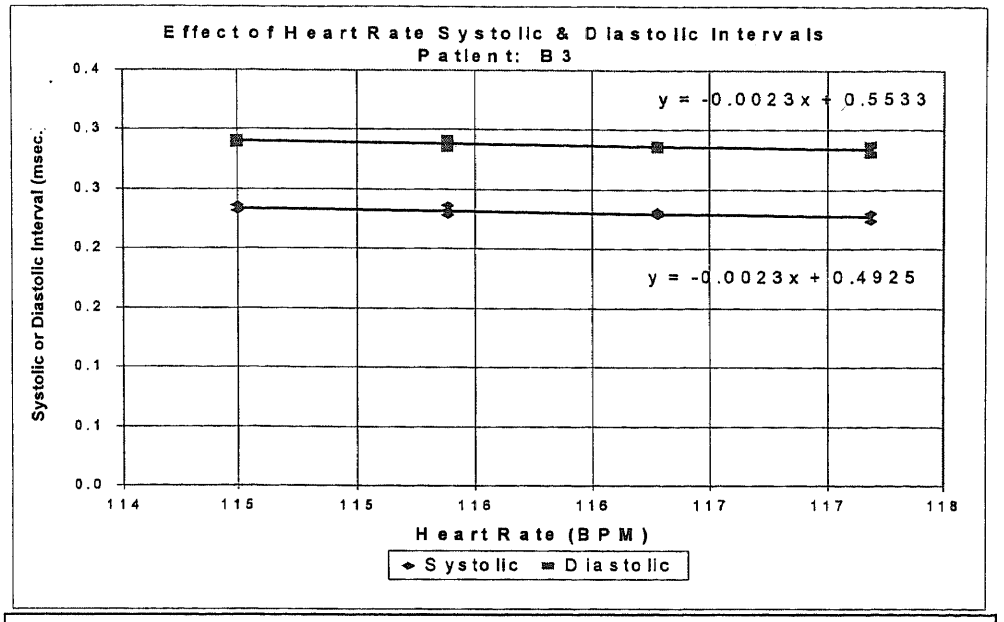

Figure 13B

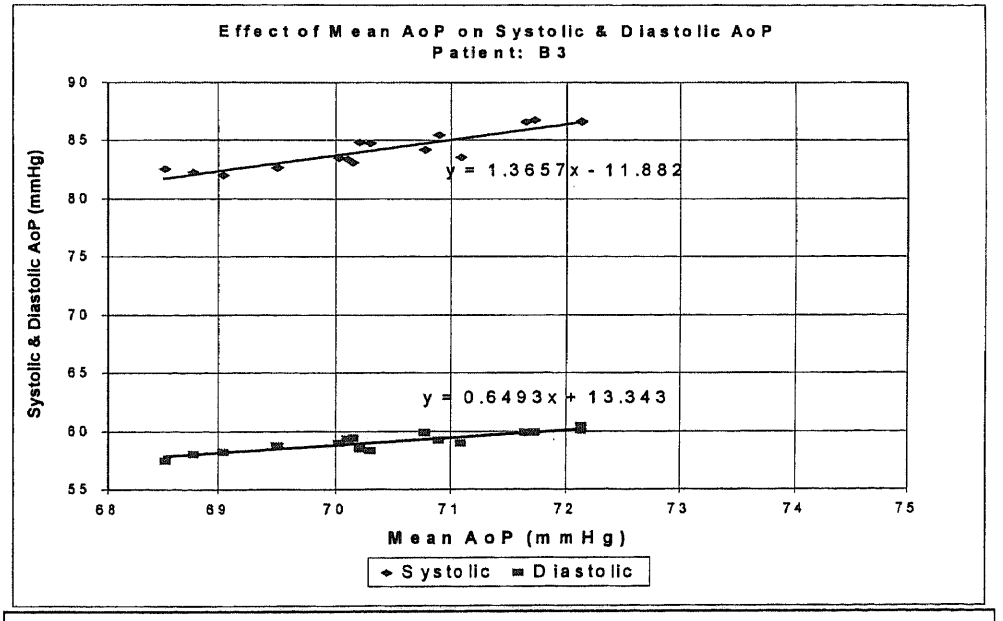

Figure 14B

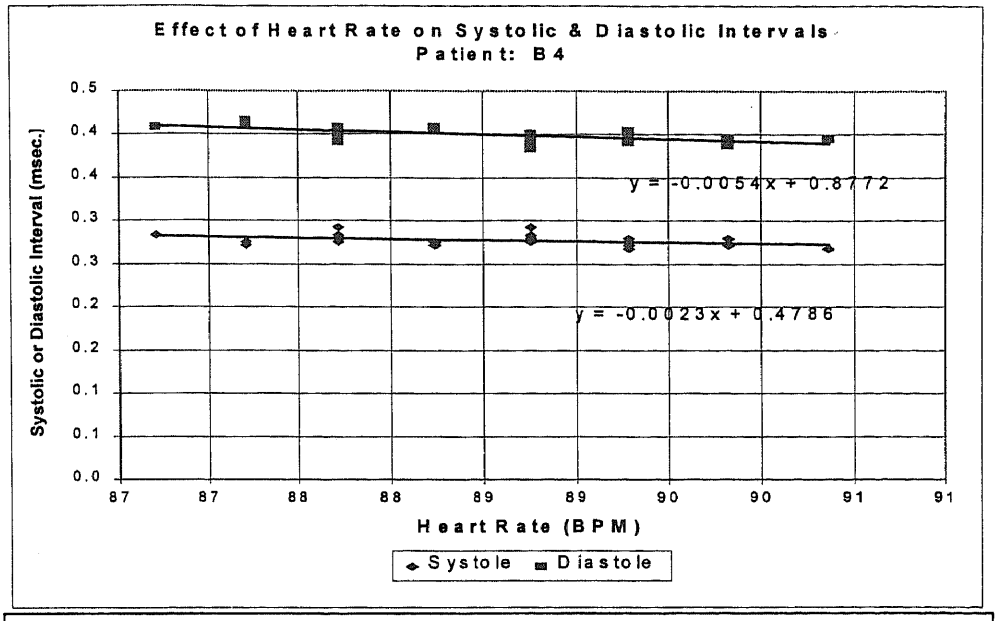

Figure 15B

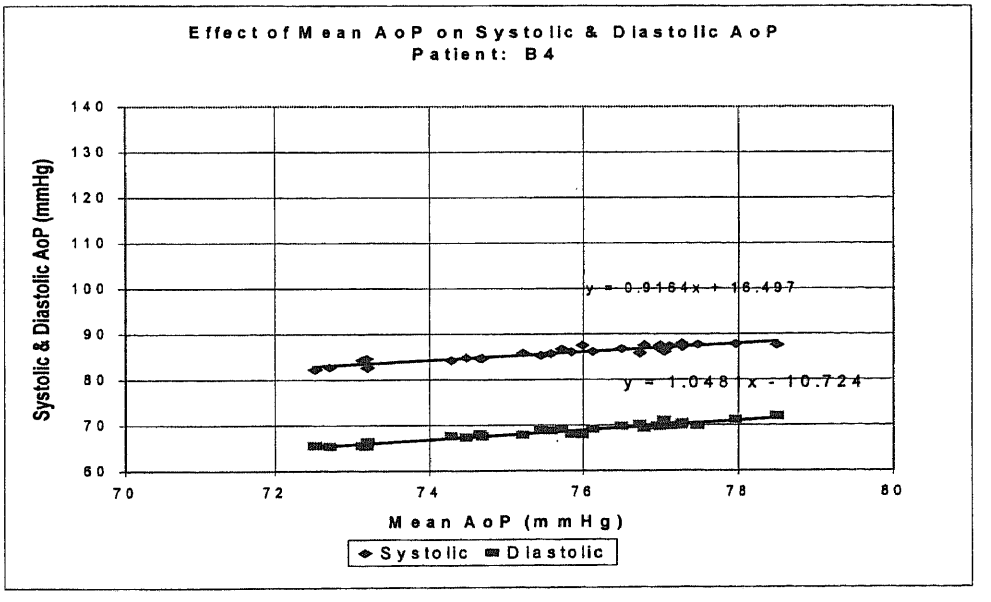

Figure 16B

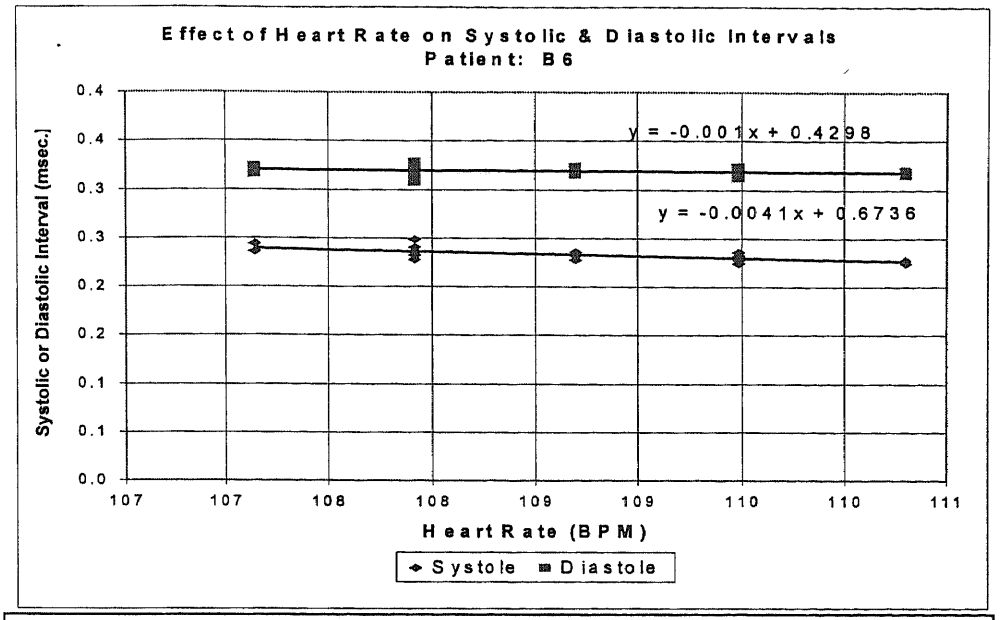

Figure 17B

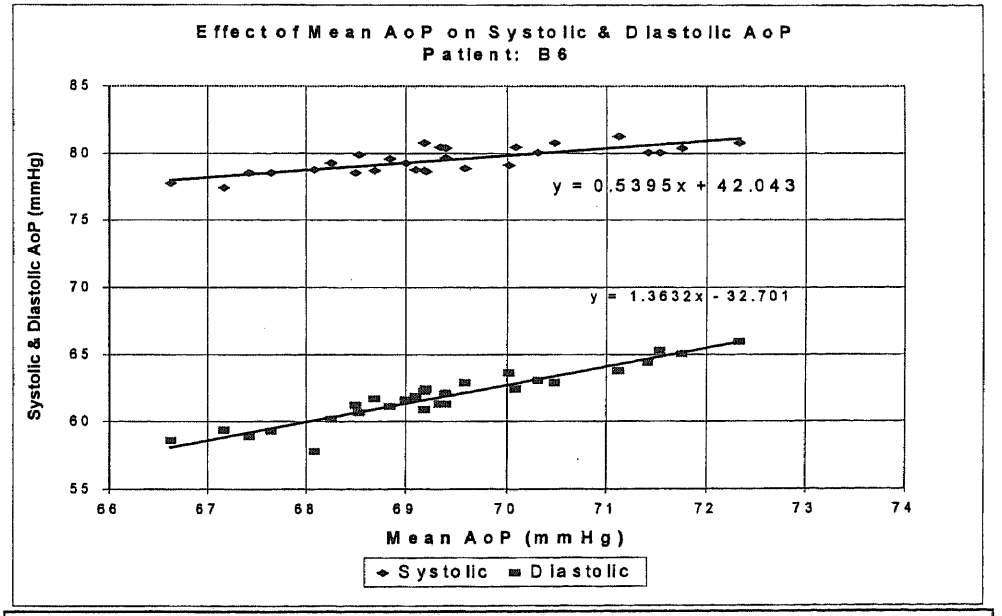

Figure 18B

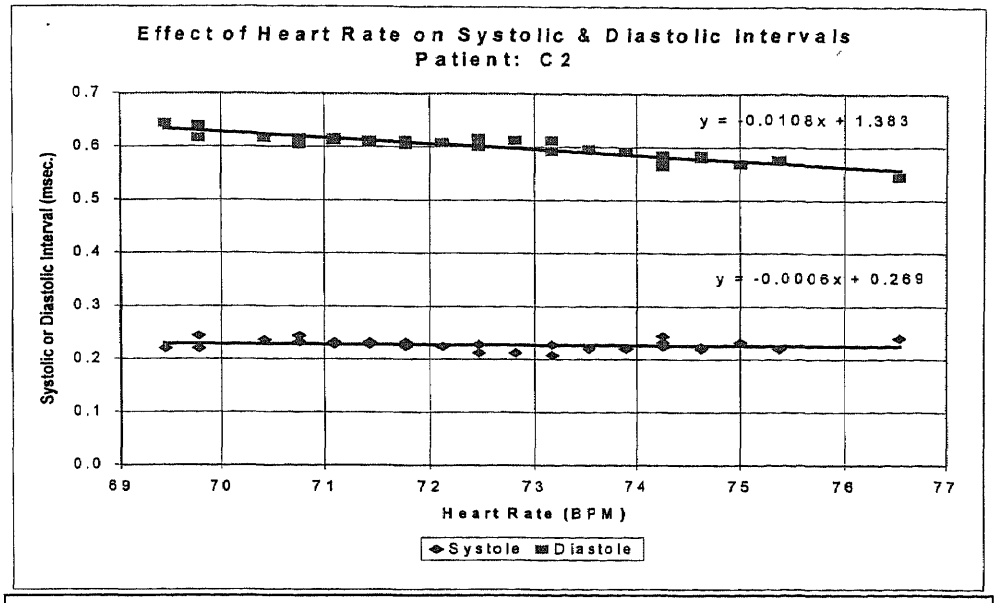

Figure 19B

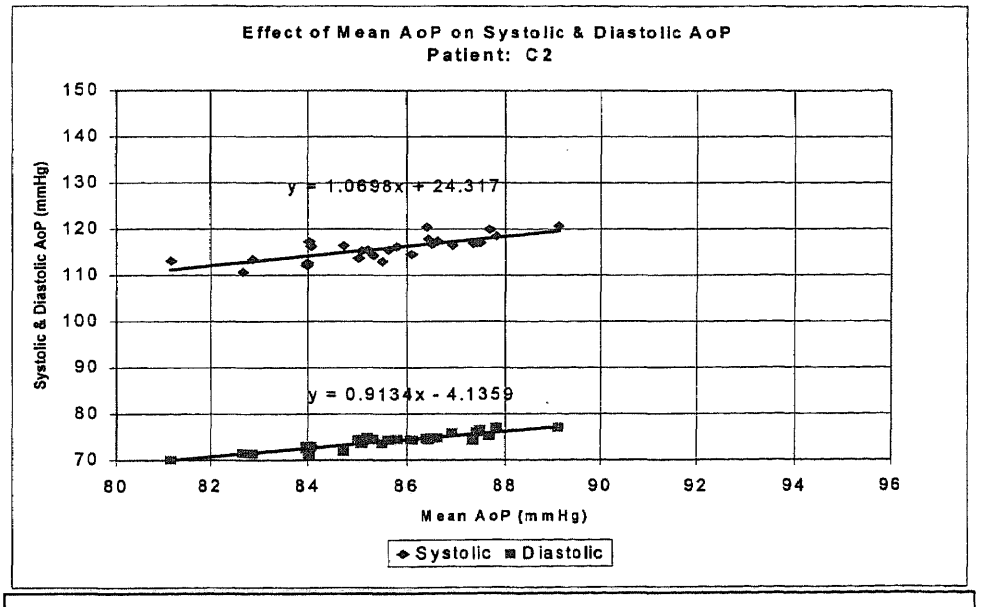

Figure 20B

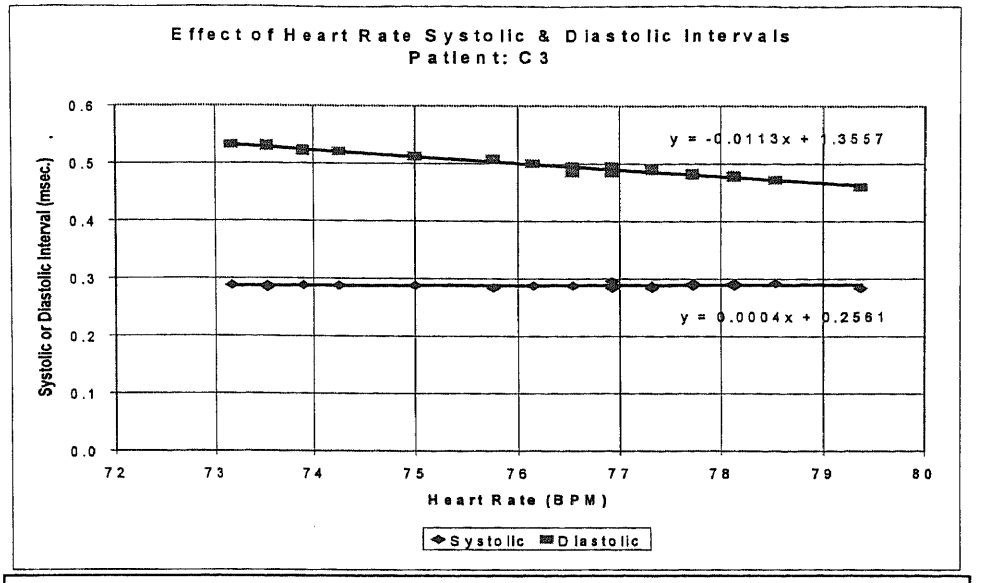

Figure 21B

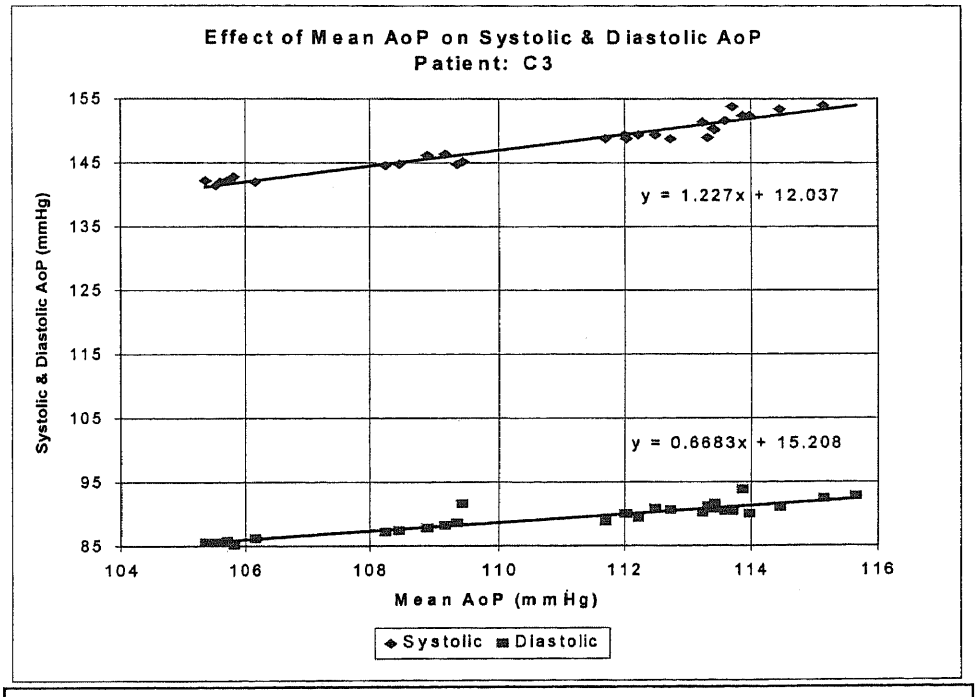

Figure 22B

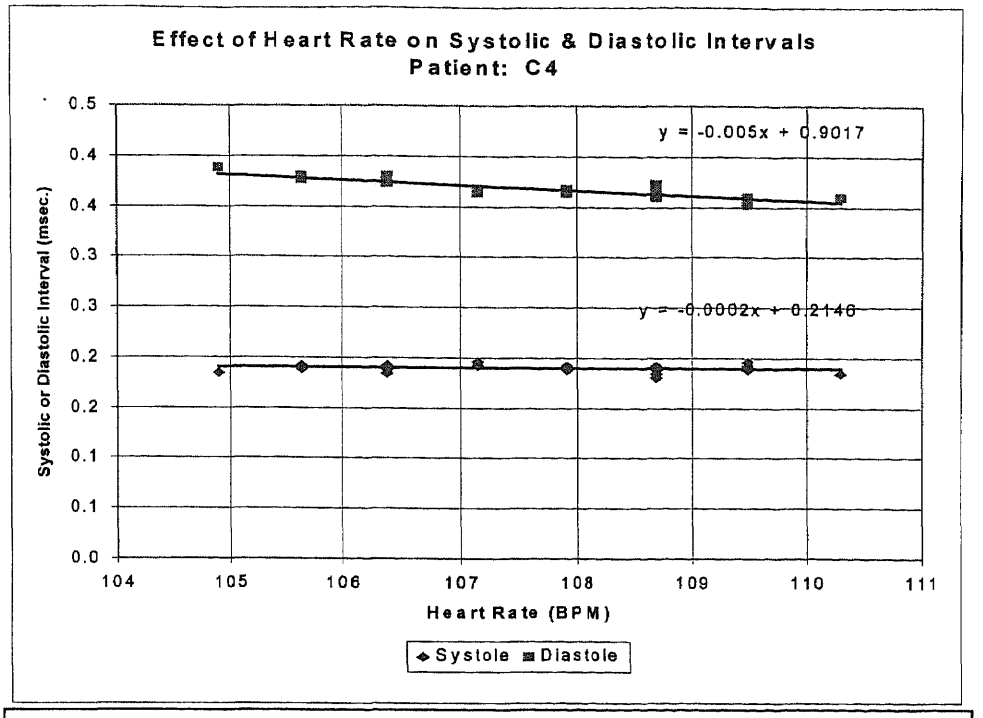

Figure 23B

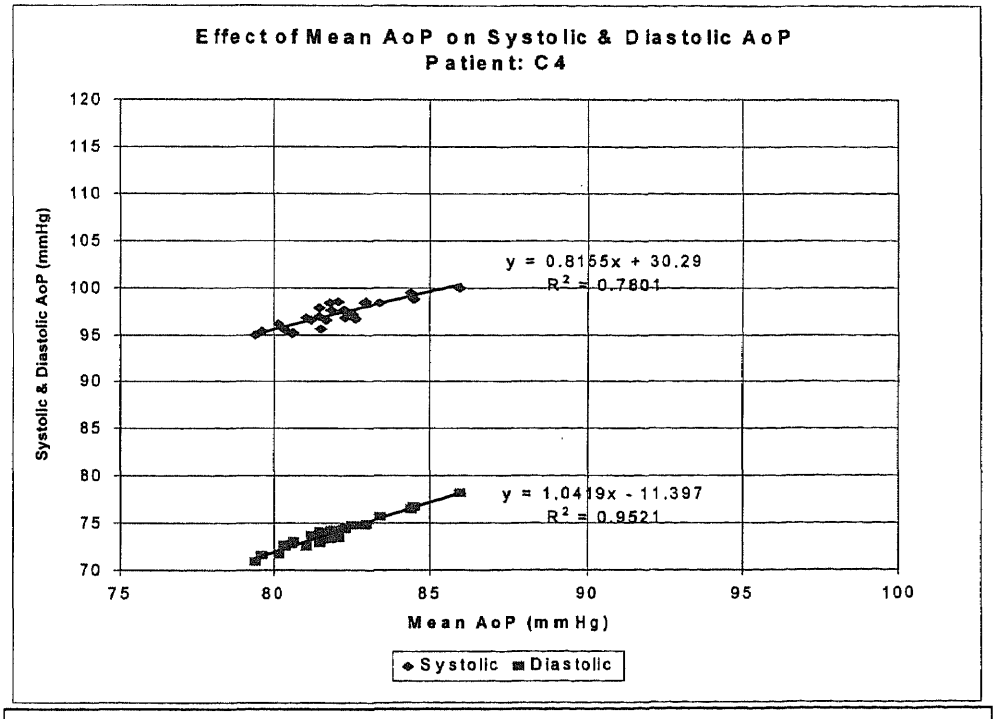

Figure 24B

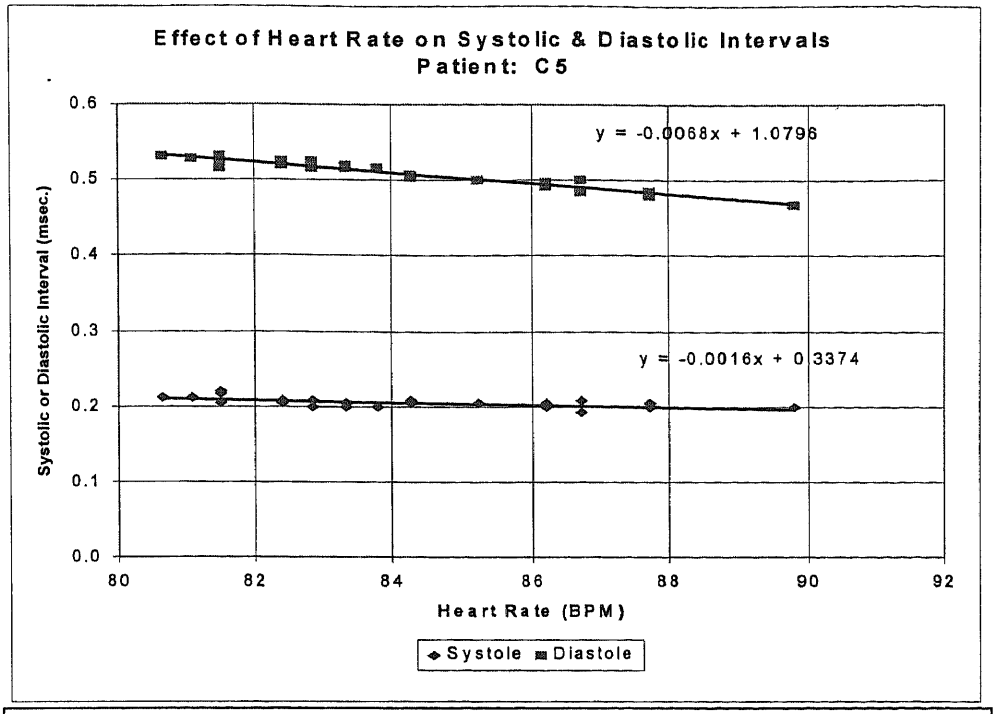

Figure 25B

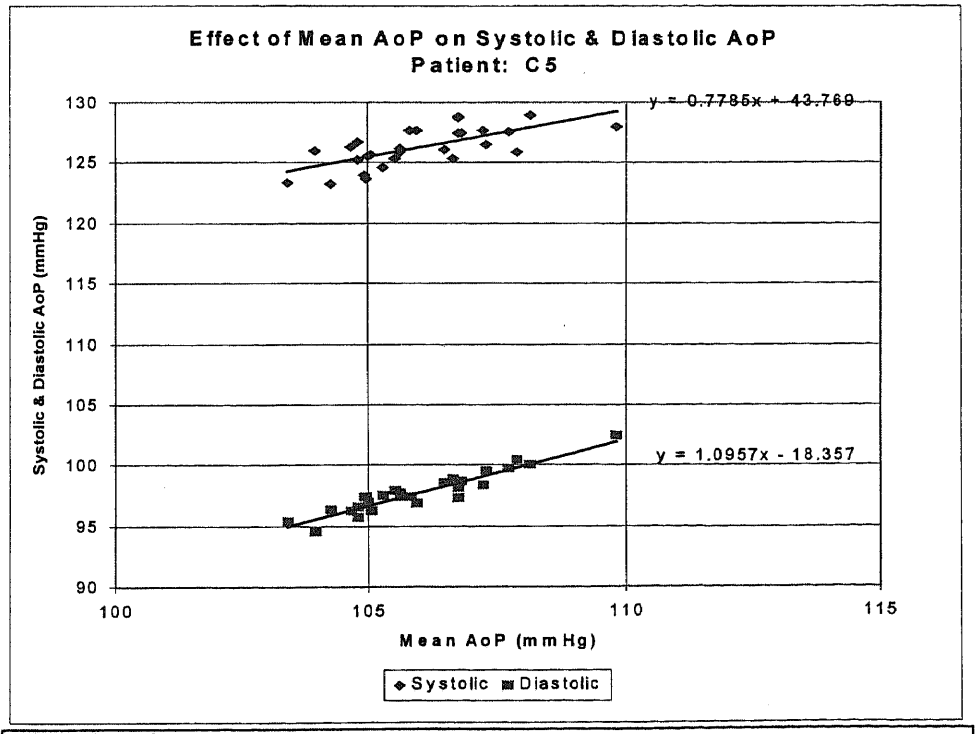

Figure 26B

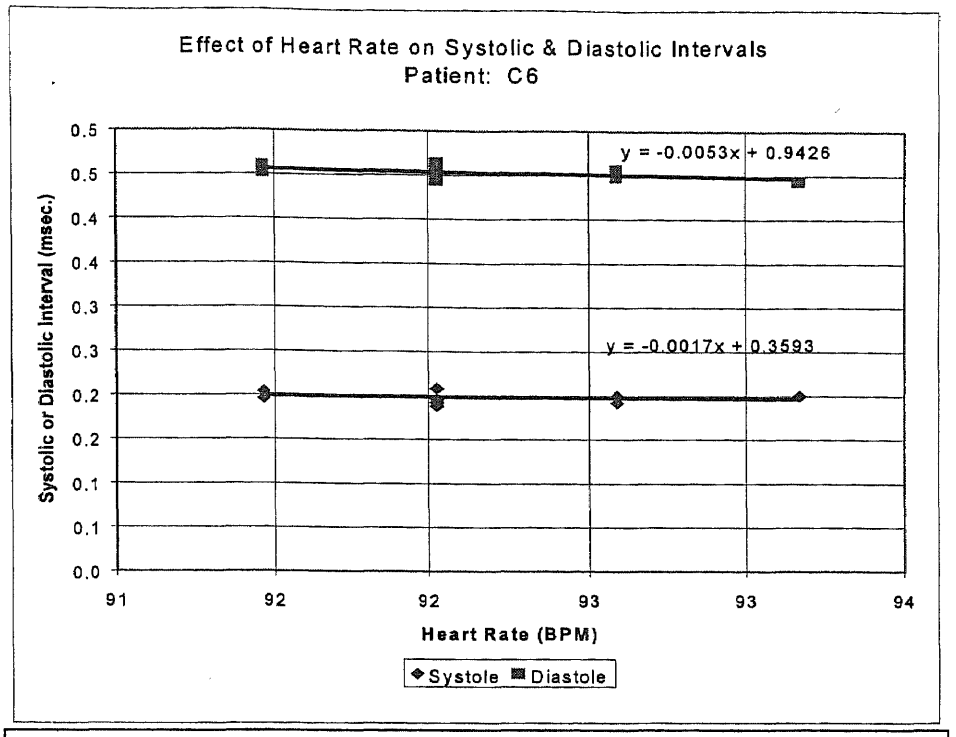

Figure 27B

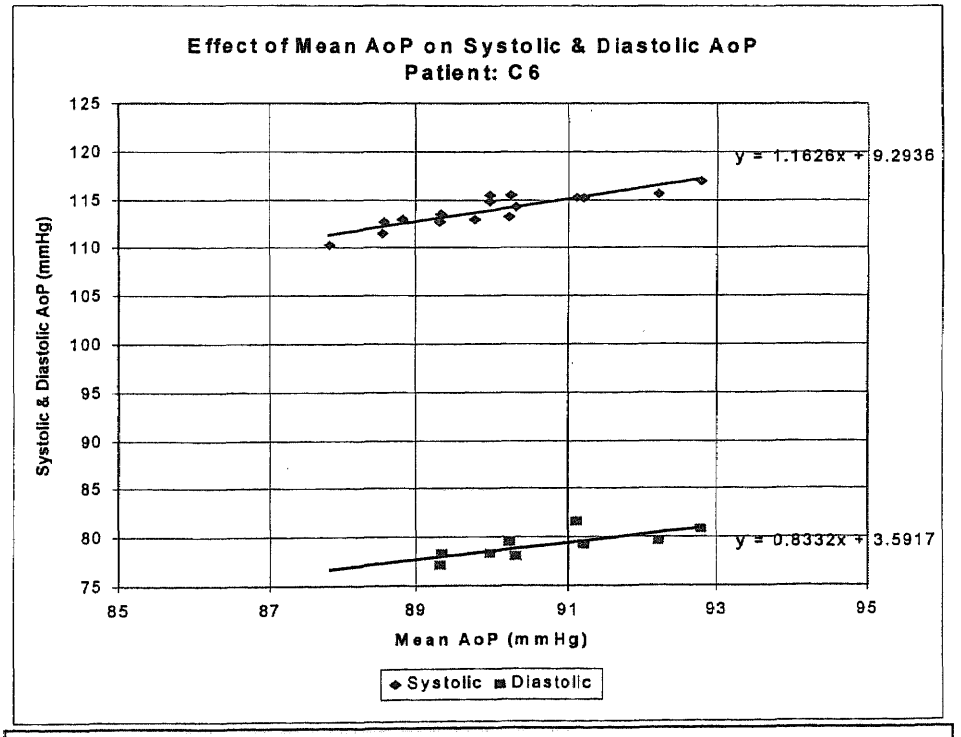

Figure 28B

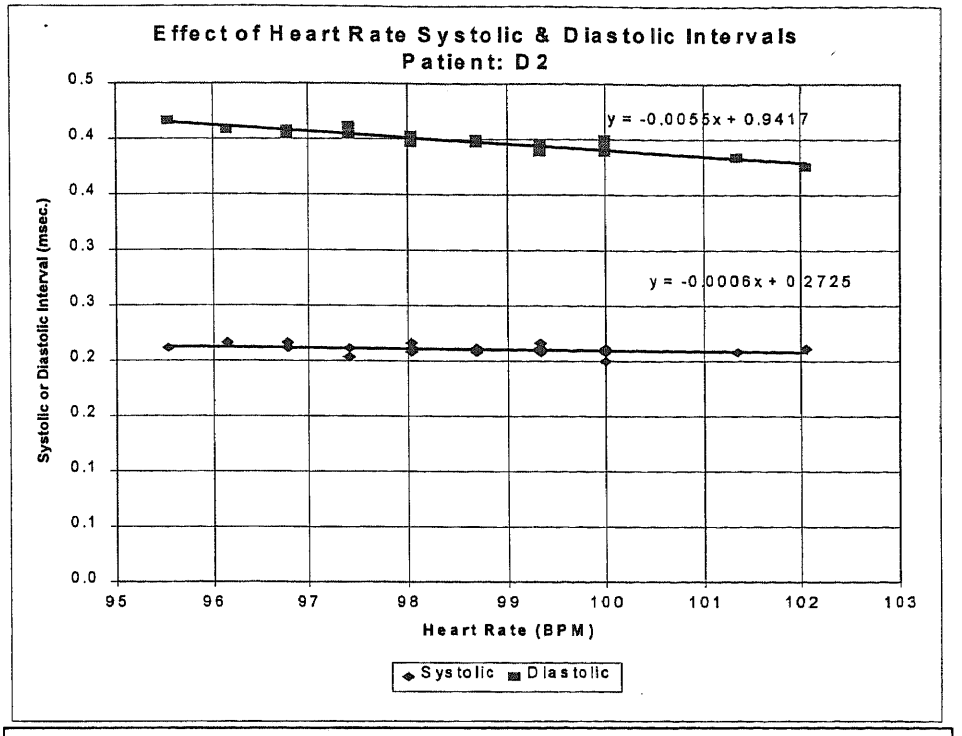

Figure 29B

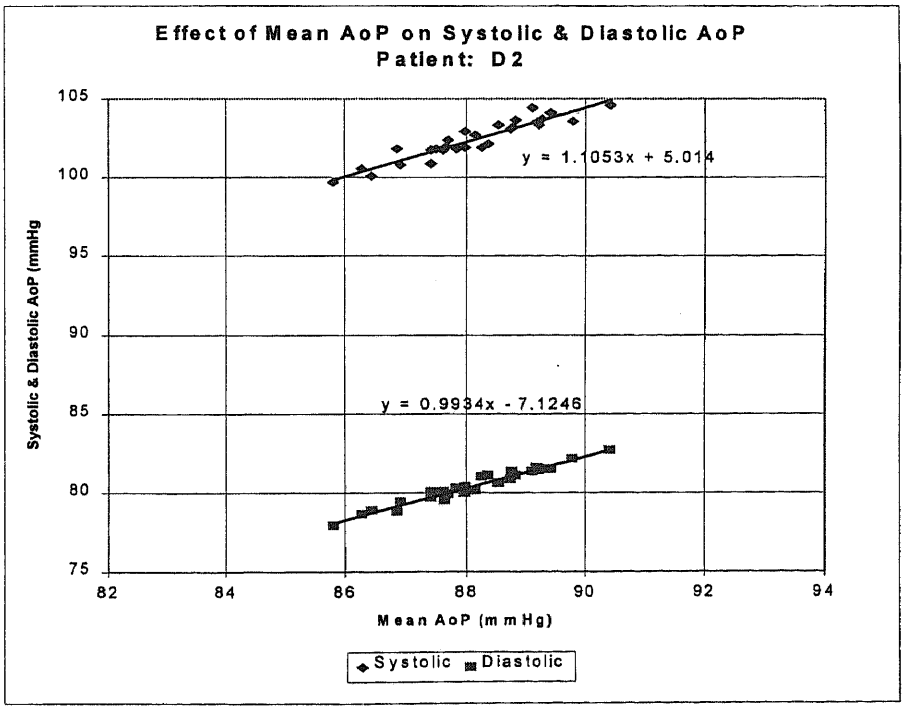

Figure 30B

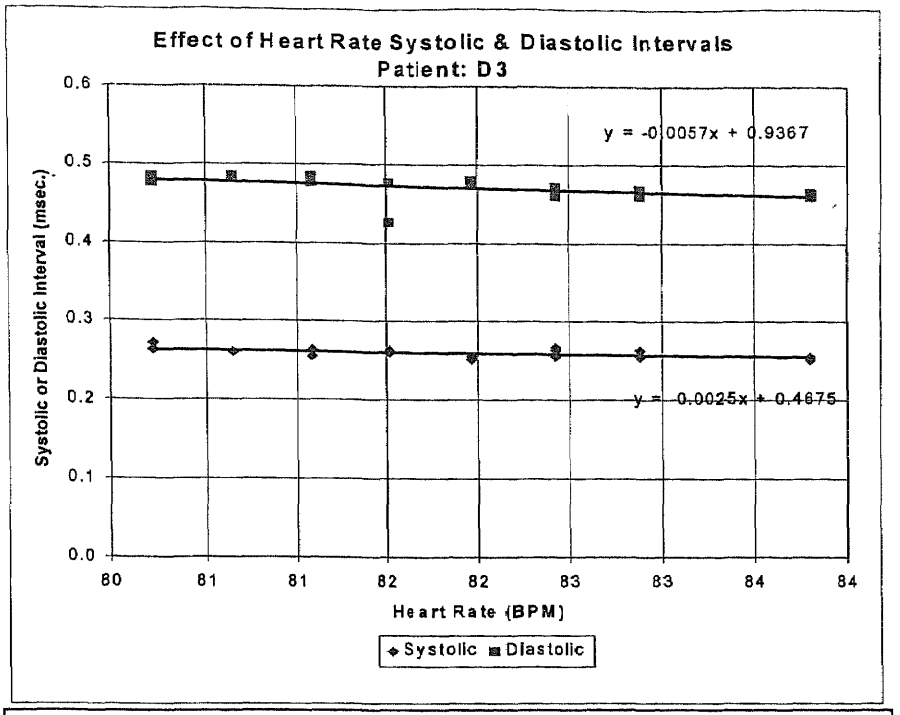

Figure 31B

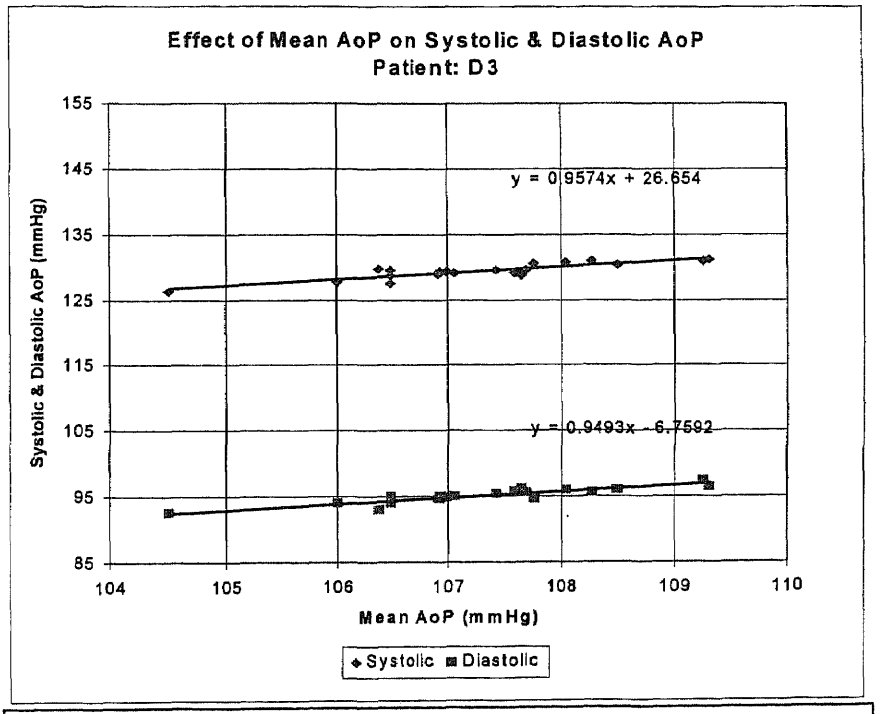

Figure 32B

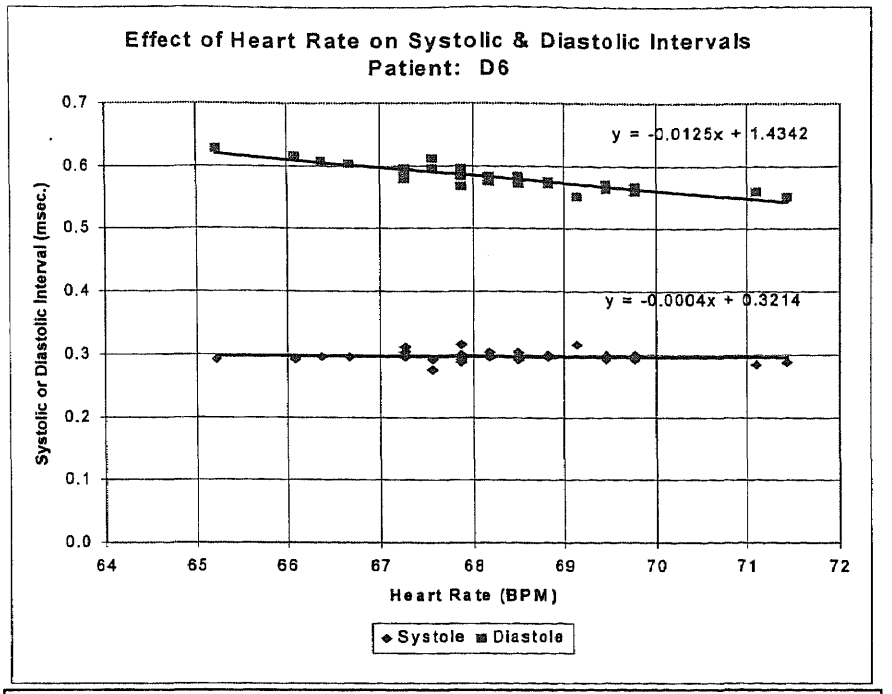

Figure 33B

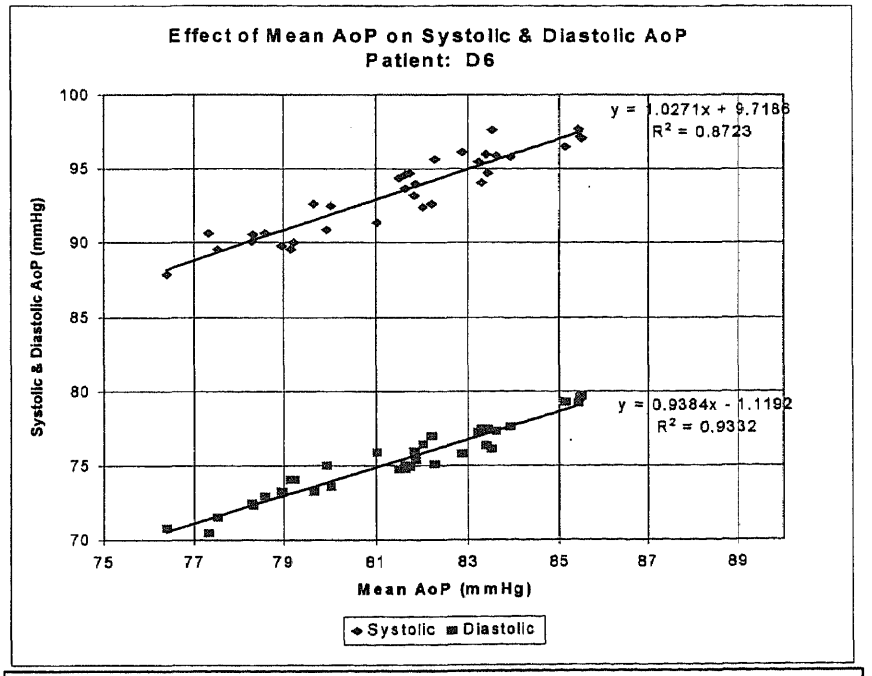

Figure 34B

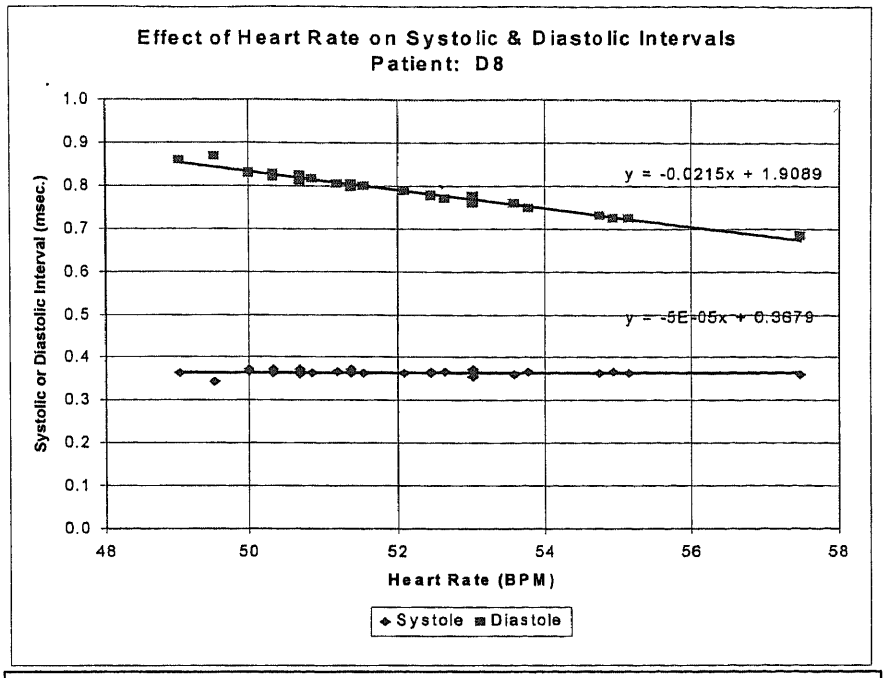

Figure 35B

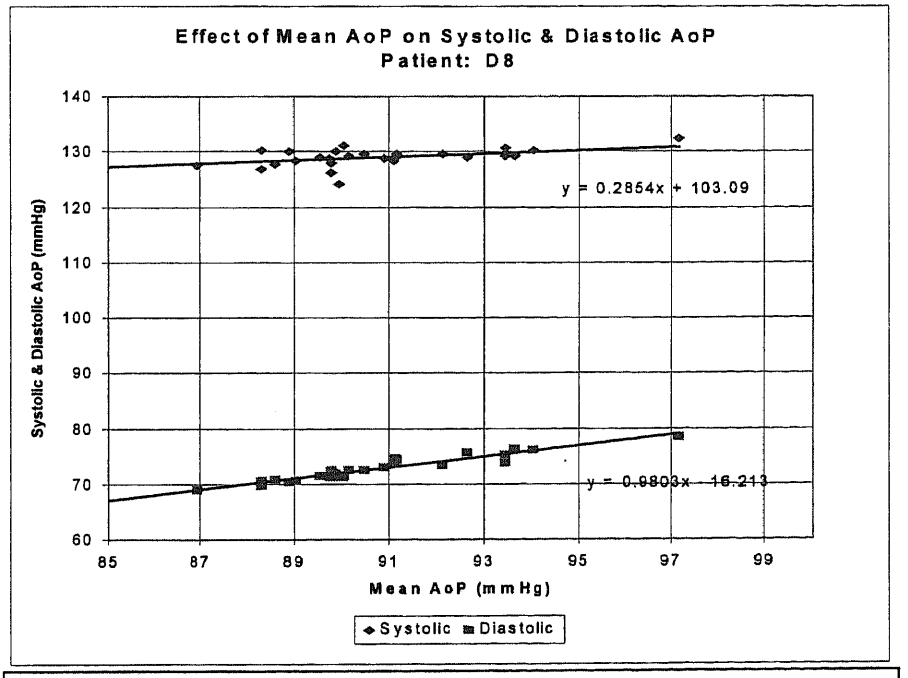

Figure 36B

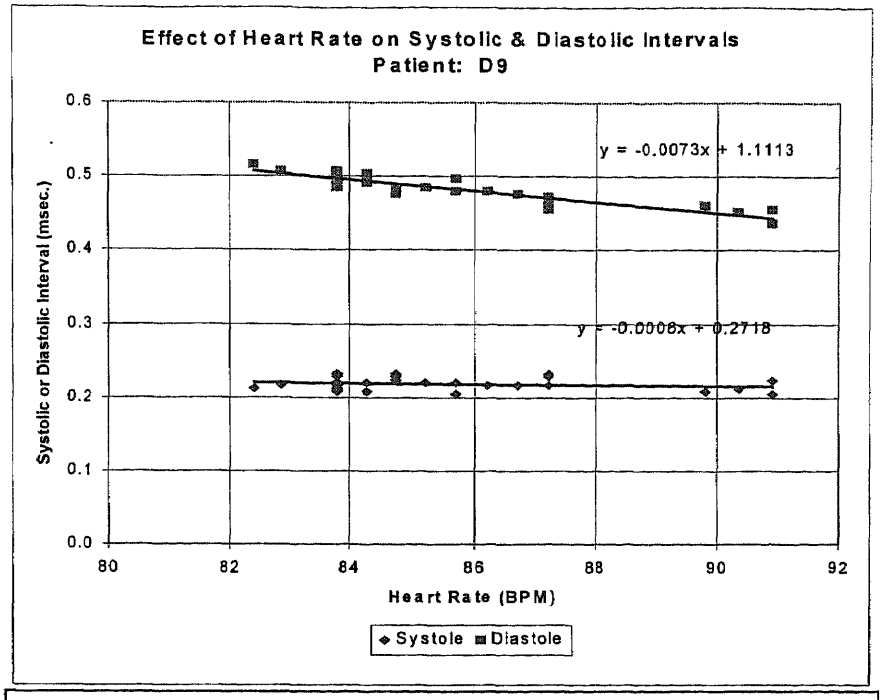

Figure 37B

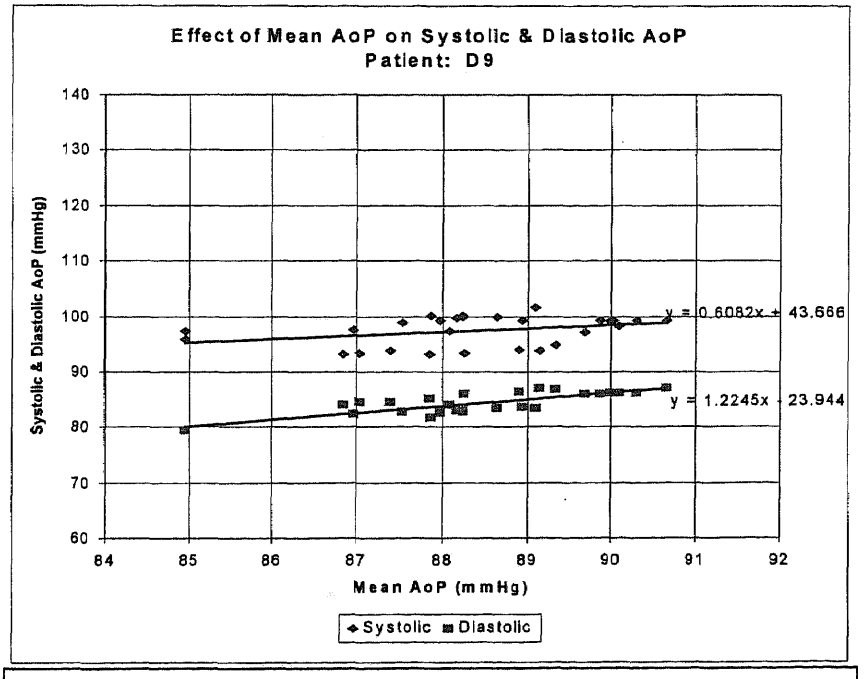

Figure 38B

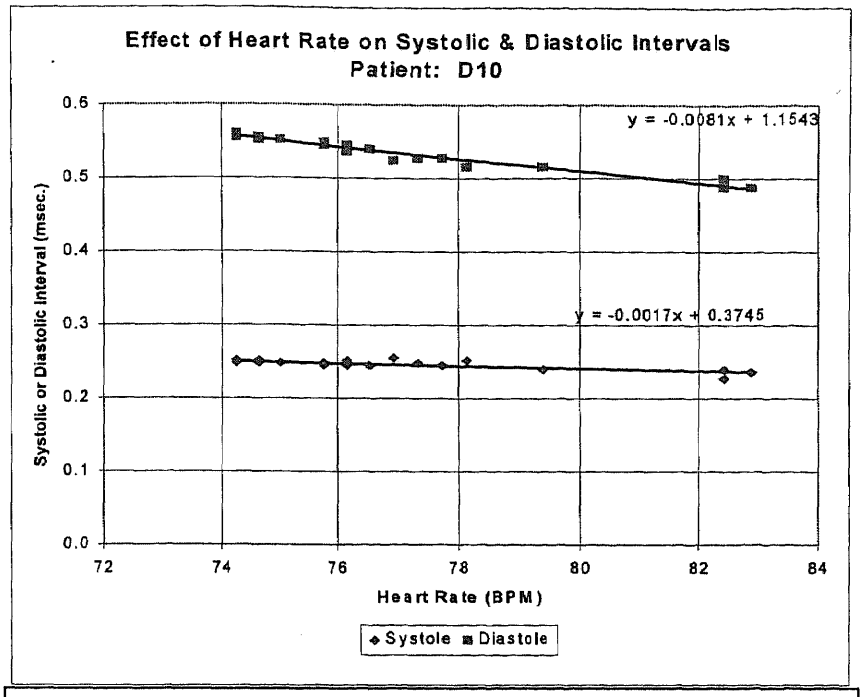

Figure 39B

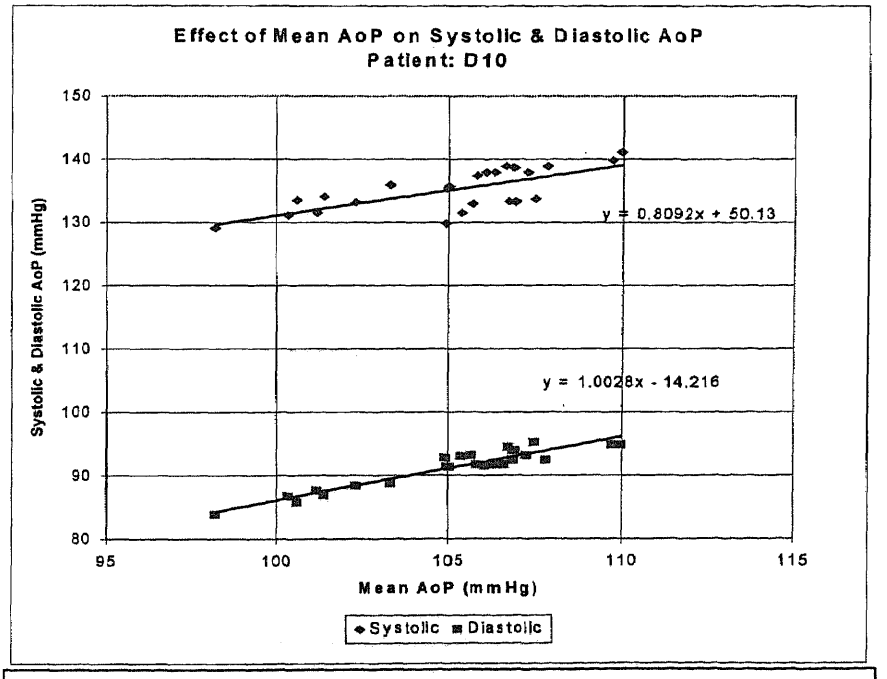

Figure 40B

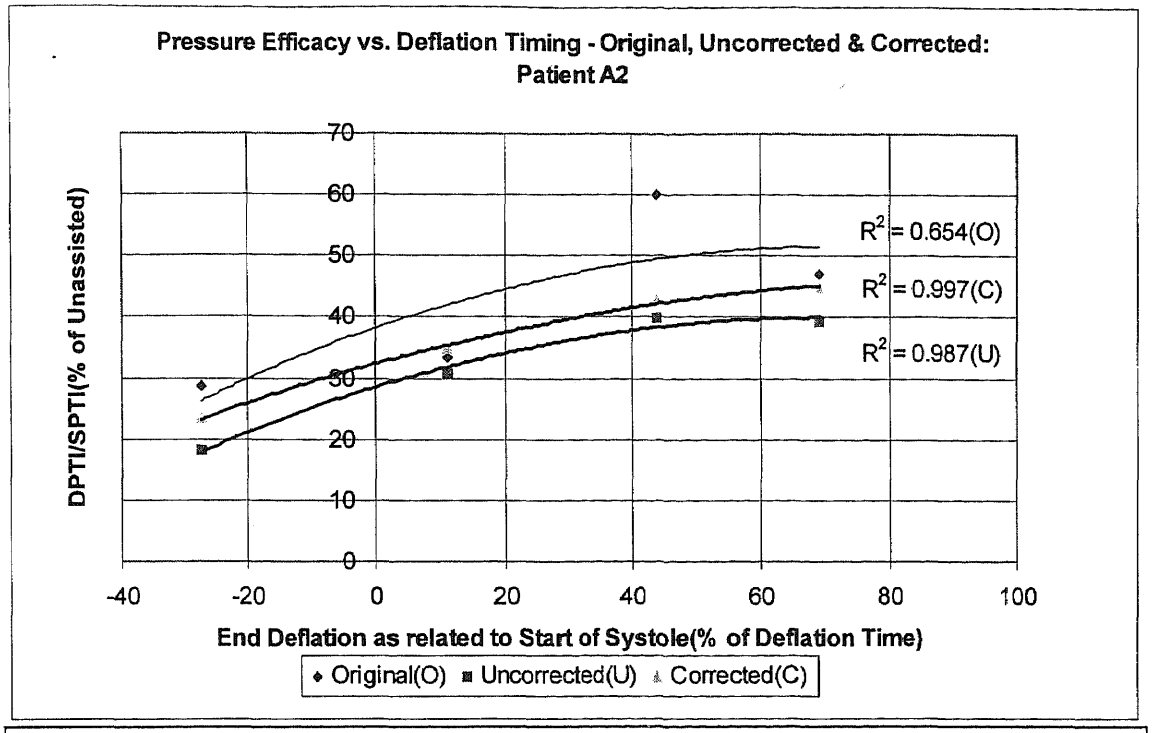

Figure 41B

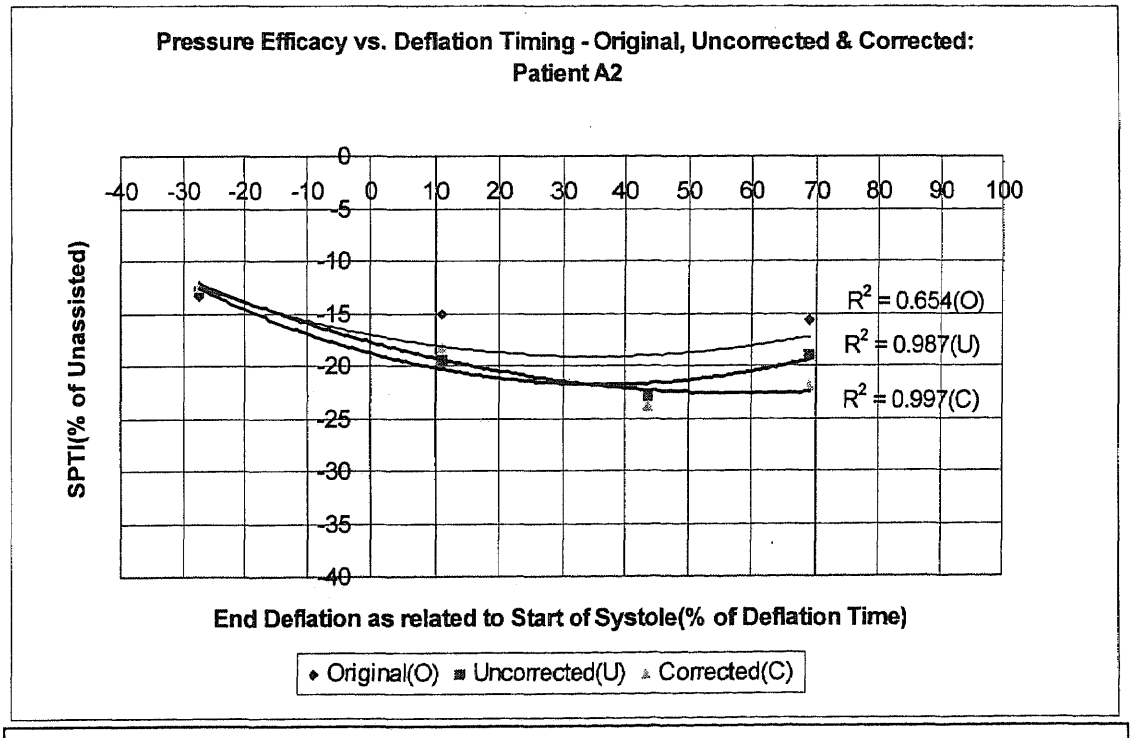

Figure 42B

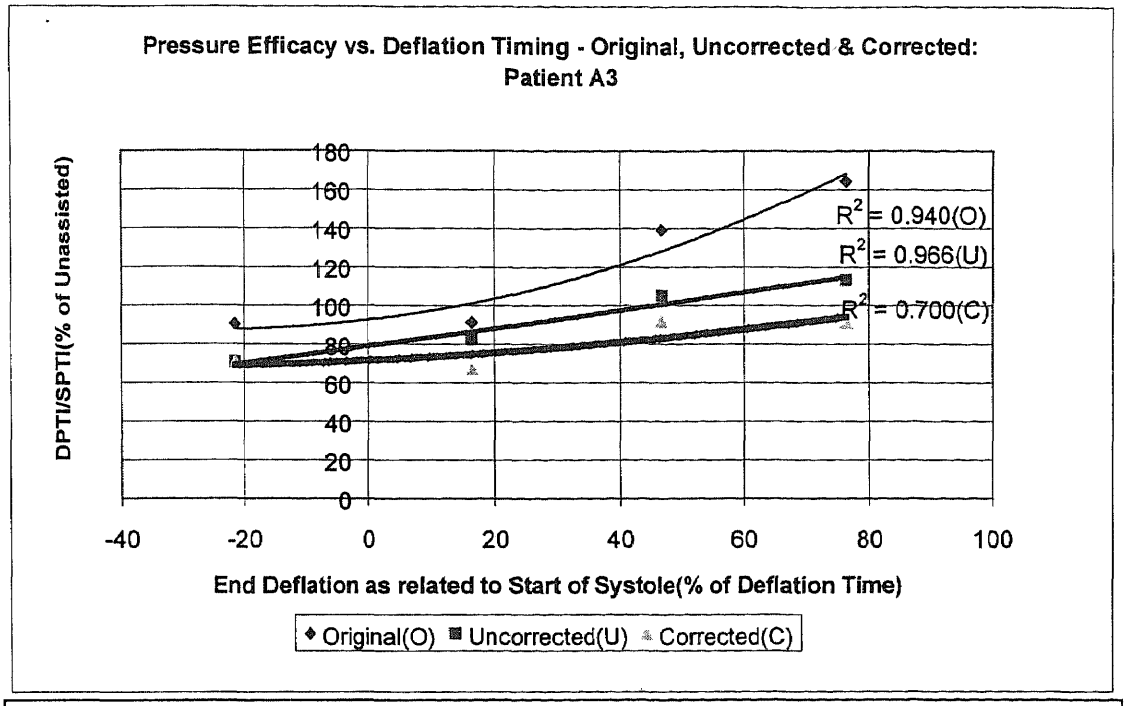

Figure 43B

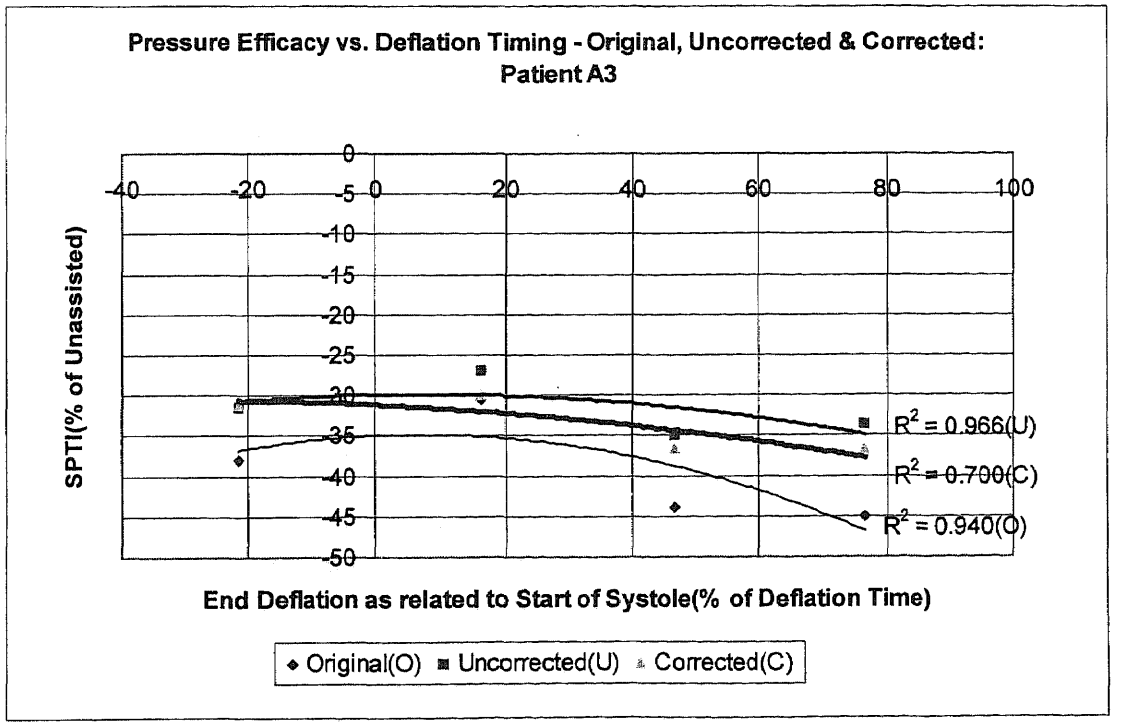

Figure 44B

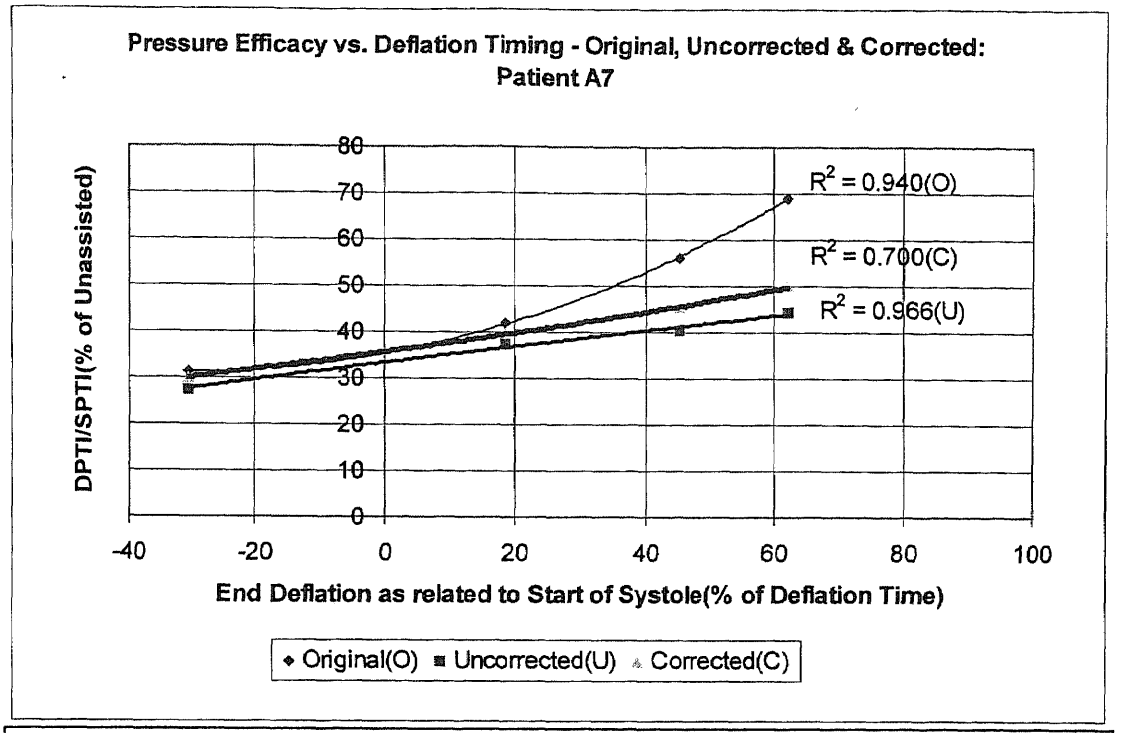

Figure 45B

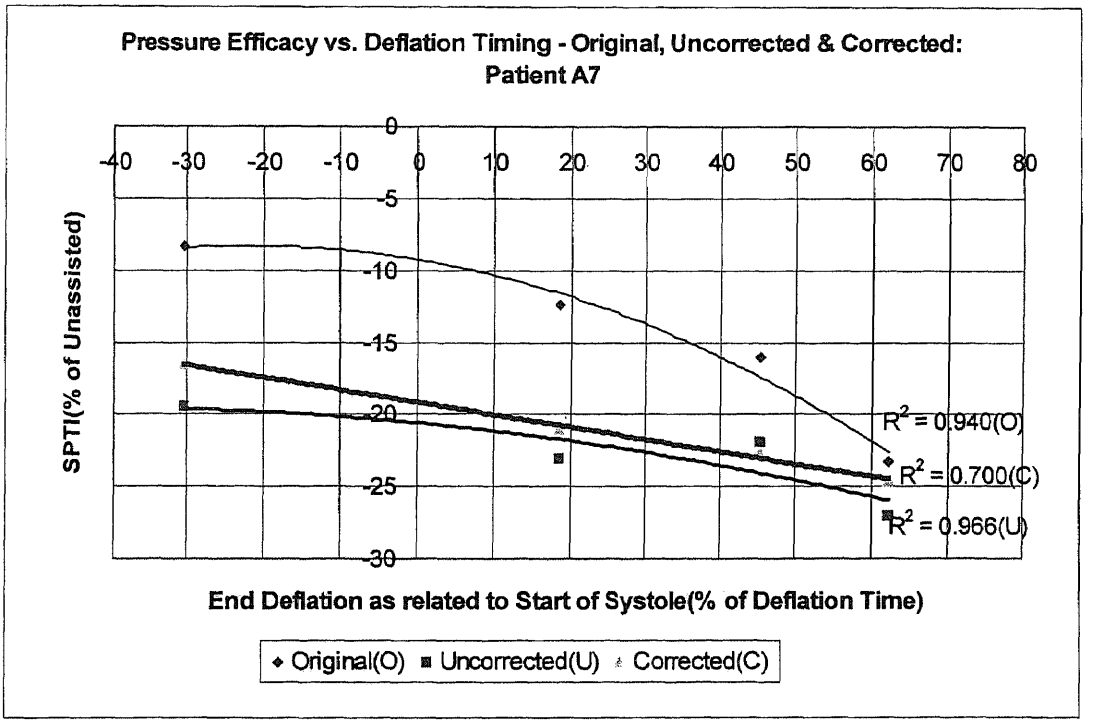

Figure 46B

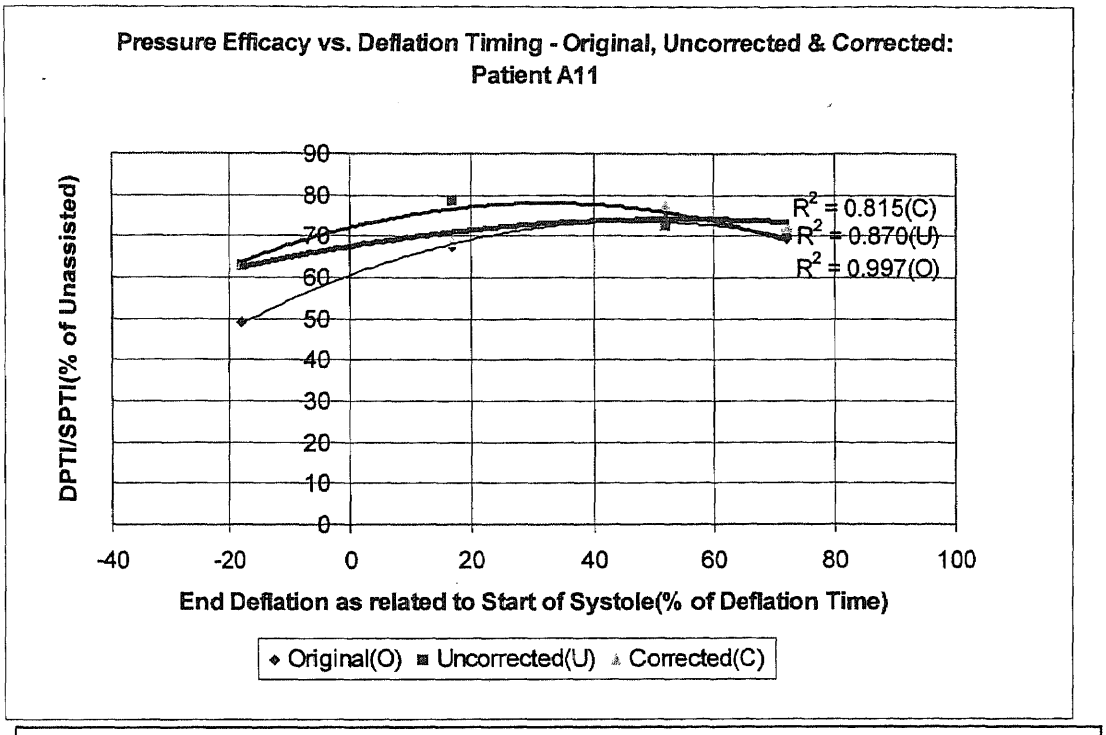

Figure 47B

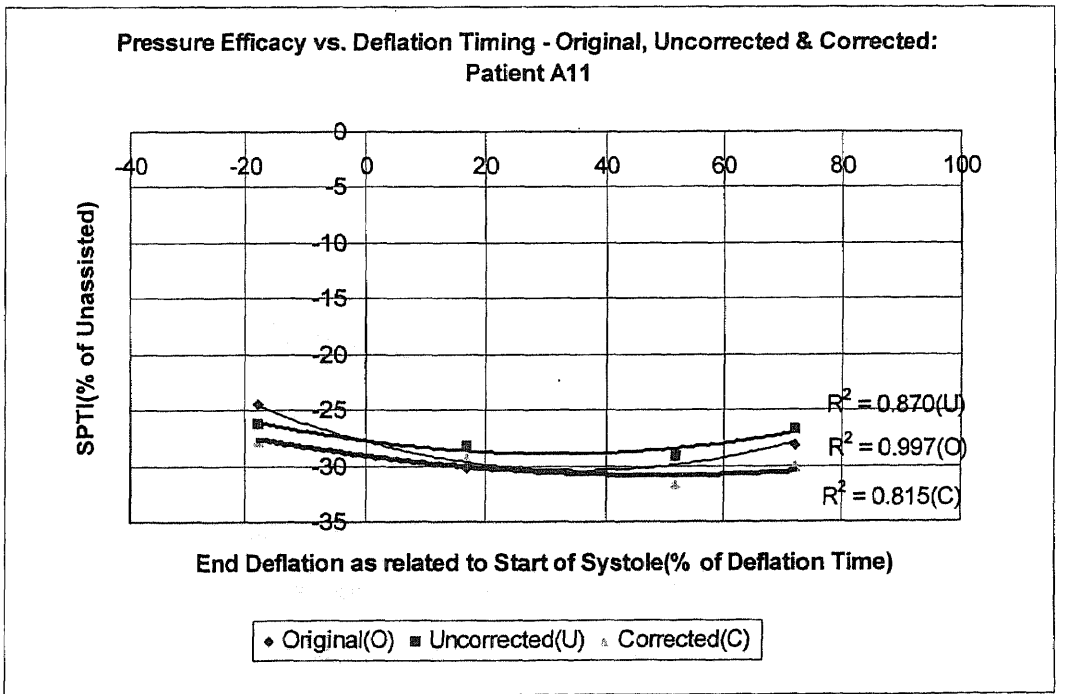

Figure 48B

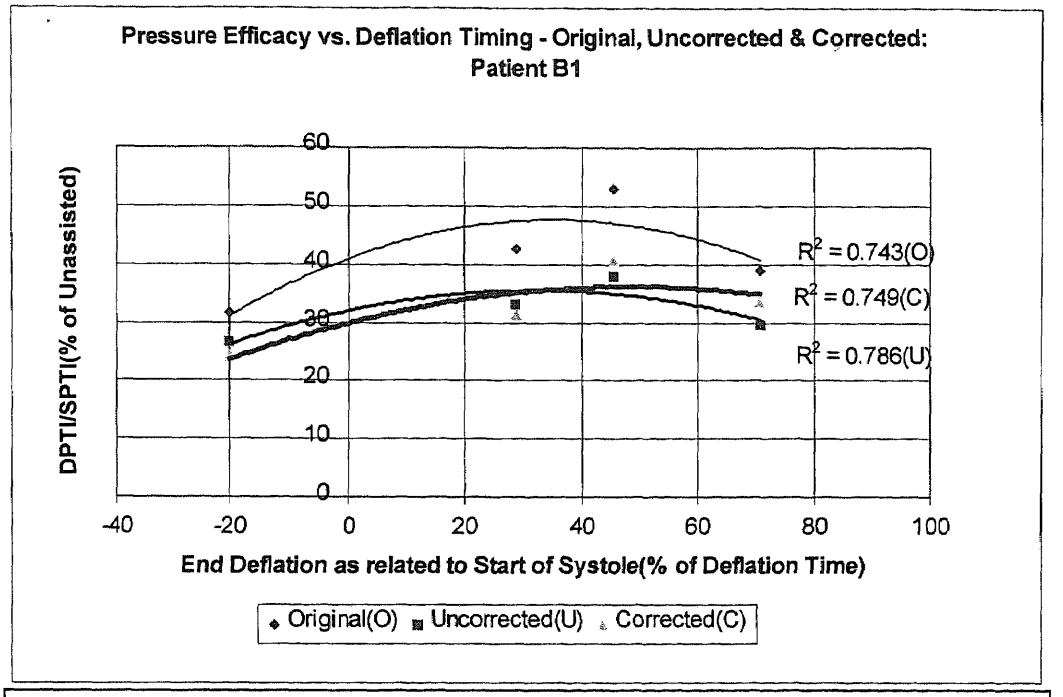

Figure 49B

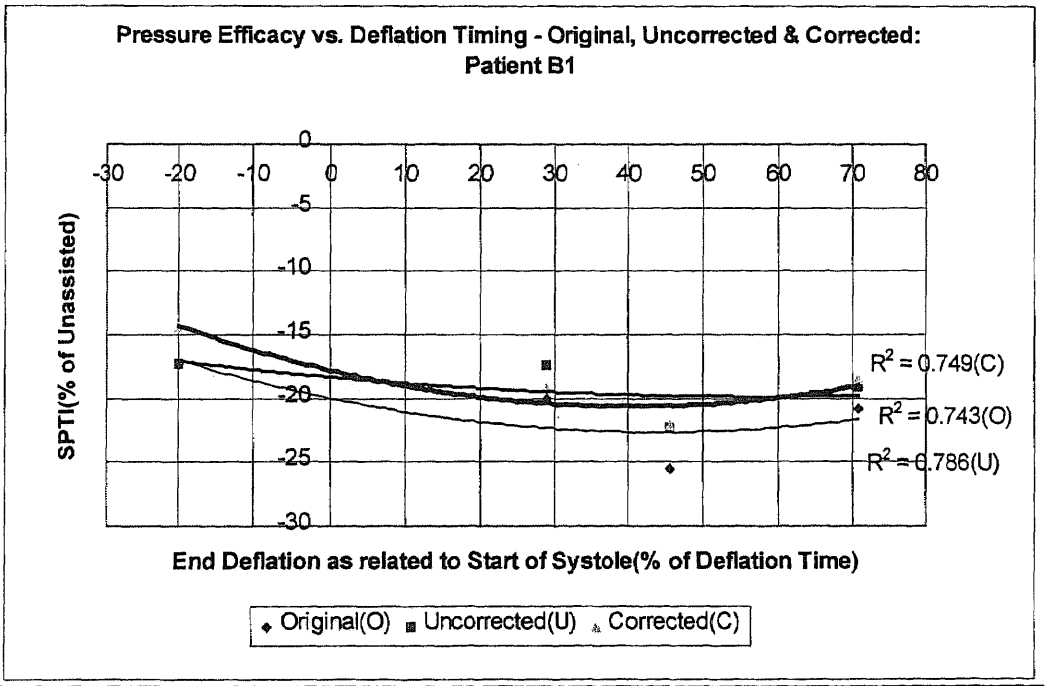

Figure 50B

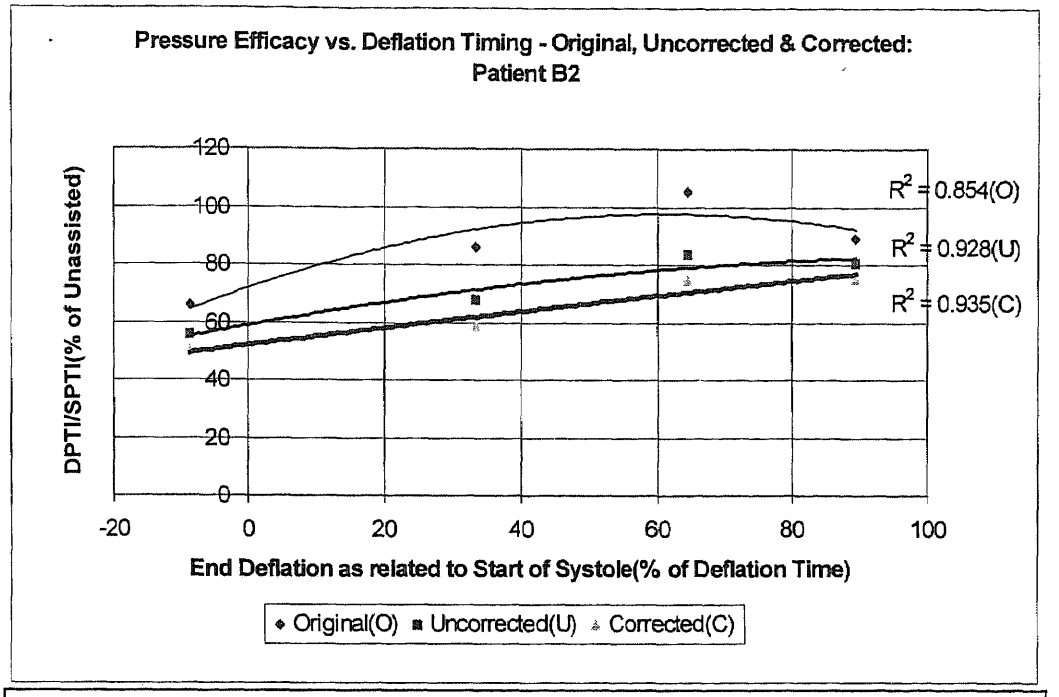

Figure 51B

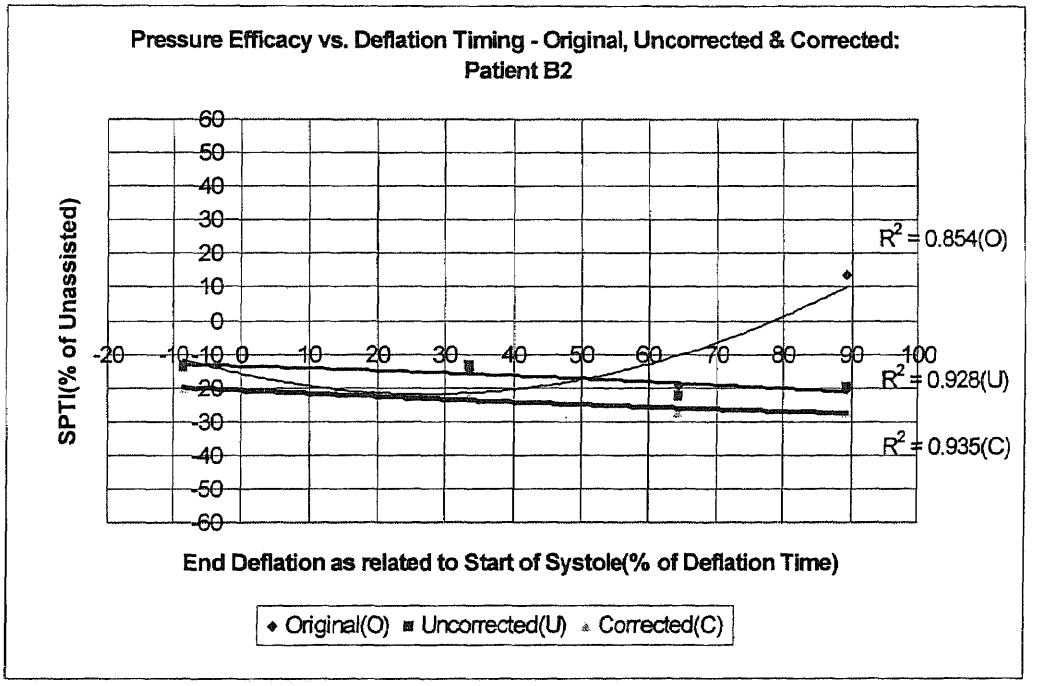

Figure 52B

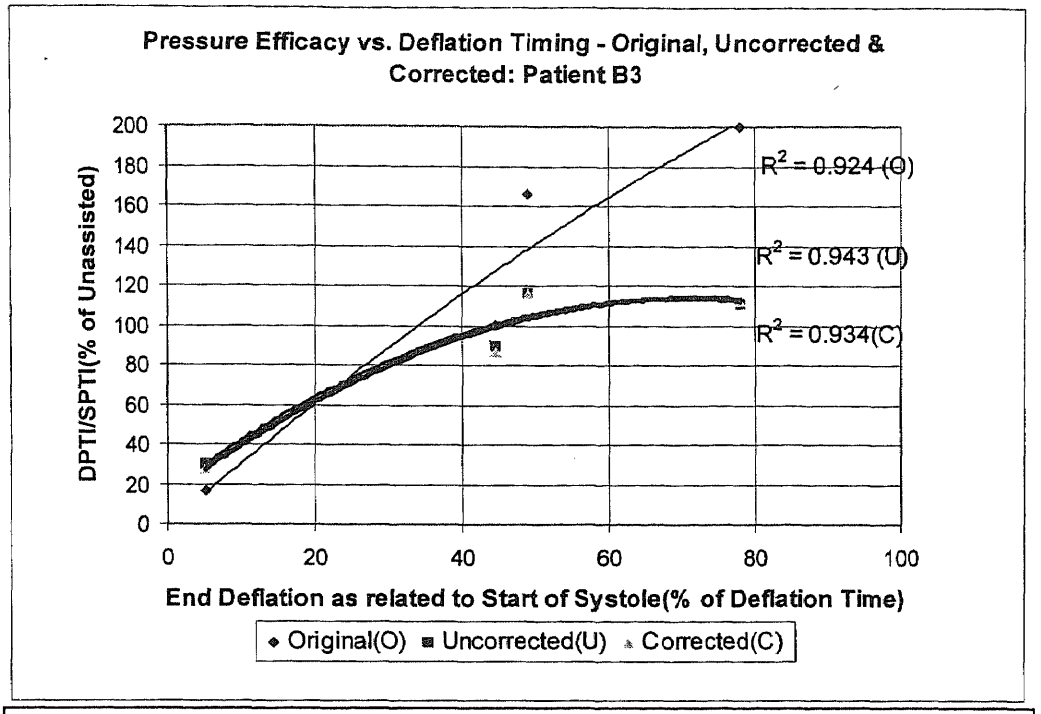

Figure 53B

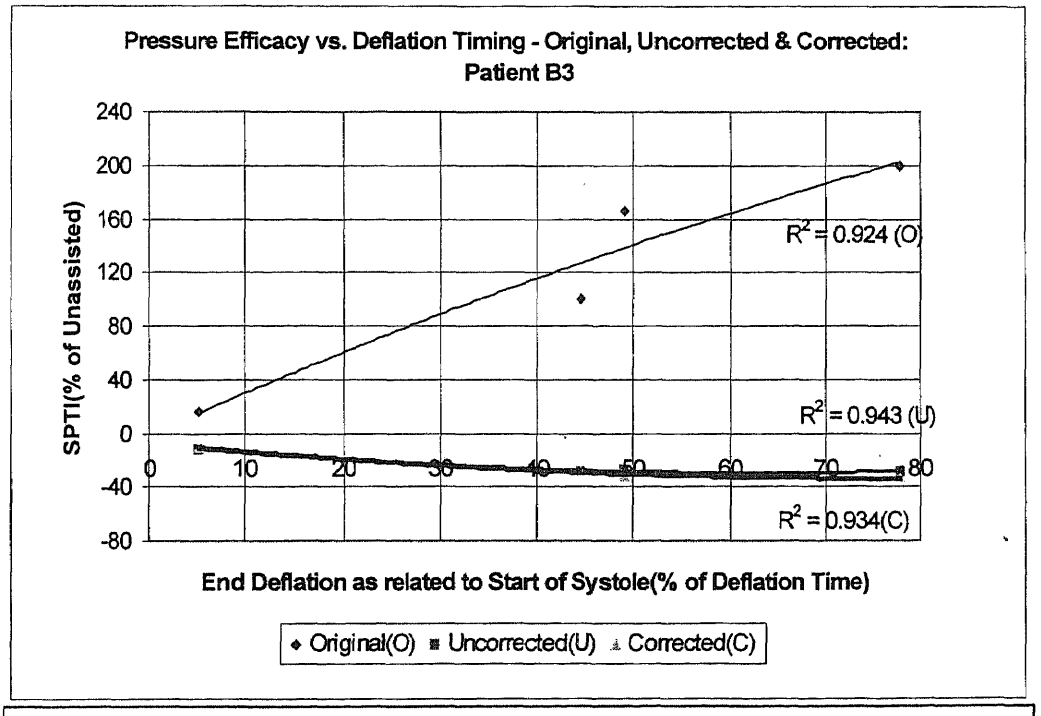

Figure 54B

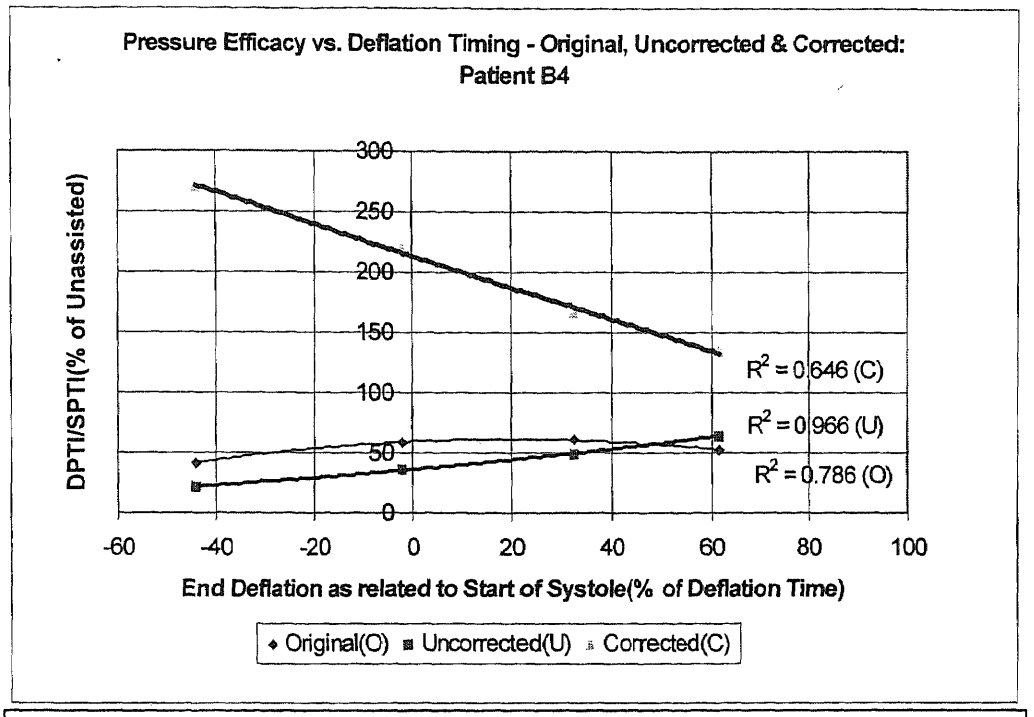

Figure 55B

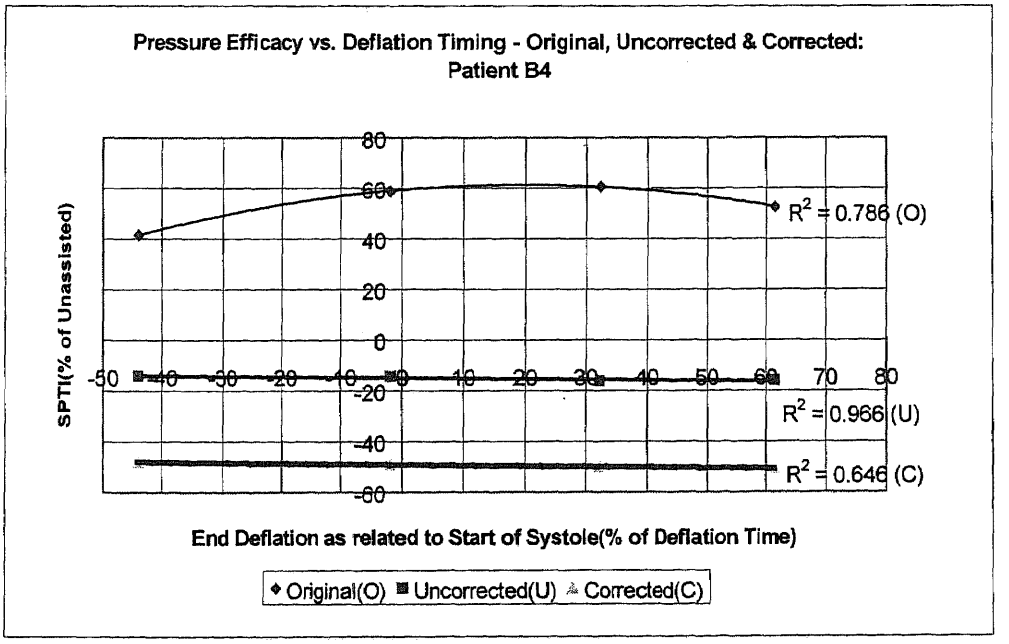

Figure 56B

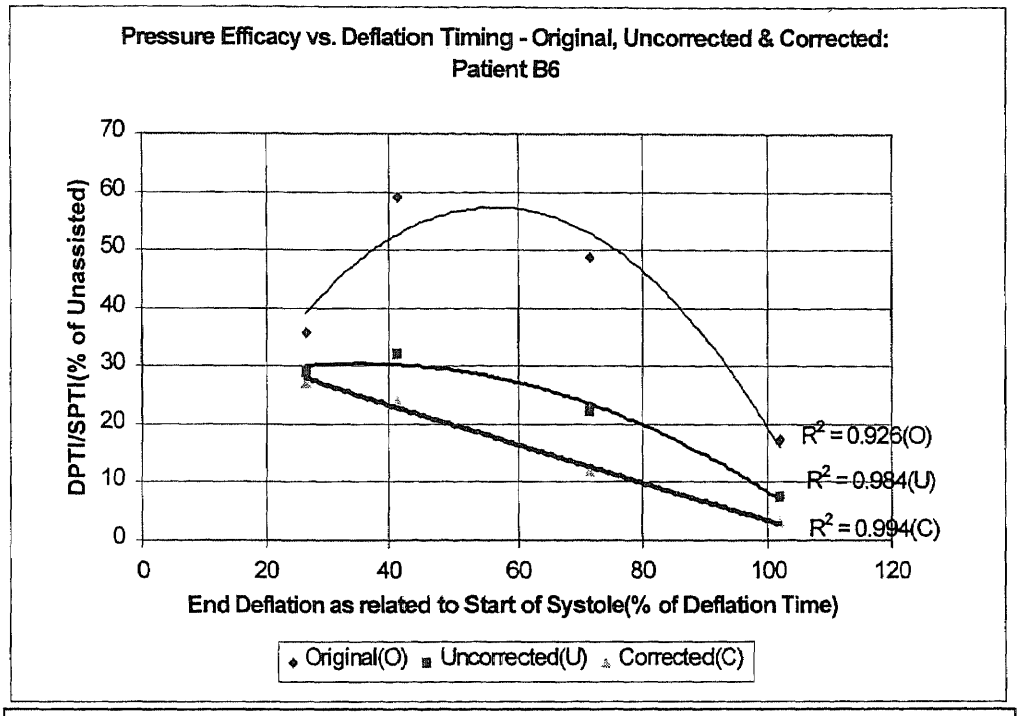

Figure 57B

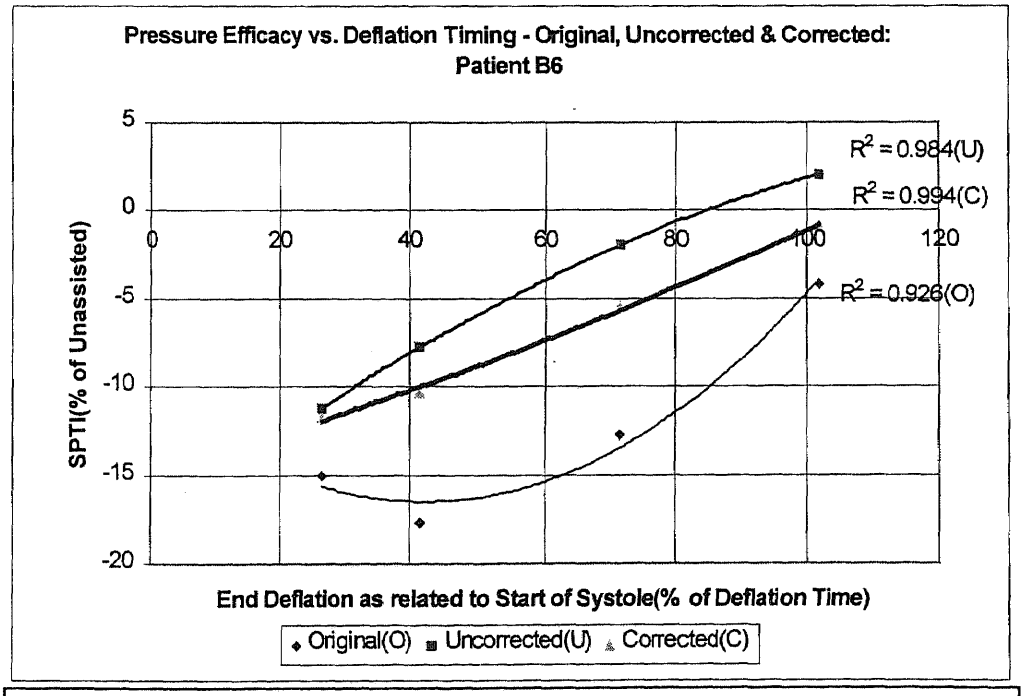

Figure 58B

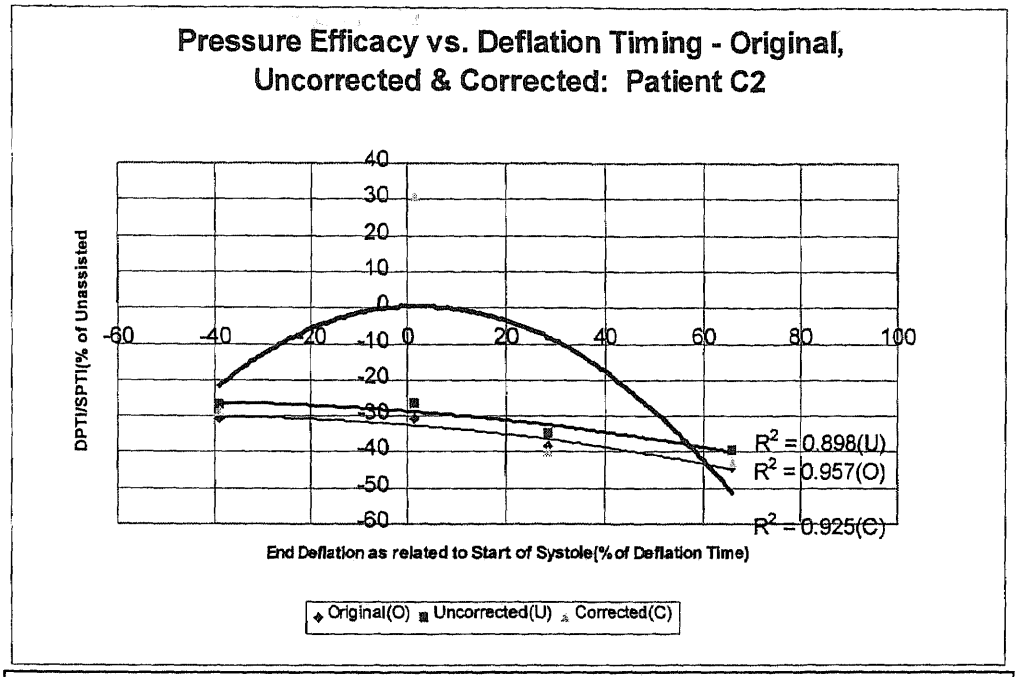

Figure 59B

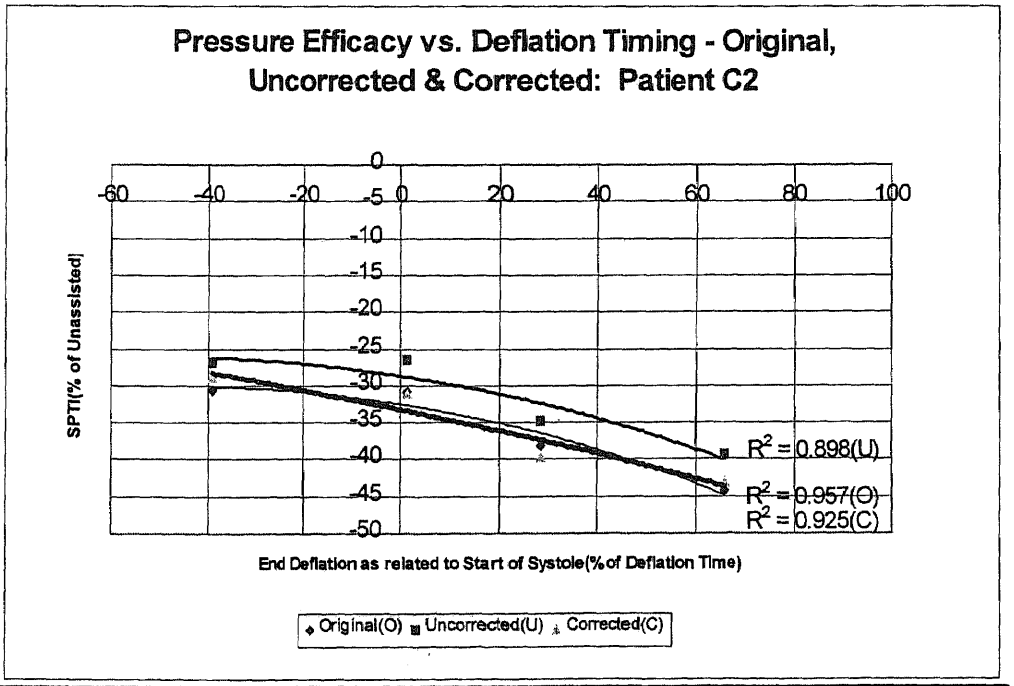

Figure 60B

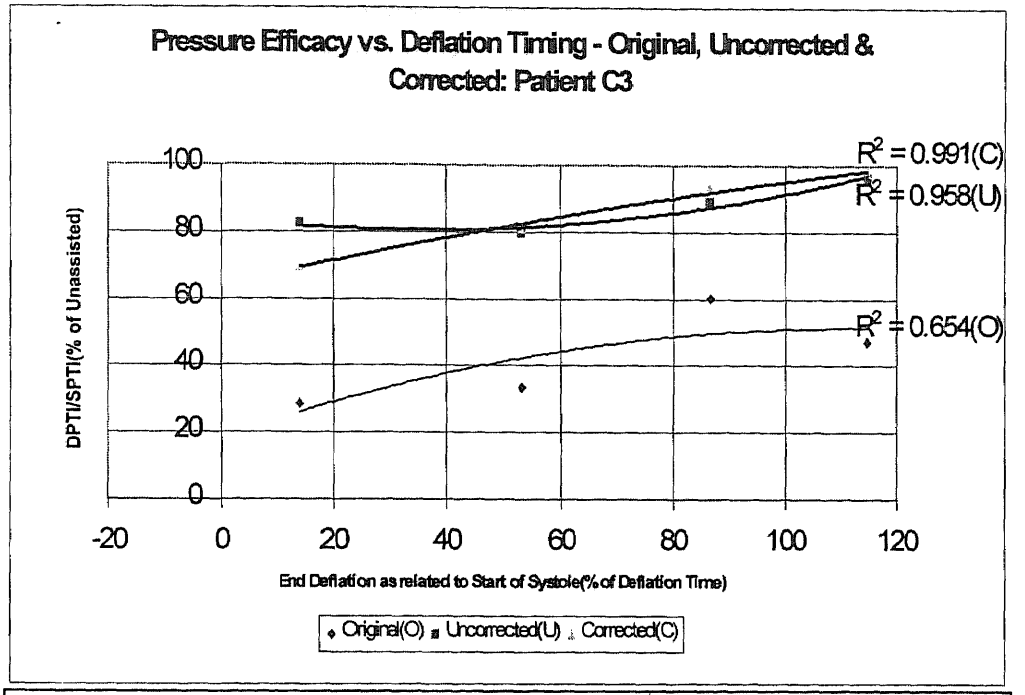

Figure 61B

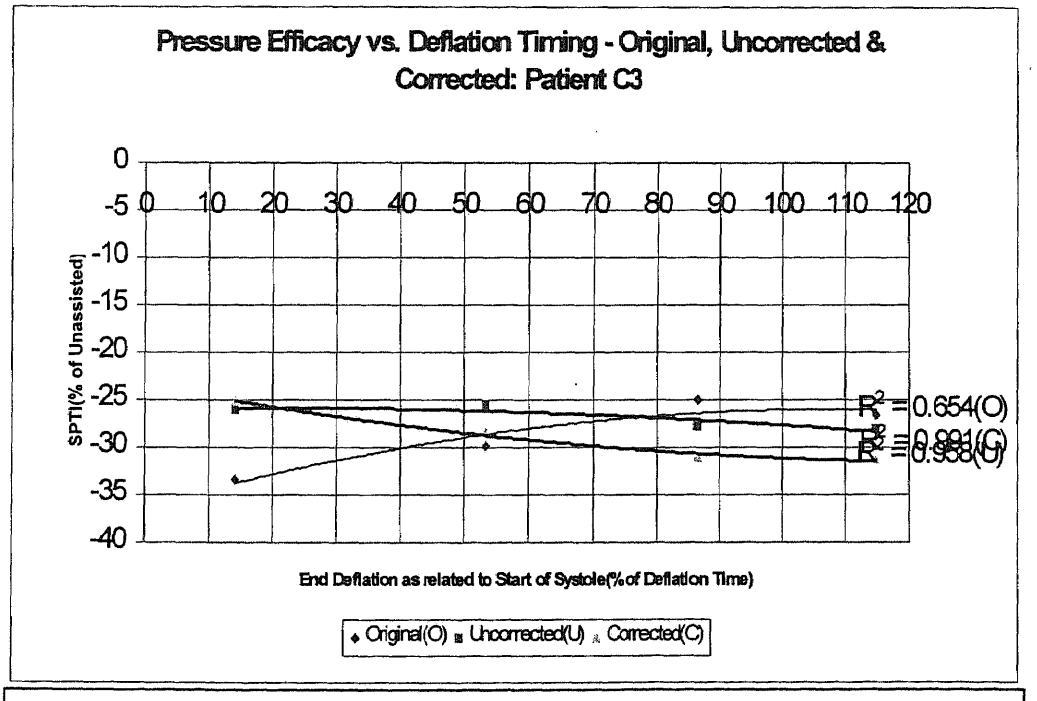

Figure 62B

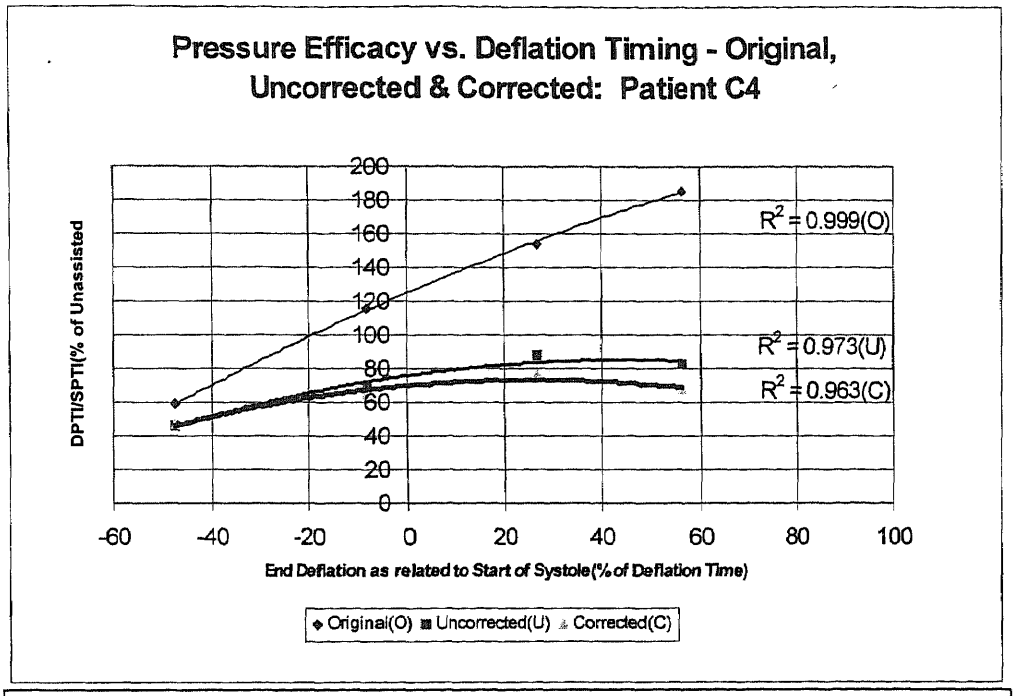

Figure 63B

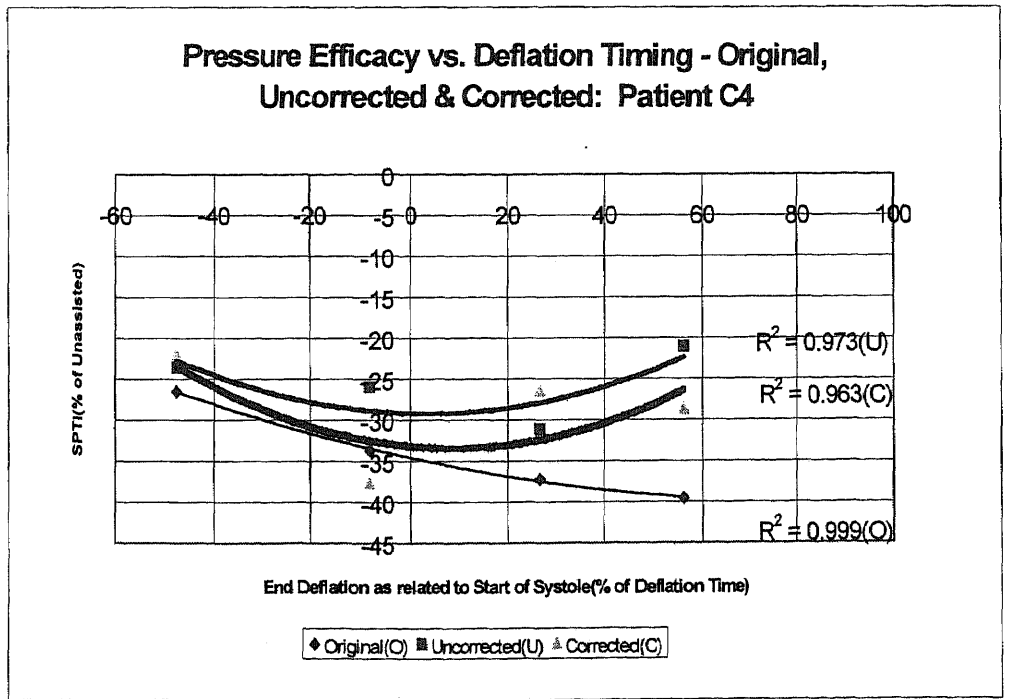

Figure 64B

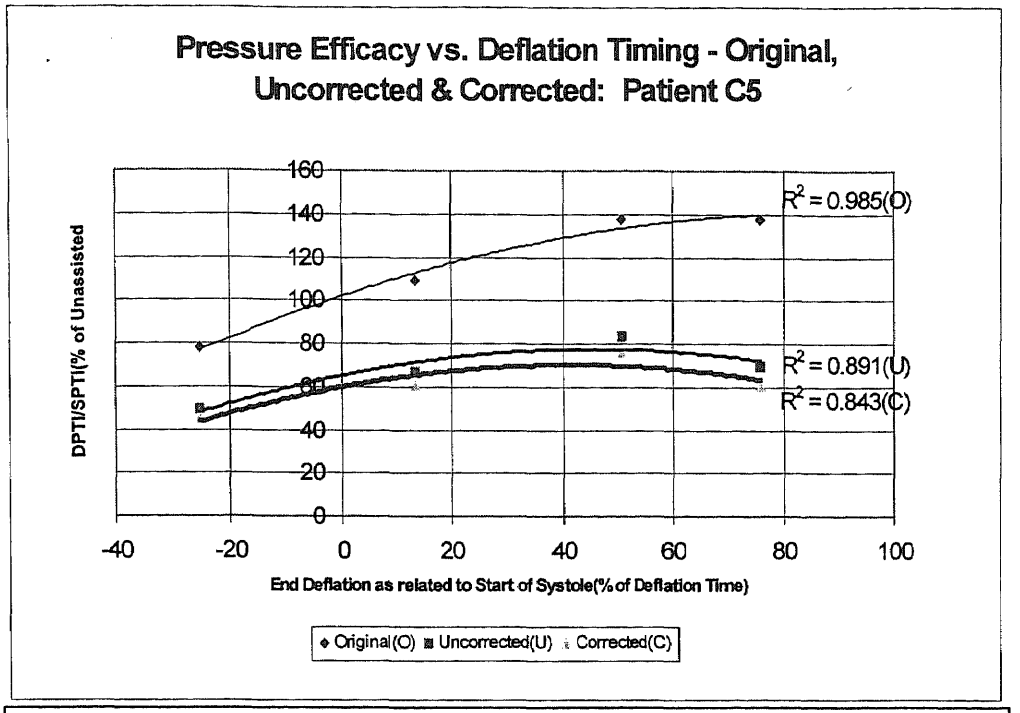

Figure 65B

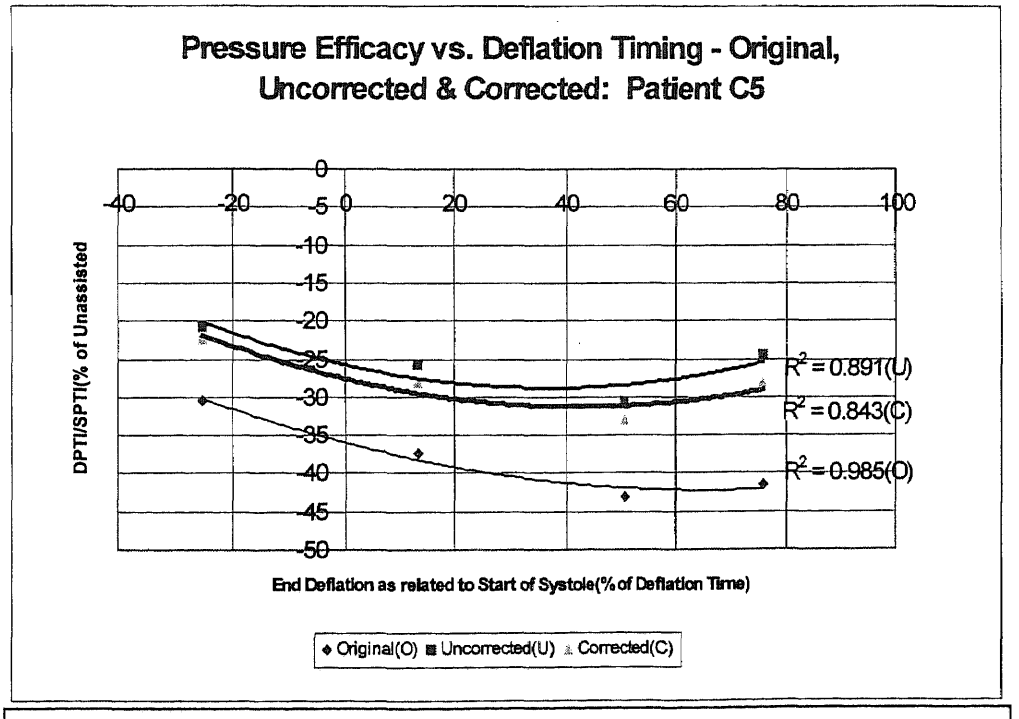

Figure 66B

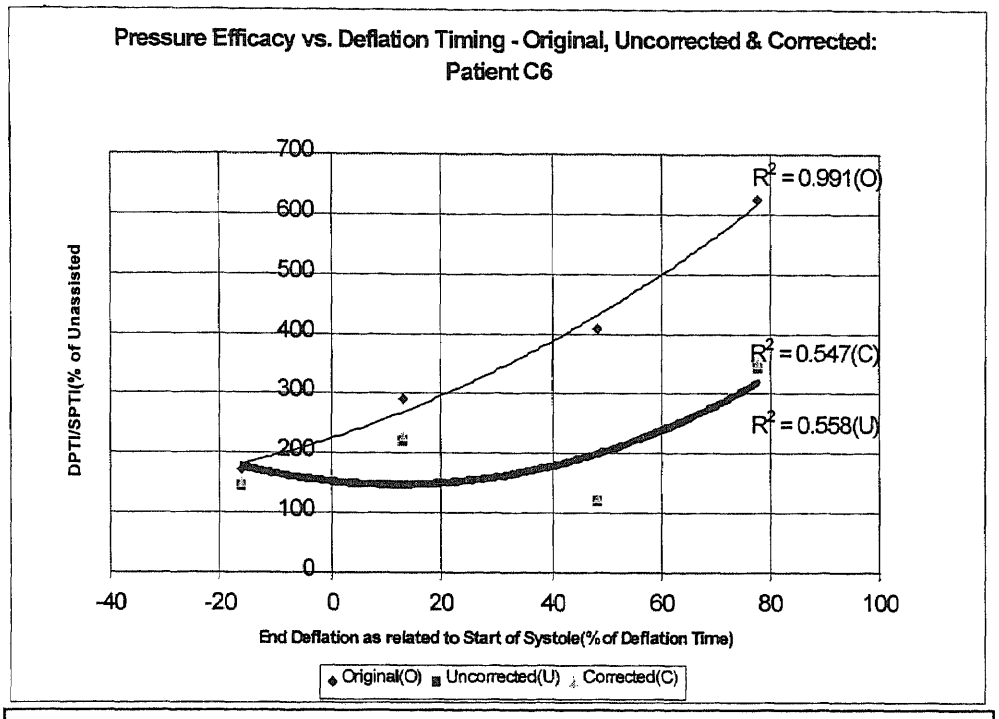

Figure 67B

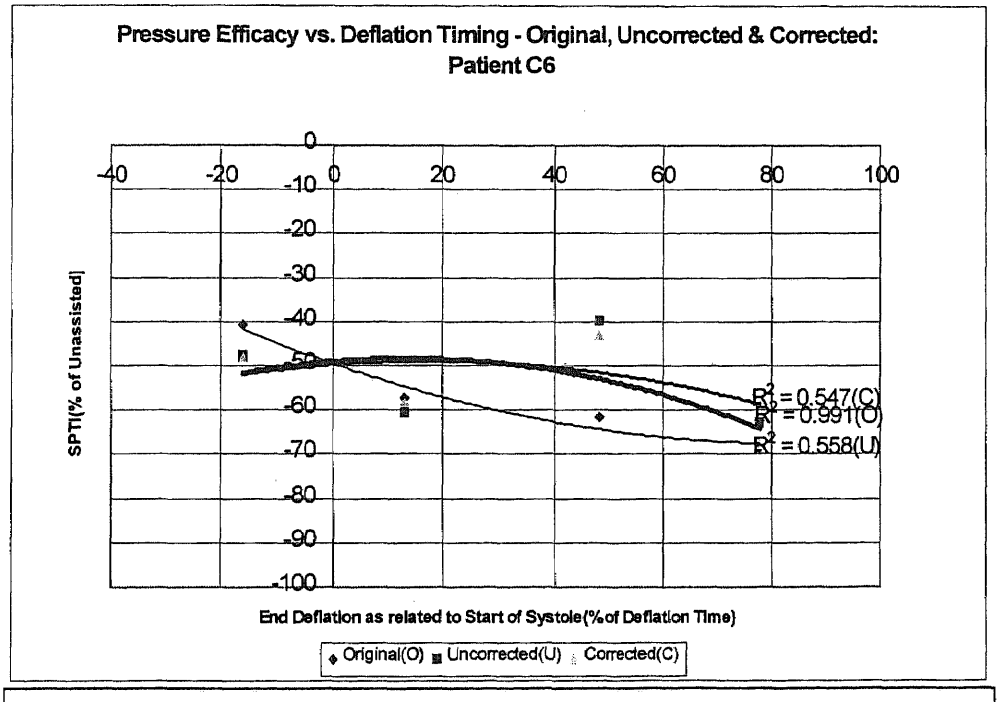

Figure 68B

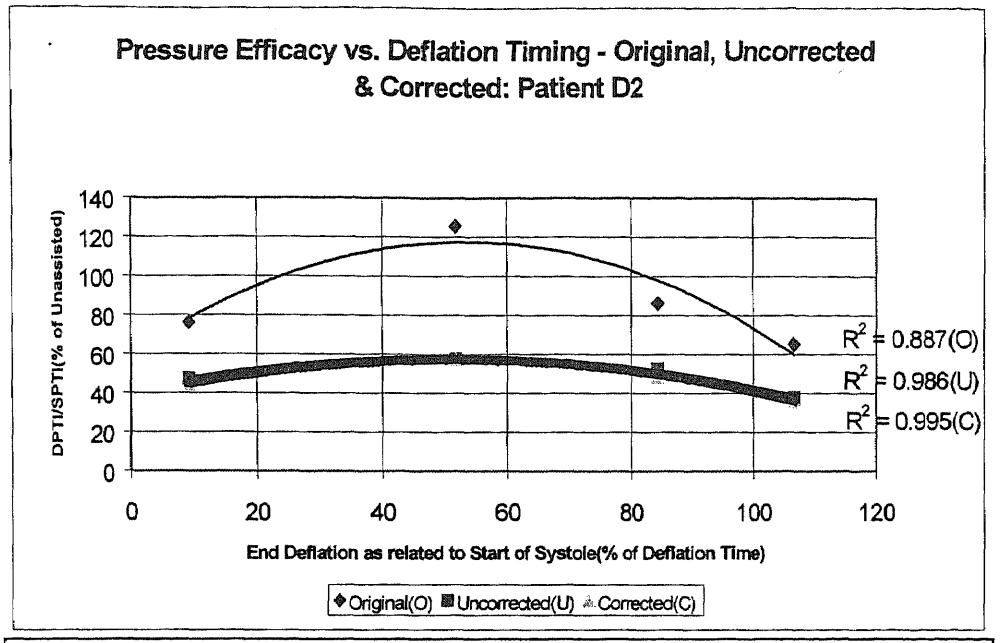

Figure 69B

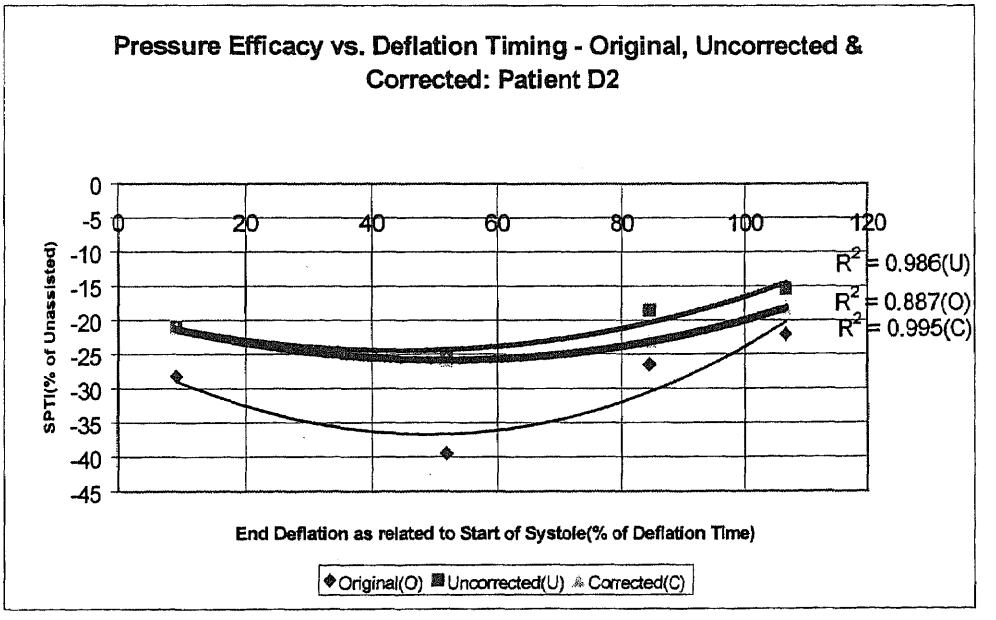

Figure 70B

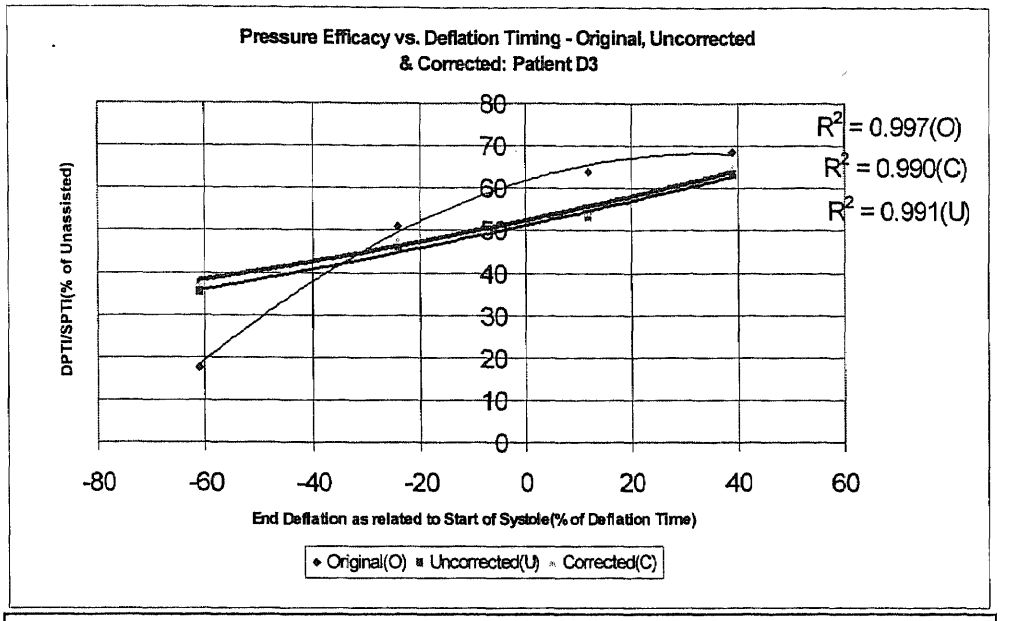

Figure 71B

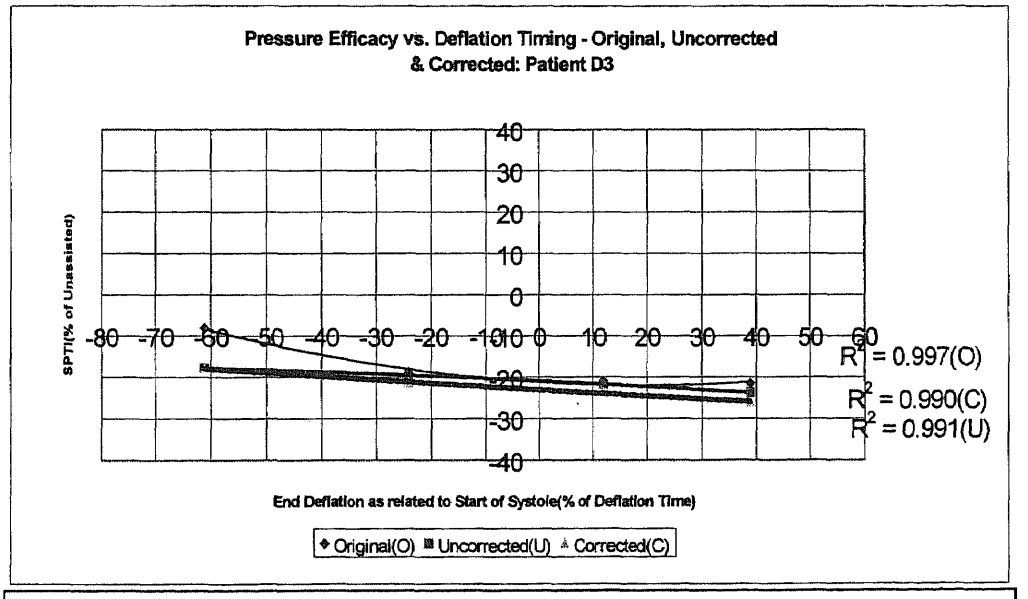

Figure 72B

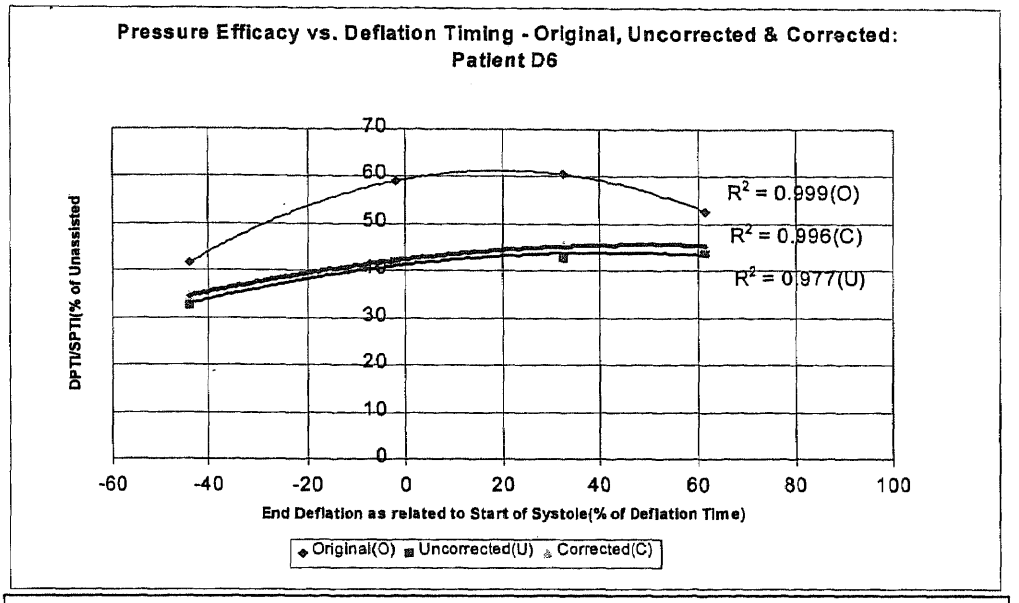

Figure 73B

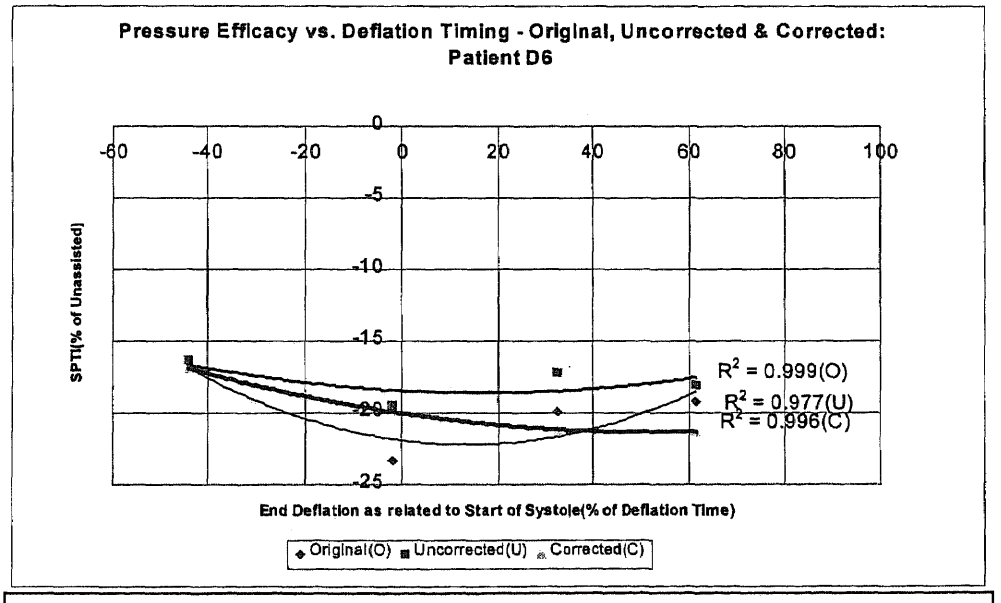

Figure 74B

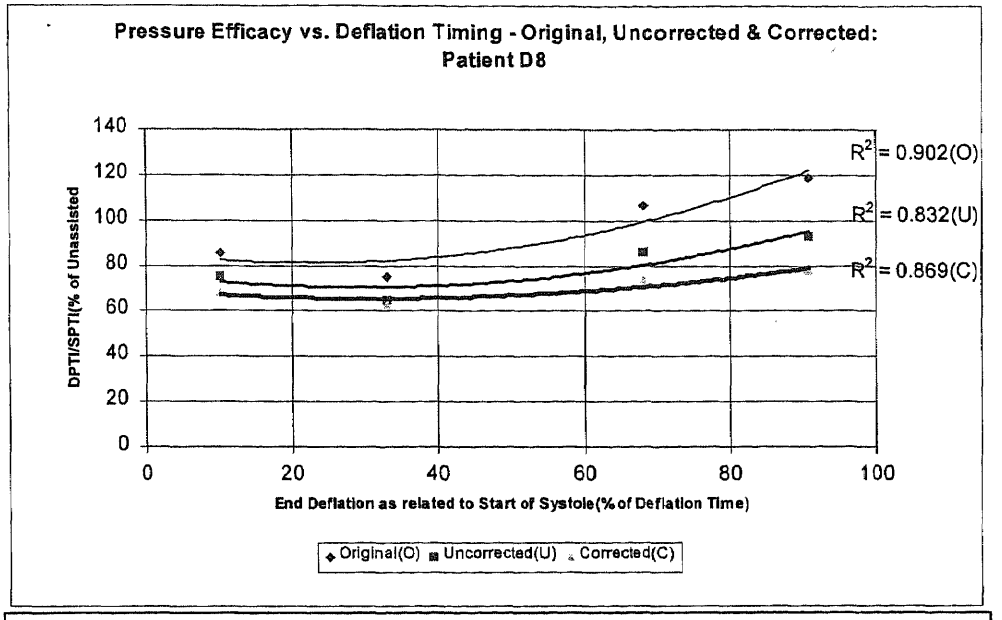

Figure 75B

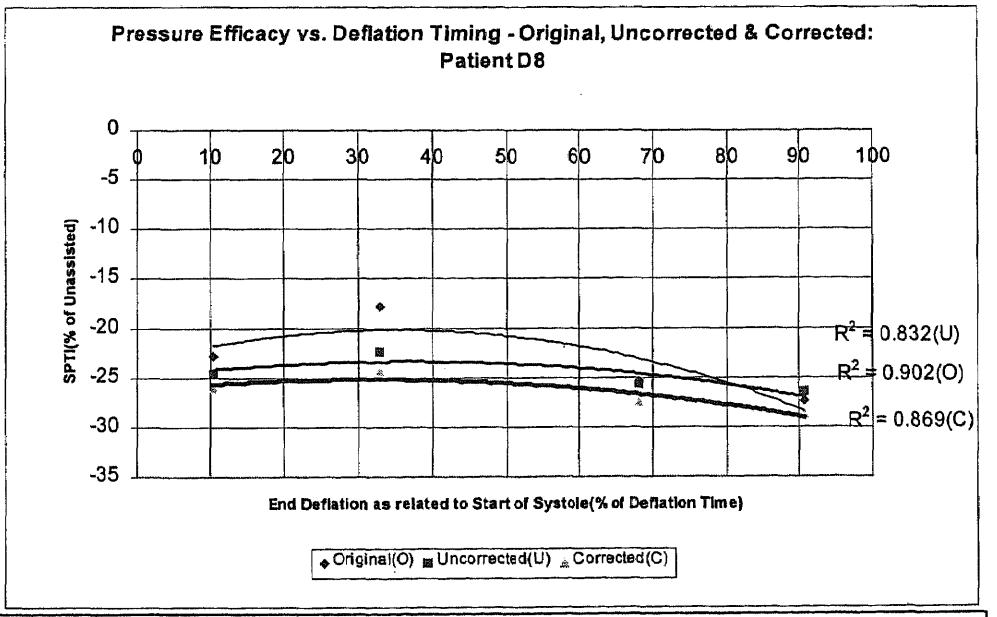

Figure 76B

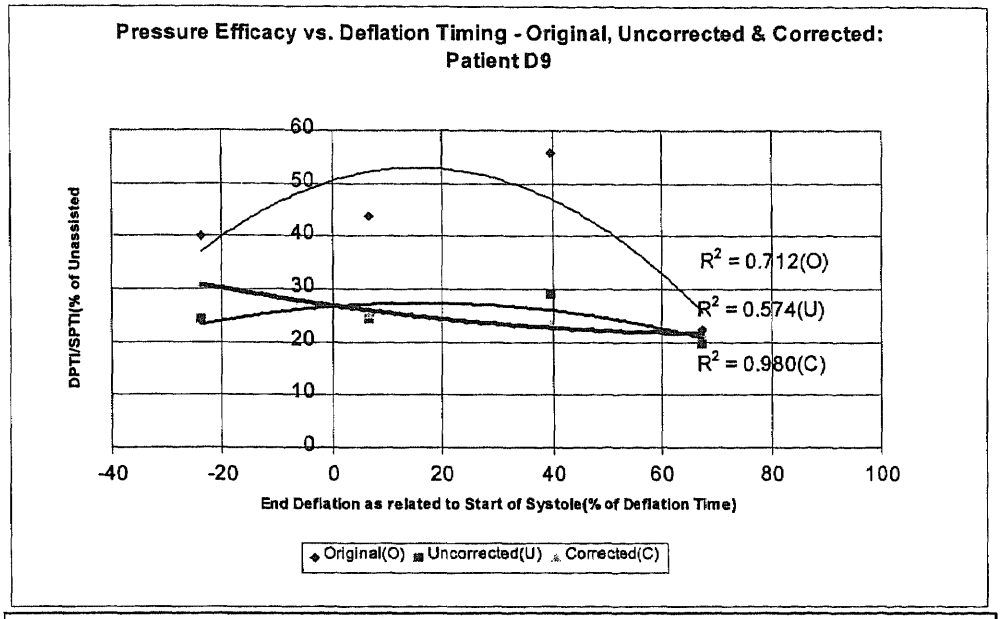

Figure 77B

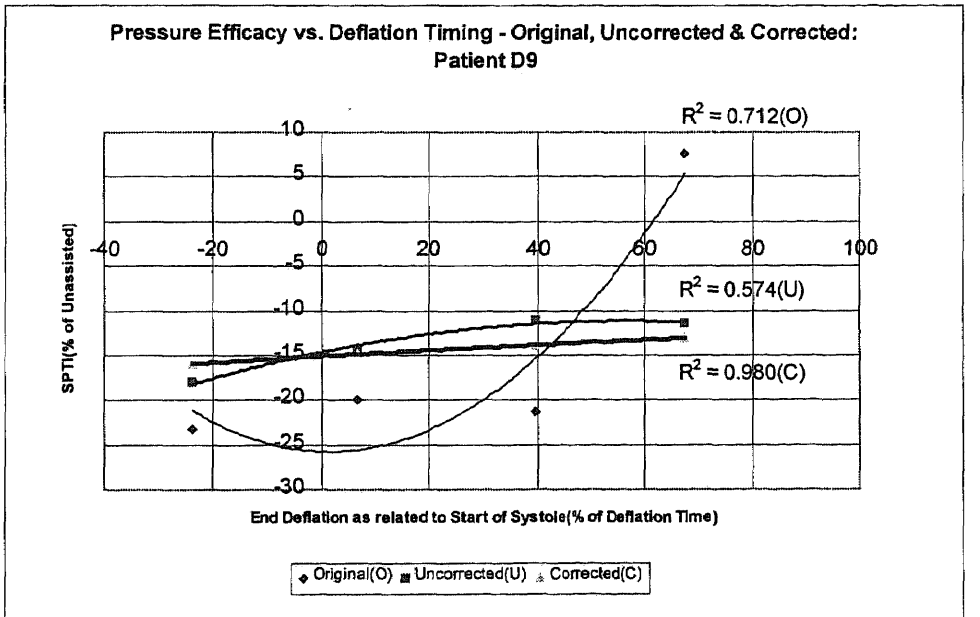

Figure 78B

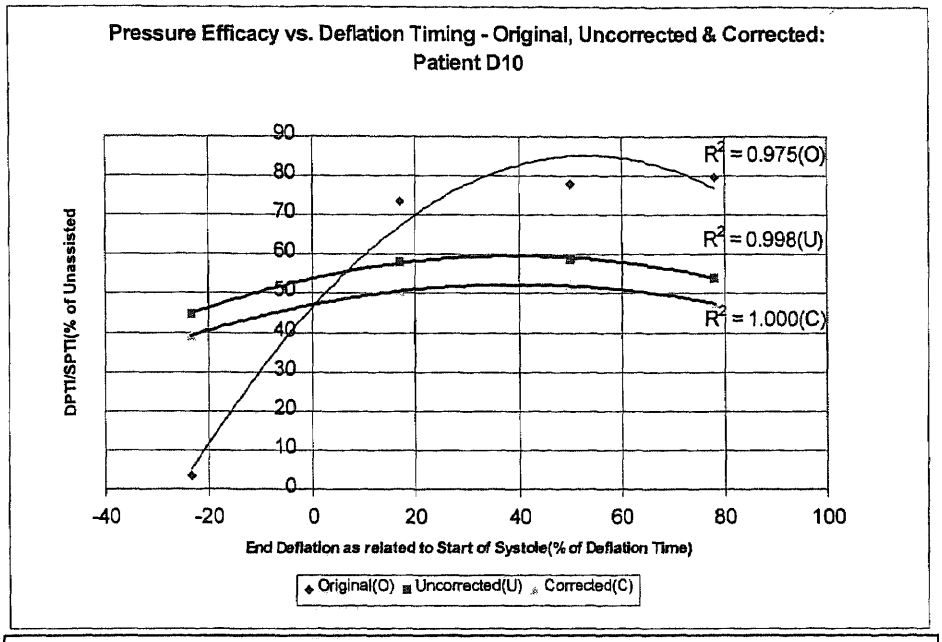

Figure 79B

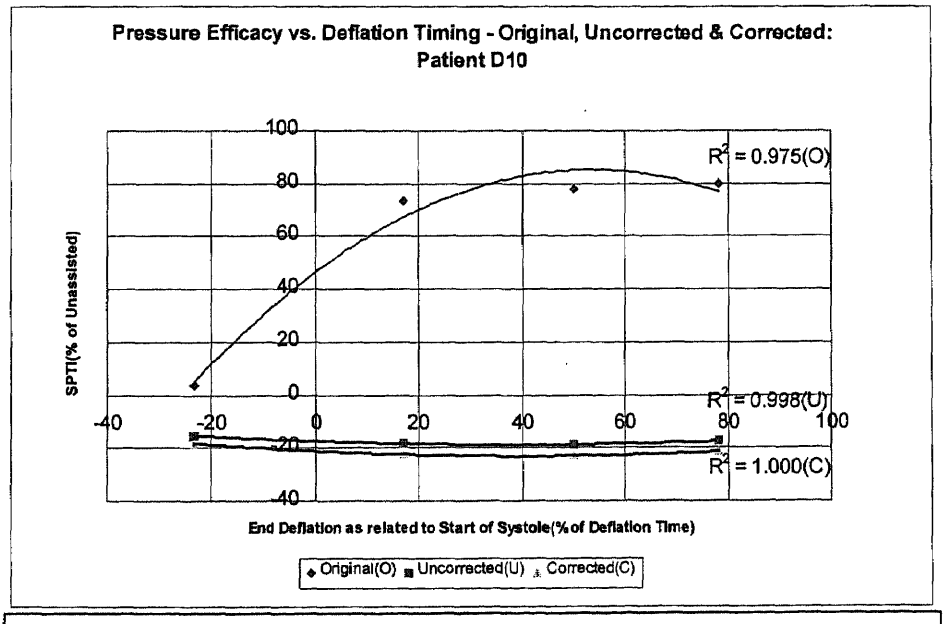

Figure 80B

APPENDIX C

SUMMARY OF DATA

In this Appendix, a summary of all the patients' files analyzed is provided. Refer to Chapter 5 for explanation of each of the hemodynamic indices calculated.

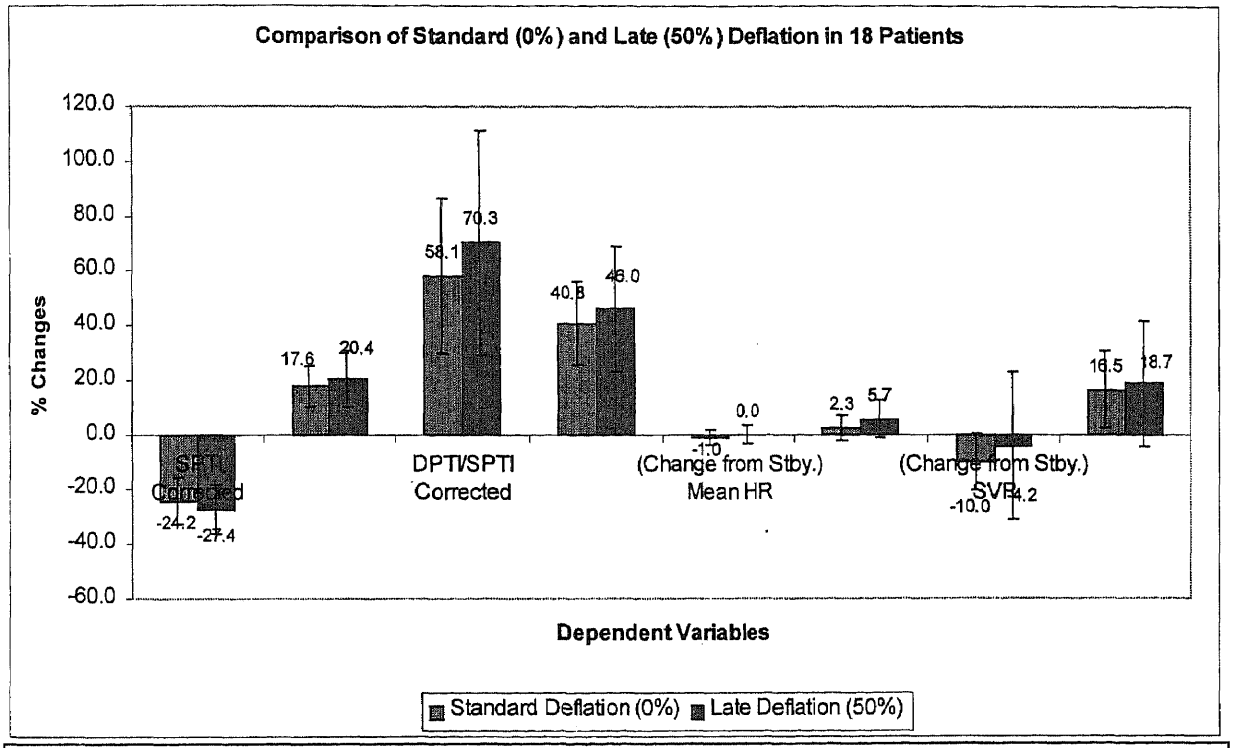

Figure 1C

REFERENCES

1. Al-Mubarak N, Roubin GS, Liu MW, et al. "Early Results of Percutaneous Intervention for Severe Coexisting Carotid and Coronary Artery Disease." *The American Journal of Cardiology* 84 (1999): 600-602.

2. Arafa OE, Pederson TH, Svennevig JL, et al. "Intraaortic Balloon Pump in Open Heart Operations: 10-Year Follow-up with Risk Analysis." *Ann Thorac Surg.* 65 (1998): 741-747.

3. Aronow WS, Ahn C, Kronzon I. "Comparison of Incidences of Congestive Heart Failures in Older African-Americans, Hispanics, and Whites." *The American Journal of Cardiology* 84 (1999): 611-612.

4. Bai J, Lin H, Yang Z, Zhou X. "A Study of Optimal Configuration and Control of a Multi-Chamber Balloon for Intraaortic Balloon Pumping." *Annals of Biomedical Engineering* 22 (1994): 524-531.

5. Barnea O, Moore TW, Dubin SE, Jaron D. "Cardiac Energy Considerations during Intraaortic Balloon Pumping." *IEEE Transactions on Biomedical Engineering* 37 (1990): 170-181.

6. Bolooki H. Clinical Application of the Intra-Aortic Balloon Pump. New York, 1998, Futura Publishing Company, Inc.

7. Christenson JT, Simonet F, Badel P, Schumziger M. "Evaluation of Preoperative Intra-Aortic Balloon Pump Support in High Risk Coronary Patients." *European Journal of Cardio-Thoracic Surgery* 11 (1997): 1097-1103.

8. Clark JW, Kane GR, Bourland HM. "On the Feasibility of Closed-Loop Control of Intra-Aortic Balloon Pumping." *IEEE Transactions on Biomedical Engineering* BME-20 (1973): 404-412.

9. Clayman CB. Your Heart. New York, 1989, Dorling Kindersley, LTD.

10. Courtesy of Datascope Corp. "Intra-Aortic Balloon Pumping: A Bibliography." (1991): 1-71.

11. Downing TP, Miller DC, Stinson EB, et al. "Therapeutic Efficacy of Intraaortic Balloon Pump Counterpulsation." *Circulation 64* suppl II (1981): II108-II113.

12. Fried GH. Biology. New York, 1990, McGraw-Hill, Inc.

13. Fuchs RM, Brin KP, Brinker JA, et al. "Augmentation of Regional Coronary Blood Flow by Intra-Aortic Balloon Counterpulsation in Patients with Unstable Angina." *Circulation* 68 (1983): 117-123.

14. Ioseliani GD, Sergei MC. "Improvement in Intra-aortic Balloon Pumping and Evaluation of its Efficacy by Electrode Methods of Control." *Artificial Organs* 7 (1983): 92-100.

15. Jonas M, Grossman E, Boyko V, Behar S, Hod H, Reicher-Reiss H. "Relation of Early and One-Year Outcome after Acute Myocardial Infarction to Systemic Arterial Blood Pressure on Admission." *The American Journal of Cardiology* 84 (1999): 162-165.

16. Kahn JK. Intra-Aortic Balloon Pumping: Theory and Clinical Applications. Michigan, 1990, Communications Media for Education, Inc.

17. Kantrowicz A. "Percutaneous Intra-Aortic Balloon Counterpulsation." *Crit Care Clin* 8 (1993): 819.

18. Katz AM. Physiology of the Heart. New York, 1992, Raven Press, Ltd.

19. Kern, MJ, Aguirre FV, Caracaciolo EA, et al. "Hemodynamic Effects of New Intra-Aortic Balloon Counterpulsation Timing Methods in Patients: A Multicenter Evaluation." *American Heart Journal* 137 (1999): 1129-1136.

20. Kim SY, Euler DE, Jacobs WR, et al. "Arterial Impedance in Patients during Intraaortic Balloon Counterpulsation." *Ann Thorac Surg.* 61 (1996): 888-894.

21. Lewis R. Life. IA, 1995, WM. C. Brown Communications, Inc.

22. Marchionni N, Fumagalli S, Baldereschi G, et al. "Effective Arterial Elastance and the Hemodynamic Effects of Intra-Aortic Balloon Counterpulsation in Patients with Coronary Heart Disease." *American Heart Journal* 135 (1998): 855-861.

23. Moulopoulos SD, Topaz S, Kolff WJ. "Diastolic Balloon Pumping (with carbon dioxide) in the Aorta-A Mechanical Assistance to the Failing Circulation." *American Heart Journal* 63 (1962): 669-675.

24. Opie, LH. The Heart: Physiology, from Cell to Circulation. New York, 1998, Lippincott-Raven Publishers.

25. Palmieri, V, Bella JN, DeQattro V, et al. "Relations of Diastolic Left Ventricular Filling to Systolic Chamber and Myocardial Contractility in Hypertensive Patients with Left Ventricular Hypertrophy (The PRESERVE Study)." *The American Journal of Cardiology* 84 (1999): 558-562.

26. Pfisterer ME, Buser P, Osswald, S, et al. "Time Dependence of Left Ventricular Recovery after Delayed Recanalization of an Occluded Infarct-Related Coronary Artery: Findings of a Pilot Study." *Journal of American College of Cardiology* 32 (1998): 97-102.

27. Powell WJ, Daggett WM, Magro AE. "Effects of Intra-Aortic Balloon Counterpulsation on Cardiac Performance, Oxygen Consumption, and Coronary Blood Flow in Dogs." *Circulation Research* 16 (1970): 753-787.

28. Puri NJ, Li J K-J, Welkowitz W. "Control System for Circulatory Assist Devices: Determination of Suitable Control Variables." *Trans. Amer. Soc. Artif. Organs* 28 (1983): 127-132.

29. Quaal, SJ. Comprehensive Intraaortic Balloon Counterpulsation. Missouri, 1993, Mosby.

30. Sakamoto T, Akamatsu H, Swartz MT, et al. "Changes of Intraaortic Balloon Volume during Pumping in a Mock Circulation System." *Artificial Organs* 20 (1996): 275-277.

31. Sakamoto T, Suzuki A, Shigeru K, et al. "Effects of Timing on Ventriculoarterial Coupling and Mechanical Efficiency during Intra-aortic Balloon Pumping." *ASAIO Journal* 43 (1995): M580-M583.

32. Sherman IW, Sherman VG. Biology: A Human Approach. New York, 1983, Oxford University Press.

33. Sherwood L. Human Physiology: From Cells to System. CA, 1997, Wadsworth Publishing Co.

34. Smith B, Barnea, Moore TW, Jaron D. "Optimal control system for the intra-aortic balloon pump." *Medical & Biological Engineering & Computing* 1991; 29: 180-84.

35. Stamatelopoulos ST, Nanas JN, Saridakis NS, et al. "Treating Severe Cardiogenic Shock by Large Counterpulsation Volumes." *Ann Thorac Surg* 1996; 62: 1110-17.

36. Sun Y. "Modeling the dynamic interaction between left ventricle and intra-aortic balloon pump." *American Journal of Physiology* 1991; 261: H1300-11.

37. Tierney G, Parissis H, Baker M, et al. "An experimental study of intra aortic balloon pumping within the intact human aorta." *European Journal of Cardio-thoracic Surgery* 1997; 12, 486-93.

38. Tranmer BI, Cordell EG, Kindt GW, Adey GR. "Pulsatile versus Nonpulsatile Blood Flow in the Treatment of Acute Cerebral Ischemia." *Neurosurgery* 1986; 19: 724-31.

39. Vander AJ, Sherman JH, Luciano DS. Human Physiology: The Mechanisms of Body Functions. New York, 1994, McGraw-Hill, Inc.

40. Weber KT, Janicki JS. "Intraaortic Balloon Counterpulsation: A Review of Physiological Priniciples, Clinical Results, and Device Safety." *Ann Thorac Surg* 1974; 17:602-36.

41. Wolf L, Cinch JM. "Mock Circulatory System for Intra-Aortic Balloon Testing." *IEEE Transactions on Biomedical Engineering* 1972; BME-19: 38-46.

42. Zehetgruber M, Mundigler G, Christ G, et al. "Relation of Hemodynamic Variables to Augmentation of Left Anterior Descending Coronary Flow by Intraaortic Balloon Pulsation in Coronary Artery Disease." *The American Journal of Cardiology* 1997; 80: 951-54.

43. Zelano JA, Li JK, Welowitz W. "A Closed-Loop Control Scheme for Intraaortic Balloon Pumping." *IEE Transactions on Biomedical Engineering* 1990; 37: 182-92.

44. Zinemanas D, Beyar R, Sideman S. "Effects of Myocardial Contraction on Coronary Blood Flow: An Integrated Model." *Annals of Biomedical Engineering* 1994; 22: 638-52.